Development of Granulated Activated Carbon using Corner Brook Pulp and Paper Mill Fly Ash for Drinking Water Treatment

Afsoon Taghizadehgan

A thesis submitted to the School of Graduate Studies

in partial fulfillment of the requirements for the degree of

Master of Engineering

Faculty of Engineering and Applied Science

Memorial University of Newfoundland

May 2019

St. John's, Newfoundland and Labrador

Abstract

Natural organic matters (NOM) interact with disinfectants and produce disinfection by-products (DBPs). One of the best available technologies to remove NOM from water to reduce DBPs formation is adsorption with activated carbon. In this study, the removal of NOM from pond water was studied using powder activated carbon (PAC), and the granular activated carbon (GAC) generated from Corner Brook Pulp and Paper (CBPP) fly ash as raw material. PAC was used in batch tests and water pH, temperature, and volume was considered as variables to determine optimized conditions for NOM removal applying response surface method (RSM); it was concluded that water pH and volume have significant effects on NOM removal. CBPP was combined with bitumen as a binder to produce GAC. Effect of binder to carbon ratio, calcination and steam activation temperature, the temperature increasing rate, and steam activation time were studied to produce GAC with high BET surface area and efficient hardness. Granules with 30:70 binder to carbon ratio, calcinated at 750 °C, activated at 950 °C for 3 hours with 15°C/min of heating rate were found to be ideal for GAC production for NOM removal.

Column tests for NOM removal were conducted using produced GAC. Results indicate that the produced GAC is effective for 60% NOM removal. Follow-up chlorination experiments illustrate that the formation of DBPs (THMs and HAAs) were significantly reduced. Used GAC was regenerated using RSM design at different regeneration temperature, time, and steam flow. The results show that regeneration at 916 °C for 43 minutes under 350 mL/min of steam would lead to optimum regeneration conditions.

Acknowledgment

I would like to express my deepest gratitude to my supervisor, Dr. Tahir Husain, for the great opportunity, his thoughtful support, and his guidance through the course of this study.

I acknowledge the Faculty of Engineering and Applied Science, Memorial University of Newfoundland (MUN), Harris Centre MMSB Waste Management, the Natural Sciences and Engineering Research Council of Canada, and Innovate NL Collaborative Research and Development for their financial support.

I would like to thank all my friends at NRPOP Control Lab in the Faculty of Engineering and Applied Science for providing a pleasant working environment. Special thanks to Ms. Victoria Alexandra Downing and Dr. Michael Katz for their great support regarding BET analysis.

I am grateful to my family for their never-ending love, encouragements, and supports.

Finally, I hope the useful results of this research would be a help to all people who are struggling for a clean environment and safe drinking water.

Table of Contents

Abstract i

Acknowledgment ii

Table of Contents iii

List of Tables viii

List of Figures x

List of Abbreviations xii

Chapter 1 Background 1

1.1 Introduction 1

1.2 Research Objectives 3

1.3 Research scope 3

1.4 Thesis Organization 4

Chapter 2 Literature Review 5

2.1 NOM and its Presence in Water 5

2.2 Carbon Activation 8

2.2.1 Physical activation 8

2.2.2 Chemical Activation 13

2.2.3 Granular Activated Carbon 15

2.3 Factors Affecting Natural Organic Matter Removal by Activated Carbon and Design of Experiment 25

2.3.1 Activated Carbon Properties 25

2.3.2 NOM characteristics 26

2.3.3 Contact time 26

2.3.4 Temperature 27

2.3.5 pH 28

2.3.6 Experimental Design 28

2.3.7 Analysis of Variances (ANOVA) 29

2.4 Activated Carbon Regeneration 31

Chapter 3 Experimental Methods 33

3.1 Water Collection and Characterization 33

3.1.1 Water Source 33

3.1.2 Water Characterization 35

- pH 36
- Total Organic Carbon (TOC) 36
- Ultraviolet Absorbance 36
- Elemental analysis 37

3.2 Adsorbents Preparation and Characterization 37

3.2.1 Carbon Source 37

3.2.2 Powder Activated Carbon Production 38

3.2.3 Granular Activated Carbon Production 39

3.2.4 Adsorbent Characterization 41

3.3 NOM Adsorption in Batch and Column Tests 47

3.3.1 NOM adsorption: Batch System 48

3.3.2 NOM Adsorption: Column Test 49

3.3.3 Chlorination 51

3.3.4 GAC Regeneration 53

3.4 Adsorption Study 54

3.4.1 Adsorption Kinetic 54

3.4.2 Adsorption Isotherm 56

3.5 Quality control 60

Chapter 4 Results and Discussion 62

4.1 Adsorbents Characterization (Powder) 62

4.1.1 Moisture Content, Ash Content, pH, MB, and IN of CBPP 62

4.1.2 Elemental Analysis (major metal content) 63

4.1.3 BET Surface Area and Pore Size Distribution of PAC 65

4.2 GAC Generation with Raw CBPP and PAC 67

4.3 GAC Generation by Washed CBPP and Bitumen 67

4.3.1 Calcination temperature 68

4.3.2 Activation Temperature 71

4.3.3 Calcination temperature increasing rate 75

4.3.4 Activation temperature increasing rate 77

4.3.5 Steam Activation, Steam Temperature 78

4.3.6 Steam Activation time 80

4.4 GAC Characterization 82

4.4.1 Elemental Analysis for produced GAC 82

4.4.2 BET Surface Area and Pore Size Distribution of GAC 83

Chapter 5 NOM Removal by Generated Adsorbents 86

5.1 Water Sample Characterization 86

5.2 NOM adsorption: Batch System 87

5.2.1 R-Squared Interpretation 91

5.2.2 Model Adequacy 92

5.2.3 Important Factors of Adsorption and Interactions 94

5.2.4 Model Validation 96

5.2.5 Adsorption Study: Kinetic Study 97

5.2.6 Adsorption Study: Equilibrium Study 100

5.3 NOM Adsorption: Column Test 103

5.3.1 Elemental Analysis for Treated water 105

5.4 Chlorination 106

5.4.1 THMs Analysis After Chlorination 108

5.4.2 HAAs Analysis After Chlorination 110

5.5 GAC Regeneration 114

5.5.1 Regeneration Optimization 119

5.6 NOM Adsorption: Column Test, Regenerated carbon 120

Chapter 6 Conclusions and Recommendations 122

6.1 Conclusions 122

6.2 Major Research Contributions 125

6.3 Recommendations and Future Works 125

References 127

Appendixes 136

List of Tables

Table 2-1: Researches on Physical Activation..... 11

Table 2-2: Researches on Chemical Activation..... 13

Table 3-1: Variables and their ranges for granulation study..... 40

Table 3-2: Factors and levels of experiment..... 48

Table 3-3: Sample collection from column test..... 51

Table 3-4: Sample collection for chlorination 52

Table 3-5: Factors and levels of experiment..... 54

Table 4-1: Raw, Washed, and Activated CBPP Characterization 62

Table 4-2: Elemental analysis for raw and washed CBPP..... 64

Table 4-3: Characterization for the effect of calcination temperature on different carbon-to-binder ratios..... 69

Table 4-4: Characterization for the effect of activation temperature on different carbon-to-binder ratios..... 73

Table 4-5: Characterization for the effect of calcination temperature increasing rate on 30% binder granules 76

Table 4-6: Characterization for the effect of activation temperature increasing rate on 30% binder-to-carbon granules..... 77

Table 4-7: Effect of steam temperature on GAC's generation 80

Table 4-8: Effect of activation time on GAC's characterizations..... 81

Table 4-9: Elemental analysis for PAC and GAC 83

Table 5-1: Water sample characterization 86

Table 5-2: Pouch Cove Water Elemental Analysis..... 87

Table 5-3: Results for NOM adsorption in batch system 90

Table 5-4: Analysis of Variance (ANOVA) 91

Table 5-5: R-Squared..... 92

Table 5-6: Validation of the model..... 97

Table 5-7: Kinetic Models Parameters for NOM Adsorption 100

Table 5-8: Isotherm Models Parameters for NOM Adsorption..... 103

Table 5-9: Elemental analysis for treated water 106

Table 5-10: Sample collection for chlorination 107

Table 5-11: THM compounds in raw and treated water..... 110

Table 5-12: HAA compounds in raw and treated water 112

Table 5-13: Results of thermal regeneration..... 116

Table 5-14: ANOVA for MB adsorption..... 117

Table 5-15: ANOVA for IN adsorption..... 118

Table 5-16: ANOVA for Hardness..... 119

Table 5-17: Optimum Condition for GAC regeneration..... 120

List of Figures

Figure 3-1: Location of St. John's and Pouch Cove 34

Figure 3-2: North Three Island Pond, Pouch Cove, NL 35

Figure 3-3: Experimental setup for column test 50

Figure 3-4: Adsorption Isotherms from (McCabe et al., 1993) 57

Figure 4-1: Isotherm plot of PAC 66

Figure 4-2: Pore Size Distribution for of PAC 66

Figure 4-3: Characterizations for the effect of calcination temperature on different carbon-to-binder ratios; a) Burn-off, b) MB, c) IN 70

Figure 4-4: Characterizations for the effect of activation temperature on different carbon-to-binder ratios; a) Burn-off, b) MB, c) IN, d) Hardness 75

Figure 4-4: Characterization for the effect of activation temperature increasing rate on 30% binder granules 76

Figure 4-5: Characterization for the effect of activation temperature increasing rate on 30% binder granules 78

Figure 4-6: Effect of steam temperature on GAC's generation 80

Figure 4-7: Effect of activation time on GAC's characterizations 81

Figure 4-8: Isotherm plot of GAC 84

Figure 4-9: Pore Size Distribution for GAC 85

Figure 5-1: Diagnostics curves for NOM adsorption 94

Figure 5-2: Model Graphs; a) Contour Graph for water volume and pH b) 3D Surface Graph for water volume and pH 95

Figure 5-3: interaction of water volume and pH 96

Figure 5-4: NOM Adsorption Kinetic Study 98

Figure 5-5: NOM Adsorption Kinetic models: a) pseudo-first-order, b)pseudo-second-order 99

Figure 5-6: NOM Adsorption Isotherm, Equilibrium Study 101

Figure 5-7: NOM Adsorption Isotherm models: a) Langmuir, b) Freundlich, c) Temkin 103

Figure 5-8: Breakthrough Cuves for NOM adsorption a)Concentration b)UV .. 104

Figure 5-9: Total THMs in raw and Treated samples after chlorination 109

Figure 5-10: Total HAAs in raw and Treated samples after chlorination 111

Figure 5-11: Breakthrough Curves for NOM adsorption using regenerated GAC 120

List of Abbreviations

AC	Activated carbon
ANOVA	Analysis of variances
BCAA	Bromochloroacetic acid
BDCAA	Bromodichloroacetic acid
BET	Brunauer–Emmett–Teller
CBPP	Corner Brook Pulp & Paper
CMC	Carboxymethyl cellulose
CS	Calcium sulfate
DBAA	Dibromoacetic acid
DBCAA	Dibromochloroacetic acid
DBP	Disinfection By-products
DCAA	Dichloroacetic acid
DFT	Density functional theory
DOM	Dissolved organic matters
DRC	Dynamic reaction chamber
GAC	Granular activated carbon
HAAs	Haloacetic acids

HPSEC	High-performance size exclusion chromatography
IN	Iodine number
MB	Methylene blue
MBAA	Monobromoacetic acid
MCAA	Monochloroacetic acid
MTBE	methyl tertiary-butyl ether
NOM	Natural organic matters
PAC	Powder activated carbon
PVA	Polyvinyl alcohol
RSM	Response surface methodology
S-CMC	Sodium carboxymethyl cellulose
TBAA	Tribromoacetic acid
TCAA	Trichloroacetic acid
THMs	Trihalomethanes
TOC	Total organic carbon
UV	Ultra Violet
VOCs	Volatile organic compounds

Chapter 1 Background

1.1 Introduction

At the beginning of the 20th century, chlorine was introduced as a disinfectant to the water supply to eliminate water-borne diseases (Tibbetts, 1995). A good disinfectant, as an oxidizing agent, should have the potential to destroy pathogenic bacteria and microorganisms (Goi *et al.*, 2005). Chloramine, chlorine dioxide, ozone, and ultraviolet radiation are other kinds of disinfectants. These disinfectants have different properties and different potentials for killing microorganisms. However, the disadvantage of these disinfectants is their reaction with the natural organic matters (NOM) in the formation of disinfection by-products (DBPs) (Amy *et al.*, 2000, Liu *et al.*, 2002).

The residual chlorine in the water reacts with the NOM such as humic acids and fulvic acids and forms unwanted by-products including Trihalomethanes (THMs) and Haloacetic acids (HAAs) (Nieuwenhuijsen *et al.*, 2000). More than 600 DBPs have been identified, but the detailed characteristics and toxicity of more than 60% of them are still being studied (Shen *et al.*, 2010).

NOM is all carbon-based compounds which can be found in surface and groundwater. This group of materials are the products of decomposition and metabolic reaction and include humic substances, proteins, and polysaccharides. NOM characteristics are highly dependent on the season, temperature, and amount of precipitation. For instance,

in Atlantic Canada, NOM levels peak during summer and fall. Also, in Newfoundland and Labrador, there has been an increasing trend in NOM levels due to climate change, change in the water quality, and human activities (Chaulk & Sheppard, 2011).

NOM is not a risk to human health while some of the DBPs are probable carcinogens and extremely hazardous. Therefore, the lower the amount of NOM in the water, the lower the chances of DBPs formation. There are different ways to remove NOM from water including coagulation, flocculation, high-pressure membranes, size exclusion membranes, air flotation, direct filtration, and adsorption (Chaulk & Sheppard, 2011). Among all of these methods, adsorption is considered to be the best option due to its simplicity, ease of design and high efficiency of removal (Dąbrowski, 2001).

Activated carbon has been widely considered as an effective adsorbent to remove natural organic matters from the water. This adsorbent, depending on its porous structure, is useful for removing odor, taste, toxic chemicals and unwanted contaminations (Kim, 2009).

Activated carbon exists in two common forms; powder activated carbon (PAC) and granular activated carbon (GAC). Usually, PAC has a better pore structure and surface area than GAC. However, due to the simplicity of GAC use, its regeneration potential, and its granular format which does not require removal from treated water, this type of activated carbon is more practical for NOM removal than PAC (GAN *et al.*, 2006).

1.2 Research Objectives

The main objective of this study is to develop a cost-effective GAC to reduce DBPs in drinking water to an acceptable level by reducing NOM from the water. To conduct the study, intake water from Pouch Cove, a small community near St. John's, was tested in the laboratory. Raw carbon from Corner Brook Pulp and Paper Mill (CBPP) fly ash was used in powder and granular formats to remove NOM from water in batch and column tests. Moreover, to have a comprehensive and efficient study, Design of Experiment for NOM adsorption in batch test and GAC regeneration was used (Vepsäläinen *et al.*, 2009, Duan *et al.*, 2012).

1.3 Research scope

This study aims to use powder and granular activated carbons to produce effective filtration media for the removal of NOM from Pouch Cove intake water. Raw carbon was extracted from the Corner Brook Pulp and Paper Mill (CBPP) fly ash to produce a low-cost adsorbent. Powder activated carbon was used in the batch system to adsorb NOM from water at different ranges of temperature, pH, and carbon concentrations in water. In the next step, granulation of raw carbon was studied. For this, different binders and activation situations was investigated to produce GAC with well-developed pore structure. The produced GAC was used in a continuous system using column tests to remove NOM from the water and develop breakthrough curves. Treated water was then chlorinated, maintaining residual chlorine in the water. DBP formation in the water for different contact

periods was investigated to determine DBP reduction efficiency using GAC. In the last step, used GACs was regenerated and used again in the adsorption system to investigate the effectiveness of regenerated carbon.

1.4 Thesis Organization

This thesis is divided into six chapters. In the first chapter, research outline and objectives are briefly discussed. In the second chapter, a comprehensive background information and literature review on activation, granulation, regeneration and natural organic matter adsorption are presented. The third chapter is about the experimental setup including water collection and characterization, a method of activation and development of granulated activated carbon, in-depth investigation of adsorption study, and different analytical methods including Design of Experiment. In chapter four, a comparative evaluation of GAC and PAC is presented. This chapter includes the characterization of raw and activated carbon, the production of GAC, and the characterization of granular activated carbon. Chapter five includes the results of NOM adsorption in batch and continuous systems, the chlorination step and DBPs formation, and the efficiency of regeneration. The last chapter of the thesis, chapter six, covers conclusions on the effectiveness of GAC and PAC and recommendations for future studies.

.

Chapter 2 Literature Review

2.1 NOM and its Presence in Water

NOM is a complex material present in all natural waters (Świetlik *et al.*, 2004). It is produced by the natural decay of plants, aquatic plants, and algae (Chow *et al.*, 2008). Concentration and characterization of NOM are dependent on factors such as the water source, seasons, climate, and geology (Fabris *et al.*, 2008). NOM can be categorized as (a) particulate organic matters with particles of diameter more than 0.45 μm filter; and (b) dissolved organic matters with a diameter of less than 0.45 μm filter (Szymczycha *et al.*, 2017).

NOM characterization can help to understand its role in water. Simple techniques such as ultraviolet (UV_{254}), total organic carbon (TOC), dissolved organic matter (DOM), and parameters such as pH, and turbidity can be employed to specify the amount and characteristics of NOM in water, although some specification such as the molecular weight distribution, hydrophobicity, and hydrophilicity of particles need complicated techniques. High-performance size exclusion chromatography (HPSEC) can be used to determine molecular weight and fractionation is a useful method to determine its hydrophobicity and hydrophilicity (Chow et al., 2008).

The presence of NOM in water will lead to adverse effects on water quality such as unpleasant odor, taste and color in drinking water distribution system (Metsämuuronen *et al.*, 2014), promoting bacterial reproduction (Korotta-Gamage & Sathasivan, 2017),

making a complex with heavy metals and increasing their solubility in water (Rao *et al.*, 2011), causing fouling in membranes, and reducing treatment efficiency (Drikas *et al.*, 2011). One of the most important and hazardous effects of NOM presence in water is their interactions with disinfectants which leads to DBP formation (Tubić *et al.*, 2013).

During the last century, water disinfection technology has been a major contributor to the reduction of water-borne diseases (Van Leeuwen, 2000). Chlorine, chloramine, ozone, and chlorine dioxide are different types of disinfectants helping in the eradication of diseases such as cholera and typhoid. If there were no disinfection, a majority of people all around the world would still not have safe drinking water (Kerwick *et al.*, 2005). A dose of disinfectant is added to drinking water at the last step of water treatment, before water distribution. Once disinfectants are added, DBPs will form as a consequence of interaction with NOM. Exposure to DBPs through ingestion, inhalation, and dermal adsorption are associated with the development of cancers including bladder cancer (Singer, 1999, Villanueva *et al.*, 2006), adverse effects on the liver, kidneys and central nervous system (Clark & Boutin, 2001). It is important to mention that the risk of cancer from DBPs is a thousand time lower than the risk of death from pathogens (WHO, 2000).

The first DBPs reported in drinking water were Trihalomethanes (THMs) which were by-products of interactions between disinfectants and organic matters such as humic acids and fulvic acids. Haloaceticacids (HAAs) was the second major group of DBPs (Bellar *et al.*, 1974). Although THMs and HAAs are considered to be the dominant groups, more than 600 DBPs have been found in water (Richardson *et al.*, 2007, Singer, 1999). The

common DBPs are Haloacetonitriles, Haloketones, Aldehydes, Oxyhalides, Cyanogen halides, and Carboxylic acids (Krasner, 1999).

Chloroform ($CHCl_3$), Bromodichloromethane ($CHCl_2Br$), Dibromochloromethane ($CHClBr_2$), and Bromoform ($CHBr_3$) are four compounds which are part of the THMs group. According to the Canadian guideline, the total concentration of THMs in water should not exceed 100 µg/L (Health Canada, 2017)

Monochloroacetic acid (MCAA), Monobromoacetic acid (MBAA), Dichloroacetic acid (DCAA), Trichloroacetic acid (TCAA), Bromochloroacetic acid (BCAA), Bromodichloroacetic acid (BDCAA), Dibromoacetic acid (DBAA), Dibromochloroacetic acid (DBCAA), and Tribromoacetic acid (TBAA) are nine different compounds in the HAAs group. According to Canadian guidelines, the maximum allowable concentration for total HAAs in water is 80 µg/L based on the concentration of five compounds including MCAA, DCAA, TCAA, MBAA, and DBAA (Health Canada, 2017).

NOM and their concentrations have significant effects on mechanisms in which DBPs are formed. Also, the disinfection dose and the retention time in the water supply system have a relationship with the concentration of DBPs in the water. Lower concentrations of NOM in the water, reduce the possibility of DBPs formation and their hazards.

Different methods for NOM removal from water are coagulation, membrane filtration, adsorption, and advanced oxidation processes. Among these, adsorption is a promising method for water treatment due to its simplicity, ease of design and operation,

and high efficiency (Dąbrowski, 2001). Among different adsorbents for NOM removal, activated carbon is the most preferred because of its high surface area, porosity and adsorption capacity (Menya *et al.*, 2017).

Activated carbon is a carbonaceous material with high porosity and large surface area (Tancredi *et al.*, 2004) with great potential for NOM removal (Menya et al., 2017). Activated carbon is considered as one of the essential adsorbents in water treatment and air purification. To have activated carbon, a raw material with a relatively high carbon content goes through either chemical or physical processing methods (Tancredi et al., 2004). The chemical method is a single step process in which precursors are carbonized in the presence of chemical agents. The physical method involves activation in the presence of gases such as carbon dioxide and air or steam. In physical activation, to obtain a well-developed carbon structure, a large portion of the internal mass should be eliminated at a controlled temperature. On the other hand, chemical activation uses dehydrating agents to influence pyrolytic decomposition at lower temperatures (Kandiyoti *et al.*, 1984).

2.2 Carbon Activation

2.2.1 Physical activation

Physical activation includes two different steps. The first step is carbonization in which an inert gas, like nitrogen, is used to develop pure carbon and the production is termed as “Char.” During the carbonization, reactive carbon separates from the structure in the format of oxides and porous structure can be developed (Humbert *et al.*, 2008). In

the second step, an oxidizing gas like CO_2, air, steam, or a mixture of them is used to improve the porous structure of the produced char at an elevated temperature (Hesas *et al.*, 2013).

Physical activation depends on factors such as oxidizing gas, activation temperature, and activation time. According to most of the literature, activation with steam obtains more porous carbon with larger pores and as a result, a better adsorption capacity (Kühl *et al.*, 1992, DeGroot & Richards, 1989, Lu & Do, 1992).

Activation is associated with the carbon burn-off for pores enlargement and pore creation. As a result, carbon weight would decrease during the process. Activation time and temperature have a significant role in the pore structure and Brunauer–Emmett–Teller (BET) surface area. Activation at a temperature below 1000 °C will result in smaller pores known as micropores (0.2-1 nm) and mesopores (1-25 nm). Increasing the activation to above 1000 °C would give pores known as macropores (>25 nm) (Everett, 1972, Manocha, 2003).

Iodine number (IN) and Methylene Blue test (MB) are techniques used to determine the internal surface of activated carbon (Simay *et al.*, 1984). A quantity of iodine and MB adsorbed by 1g of carbon indicates the IN and MB value, respectively (Saka, 2012). MB has large molecules, and the quantity of MB adsorbed by AC indicates the mesoporosity of AC (Simay et al., 1984). On the contrary, IN is a technique to assess the microporosity of AC (Baccar *et al.*, 2009) and an empirical rule shows that each gram of iodine adsorbed by AC, indicates 1 m^2 of BET surface area (Simay et al., 1984).

Temperature has an effective role in the mesoporosity and microporosity development. In low-temperature ranges (usually <500 °C), an increase in temperature would result in significant IN increasing due to micropores creation. However, a further temperature increase would cause the micropores to collapse and mesopores to create. As a result, IN would decrease (Patnukao & Pavasant, 2008).

In Table 2-1, previous studies on physical activation at different times, temperatures, and activation conditions are summarized. Provided information in each article about IN, MB, BET surface area or any specific results are stated in the table.

Table 2-1: Researches on Physical Activation

Raw Material	Activation Agent	Carbonization Condition	Activation Condition	Optimum Condition and Carbon Properties	Reference
Maize tassels	Steam	Temp: 500 °C Time: 1 h Gas: Argon Flow: 200 mL/min	Temp: 700,750, 800 °C Time: 20, 40, 60 min	IN increasing with temperature up to 750 °C and decreasing afterward.	(Olorundare *et al.*, 2014)
Bamboo	Steam	Gas: N_2 Temp: 650, 700, 750, 800, and 850 °C with 5 °C/min	Temp: 650, 700, 750, 800, 850 °C Time: 40 min Steam flow: 8 g/min	IN increased with temperature increasing up to 800 °C and then decreased. Highest BET was 2024 m^2/g attained at 850 °C.	(Ma *et al.*, 2014)
Rice Husk	CO_2	Gas: N_2 Gas flow: 500 mL/min Temp: 400 °C, 20 °C/min Time 1hr	Temp: 650, 750, 850 °C CO_2 flow: 200 mL/min	Highest BET at 850 °, 350.1 m^2/g and mostly microporous	(Li *et al.*, 2016)
Sawdust	Steam	Gas: N_2 Temp: 500 °C Time: 1 hr	Temp: 800 °C Time: 1 hr	Bulk density: 0.38 (g/ml) Surface area: 516.3 m^2/g	(Malik, 2003)

Rice husk	Steam	Gas: N_2 Temp: 400 °C Time: 1 hr	Temp: 600 °C Time: 1hr	Bulk density: 0.73 (g/ml) Surface area: 272.5 m^2/g	(Malik, 2003)
Bituminous coal	CO_2	Gas: N_2 Flow: 100 mL/min Temp: 750 °C Time: 2 hr	Flow: 150 mL/min Temp: 800°C Time: 6,10,31,60 hr	Highest BET: 754 m^2/g for activation of 60 hr	(Ahmadpour & Do, 1996)
Bituminous coal	CO_2	Gas: N_2 Flow: 100 mL/min Temp: 750 °C Time: 2 hr	Flow: 150 mL/min Temp: 900 °C Time: 3, 8, 15, 20 hr	Maximum BET of 751 m^2/g for activation of 8 hr	(Ahmadpour & Do, 1996)

As it is clear from Table 2-1, in most researches, increasing activation temperature and time would result in better porosity and hence, better surface area. In physical activation, char is obtained in the first stage, carbonization of raw material at a temperature range of 400–700 °C, using N_2. The produced char exhibits minimal adsorption capacity due to blocked and undeveloped pores. After the activation process, at leveled temperatures of 600–1000 °C by using suitable oxidizing gases such as carbon dioxide, steam, air or their mixtures new porosity is created. Consequently, after the activation process, activated carbon with well-developed pore structure and relatively large BET surface area is formed. However, weight loss during physical activation at a high level of temperature and time is a negative aspect and require optimization.

2.2.2 Chemical Activation

Chemical activation is another method to prepare activated carbon. In chemical activation, a raw material is mixed with the chemical agents, as dehydrating agents and oxidants, and then it is activated under N_2 at relatively low temperature (Ioannidou & Zabaniotou, 2007). The chemical agent used for chemical activation can be acidic like nitric acid (HNO_3), hydrochloric acid (HCl), phosphoric acid (H_3PO_4), and sulfuric acid (H_2SO_4), neutral like potassium carbonate (K_2CO_3) and zinc chloride ($ZnCl_2$), or basic like potassium hydroxide (KOH) and sodium hydroxide (NaOH) (Din *et al.*, 2017).

Chemical activation has some advantages over physical activation including lower burn-off, activation at a relatively lower temperature (400-700 °C), and well-developed pores. However, the high cost of activating agent and its leaching in the water are the disadvantages of chemical activation (Maciá-Agulló *et al.*, 2004)

The scientific literature on chemical activation is summarized in Table 2-2.

Table 2-2: Researches on Chemical Activation

Raw Material	Activation Agent	Activation Condition	Optimum Condition and Carbon Properties	Reference
Bituminous coal	KOH	Agent to carbon ratio: 25% and 100% Time: 60,120,180 min Temp: 500, 600, 700, 800 °C	Higher impregnation ratio, higher BET Highest BET: 925 m^2/g for activation at 700 °C for 60 minutes	(Ahmadpour & Do, 1996)

Jute stick	60% H_3PO_4	Agent to carbon ratio: 1:1 Temp: 200 °C for 15 min, then increased to 400-700 °C	Highest BET: 1910m^2/g Best temp: 475 °C with IN of 1205 mg/g	(Jahan *et al.*, 2008)
Grape seed	7.7M H_3PO_4	Agent to carbon ratio: 1:1,2:1,3:1,4:1 N_2 flow: 100 mL/min Temperature: 350, 400, 450, 500 °C (10 °C/min) Time: 2 hr	Highest BET: 1139m^2/g Best temp: 500°C with 3:1 agent to carbon ratio	(Al Bahri *et al.*, 2012)
Palm shell	10%,20%,30% H_3PO_4	Agent to carbon ratio: 20 g carbon in 100mL agent Temperature: 650 °C (10 °C/min) Time: 2hr	Highest BET: 1000 m^2/g Best H_3PO_4 concentration: 30%	(Rahman *et al.*, 2012)
Heavy oil burning fly ash (HOFA)	H_3PO_4	Agent to carbon ratio: 10g carbon in 2 and 5mL of H_3PO_4 Temperature: 550, 800 °C Time: 30,60 min	Highest BET: 143.8 m^2/g At highest temperature, the volume of agent and time	(Mofarrah *et al.*, 2014)

Temp= Temperature

According to Table 2-2, it is clear that chemical activation has lower energy cost compared to physical activation since it usually takes place at lower temperature ranges. Also, phosphoric acid (H_3PO_4) is the most common chemical agent due to its potential to provide activated carbon with well-developed porosity and high BET surface area.

Moreover, phosphoric acid has lower toxicological and environmental limitations (Al Bahri et al., 2012).

2.2.3 Granular Activated Carbon

Activated carbon is an important adsorbent and has wide applications in industries including air purification and water treatment processes. Activated carbon can be found in two common forms; Powdered Activated Carbon (PAC) and Granular Activated Carbon (GAC). Although PAC has well-developed pore structure and high specific surface area with strong adsorption ability, when used in the water treatment process creates difficulty in the separation of PAC from the treated liquids. Also, the finer the PAC particles is, the higher chances of blocking filter surfaces, which leads to a gradual decrease in the filtration flow rate and filtration effectiveness (GAN et al., 2006). Unlike PAC, GAC has a certain size and shape, higher bulk density and, higher strength. Although the surface area per unit mass is reduced due to the granulation process, GAC has a higher surface area per unit volume because of higher bulk density (Pendyal *et al.*, 1999a). It is easier to store, transport, recycle and regenerate GAC. The GAC with all these advantages has therefore been utilized in widespread applications. Thus GAC plays a leading role in the carbon market (Markets, 1994).

GAC should be investigated regarding activity and strength. Strength is due to specific adhesion using binders and needs primary valances to link carbon molecules to each other. On the other hand, activity is for chemical adsorption and needs a great number of free valances to adsorb particles. Consequently, increasing strength would lead to a

decrease in the activity and vice versa. As a result, optimum conditions appear to be the minimum use of binders to produce strong granular activated carbon with maximum possible activity.

Granulation steps mentioned in the literature consists of either granulation of activated carbons or a heat treatment applied to molded pellets or extrudates. The latter one is more efficient due to a better response to the environmental conditions, better thermal conductivity and, higher hydrophobicity. The binder, however, might be the restriction under baking condition (Machnikowski *et al.*, 2010).

Calcination is an essential step in granulation. Calcination can improve binder properties related to strength and stability in water filtration. On the other hand, uncontrolled calcination may lead to pore blockage (Lozano-Castello *et al.*, 2002).

What happens during the heat treatment can be illustrated using thermogravimetric analysis. The thermogravimetric method is a thermal analyzer method which measures the weight loss during heat treatment, calcination part, in the range of 10 to 1000 °C and shows that usually, each calcination has three major weight loss. The first step, normally up to around 150 °C, is water loss and mostly the weight loss is due to water evaporation. The second step is organic material decomposition up to 650 °C and losing volatile organic matters and depends on raw material and binder. The last step happens at a temperature above 650 °C in which activation of carbon and generation of ash happens (Liang *et al.*, 2016).

Different methods can be applied to characterize granular activated carbon. To characterize pores structure, one method is the nitrogen (N_2), mercury and CO_2 adsorption. Machnikowski et al. (2012), used N_2 adsorption at 77 K to measure pores more than 0.6 nm. They used CO_2 adsorption at 273 K to define pores less than 0.7 nm and mercury adsorption to determine pores between 3.6 nm-15µm (Machnikowski *et al.*, 2012).

Granulation of carbon can be done using Extrusion or Hydraulic Press. Literature about GAC production using different binders, instrument, and source of carbon is reported below.

Tancredi et al. (2004) used a manual extruder to produce granular activated carbon using activated sawdust combined with Carboxymethyl Cellulose (CMC). They added kaolin to increase the stability of granules in water and improved the reinforcement. They used produced GACs to adsorb phenol from water and to determine the chemistry of the adsorption, they used the thermogravimetric method. By spotting the temperature in which the major peaks happened, they found out 20 percent total phenol adsorption was chemisorption and to desorb this amount, the temperature was increased to more than 800 °C (Tancredi et al., 2004).

Carvalho et al. (2006) granulated cork waste which was activated through the chemical method using potassium carbonate (K_2CO_3). They mixed activated carbon with different amount of binders, montmorillonite, and laponite which are two different types of clay. After mixing with the water, they passed the dough through an extruder to produce extrudates with 4mm diameter and 9mm length and calcinated them under N_2 at different

temperatures. They studied the effect of binders' quantity and calcination temperature on BET surface area and thermal and mechanical stability of granular activated carbon. To investigate the thermal resistance of extrudates, they increased the calcination temperature to 600 °C and found that the adsorption capacity remained unchanged. For mechanical strength, they measured the number of impacts required for breaking the granules by dropping from a 50 cm height into a steel pan; more than 25 drops considered to be satisfactory. The study shows that the calcination at lower temperature gives a better strength than at higher temperature and the ideal temperature was 300 °C. On the other hand, the extrudates were immersed in the water and found out that the only extrudates which remained aggregate were the ones with the calcination temperature above 400 °C (Carvalho *et al.*, 2006).

Liu et al. (2014) used calcium sulfate as a binder and activator to produce granular activated carbon out of sewage sludge. For granulation, they extruded 5-40% of binder mixed with raw carbon following activation at different times, temperatures, and temperature increasing rates. They used the gained product to adsorb methylene blue (MB) to estimate mesoporous structure. For activation temperature, they stated that increasing the activation temperature up to 700 °C would lead to better MB adsorption due to more burn-off and pore widening. However, after 700 °C pore blockage and pore widening to produce macro-pores led to a decrease in MB adsorption. Increasing the binder amount up to 30% led to a better MB removal which indicates the importance of binder (calcium sulfate) activation. However, after 30% pores were further widened causing a decrease in the mesopore area. According to their results, increasing activation time up to 1 hour led

to a better MB adsorption, whereas further increase would cause pore blockage and macropore production and a decrease in the MB adsorption. It was concluded that the slow heating rate was better for mesopore production than fast heating rate; however, energy consumption at a slow heating rate can be an issue (Liu *et al.*, 2014a).

Liu et al. (2014b) also studied the effect of different binders in the granulation process of sewage sludge. They used different binders including starch, CMC, sodium silicate, calcium sulfate, and no binders for their tests and compared the porous properties and specific surface areas of the test samples. For their granulation they first dried the sludge, crushed and sieved it into less than 2 mm diameters. Then they mixed the powder with binders in an optimized binder to carbon ratio of 10:30. In the next step, they passed the paste through an extrusion with the product extrudates of 4 mm in diameter and 9 mm in length. In the last step, the extrudates were activated at 700 °C. It was concluded that extrudates with starch as a binder had the highest surface area which showed that the organic binders are beneficial for pore structure (Liu *et al.*, 2014b).

Clark and Marsh (1989) studied the effect of breeze (recycled or broken carbon briquettes) addition and the size (<3.35 mm or <1.7 mm) of high-rank coal as raw material to increase the strength of produced granular activated carbon. In this regard, they used high-rank coal and pitch for the binder. For their granulation, they added 7% of the binder to the raw material and pressed 40 g of the blend in a cylindrical mould for 1 second. The carbonization step was at 1070 K. As a result, they found out that although it is economically desirable to add breeze (recycled carbon briquettes) to the blend, after carbonization the strength of the briquettes decreased by increasing the level of the breeze.

They also concluded that finer crushing would decrease the chance of interaction between carbon and binder and would result in soft granular carbon. On one hand, the smaller size of coal would lead to a higher surface area, but the strength of the developed GAC would decrease (Clarke & Marsh, 1989).

Sun et al. (1997) produced granular activated carbon from coal using hydraulic pressure while measuring different factors such as BET surface area, mesopore formation, and bulk density of products. The first factor was pre-oxidizing raw carbon before activation using air at 225 °C. They found out that the pre-oxidization would give a high volume of mesopores, high bulk density and, better capacity to adsorb methane rather than no oxidization. The second step was to find out the differences between CO_2 activation and steam activation which was lower BET surface area and micropore volume for CO_2 activation. The third step was the difference between physical activation and chemical activation which turned out that chemical activation resulted in a better BET surface area and micropore volume and lower bulk density. In the last step, they found out the combination of chemical and physical activation can result in lower micropore volume and bulk density rather than steam activation to produce granular activated carbon (Sun *et al.*, 1997).

Johns et al. (1998) examined the effect of oxidization on granular activated carbon for heavy metal removal. In this regard, they used sugarcane molasses as the binder in different ratio mixed with the agricultural by-products such as rice straw and peanut shell. After pelletizing, activation was done under carbon dioxide or steam. Oxidation was either physical or chemical; physical oxidation was under a mixture of O_2 and N_2 at 300 °C, and

chemical oxidation was with ammonium persulfate ($(NH_4)_2S_2O_8$). They concluded that neither carbon dioxide nor steam helped in the heavy metal removal, whereas physical oxidation increased the capacity for heavy metal removal. Chemical oxidation did not help regarding heavy metal removal (Johns *et al.*, 1998).

Pendyal et al. (1999a and 1999b) used rice hulls, rice straw, and sugarcane bagasse to produce granular activated carbon. They studied the effects of the amount of binders including coal tar, sugarcane molasses, sugar beet molasses, and corn syrup on surface properties and sugar colorants adsorption. For the granulation process, they crushed raw materials to 5-10 mesh size and mixed them with binders at the carbon to binder ratio of 1:1 and 1:0.5. Then they placed the blend in a stainless-steel cylinder of 5.7 cm diameter and 0.7 cm height. Hydraulic pressure of 7000 psi applied for 5 minutes to form briquettes. Briquettes were pyrolyzed under nitrogen flow at 700 °C for 1 hour. The products were crushed and sieved to 12-40 mesh size and used for activation. As a result, they found out that the highest surface area produced with the mixture of sugar bagasse with beet molasses at the ratio of 1:1. Also increasing the burn-off to 40-50% during activation would lead to pore enlargement. They also found out that the role of binders in defining chemical and physical characteristics of GACs including pH, bulk density, and hardness is far more important than the role of raw materials. In another article, they mentioned the use of the produced GACs in removing sugar colorants from the water. In contrast to previous research, they found out that the removal ability of GACs is more dependent to raw materials rather than any binder (Pendyal *et al.*, 1999b, Pendyal et al., 1999a).

Rubio et al. (1999) used a slightly different method to produce granular activated carbon from low-grade coal char using pitch as the binder. In this method, they first pyrolyzed the char under nitrogen at different temperatures (500,700,850 °C) and then carbonized product was mixed with different amounts of pitch (10-25% by weight), and the blend was pressed for 4 minutes. The resultant briquettes were then oxidized with steam at 200 °C and activated under different temperature (500 and 700 °C) for 2 hours. To determine the best condition to produce GAC, the conducted mechanical strength test by dropping granules repeatedly onto a concrete floor from 2m height and the number of drops and pieces after breakage was counted. The results showed mechanical strength is highly dependent to pyrolysis temperature and pitch content. High temperature (700 °C) and a minimum of 18% pitch can lead to significantly strong granules (Rubio *et al.*, 1999).

Ahmedna et al. (2000) used sugar cane bagasse to produce granular activated carbon. Natural binders such as corn syrup and coal tar pitch were used, under physical activation process. For granulation, they mixed sugar cane with binders at ratios of 1:1 and 1:2 (binder to carbon) and activated the briquettes under CO_2 at 900 °C. The percent of weight loss tested mechanical stability of produced GACs after dropping the extrudates from 50 cm height for 30 times was calculated. Their study shows that mixing sugarcane bagasse with corn syrup at the ratio of 1:1 would lead to larger surface area ($337 m^2/g$), well-developed macro and mesopores and minimal surface charge (Ahmedna *et al.*, 2000).

Lozano et al. (2002) used six different binders with powder activated carbon to produce microporous granular activated carbon for methane removal. They studied the effect of each binder including a humic acid-derived sodium salt (HAS), polyvinyl alcohol

(PVA), phenolic resin, Teflon, adhesive cellulose-based binder and, a commercial binder (WSC) on Porous texture of granules. The study shows that the phenolic resin, Teflon, adhesive cellulose and, WSC caused the least pore blockage. PVA and HAS led to considerably low removal capacity. The amount of pore blocking binders for different ratios was studied, and it was concluded that using 15% of binders in the mixture can lead to high-density granules with significant mechanical strength and high methane delivery value (Lozano-Castelló *et al.*, 2002). The same method was applied by Balathanigaimani et al. (2009) using PVA, CMC (carboxymethyl cellulose), and PVP (polyvinyl pyrrolidone) as binders. The study shows that using 5% CMC would give the least surface area reduction with the highest package density (Balathanigaimani *et al.*, 2009).

Deiana et al. (2004) used an experimental design to study the effect of particle size, types of binder, different char to binder ratio, the pressure at conformation, heating rate, oxidation, activation temperature, activation time, and water rate on granulation. For this study, Eucalyptus wood was used as raw material and grape must, asphaltic paint, and asphaltic emulsion as binders. For granulation two different sizes (mesh 20 and 80) of raw materials were mixed with the binder at 3:1 and 4:1 ratio and pressurized the blend at 140 or 280 MPa. The briquette was then activated under steam and N_2 at the heating rate of 5 to 15 K/min, the temperature of 1123 K and 1153 K with 1 and 0.7 gram of steam per gram of char at each hour for 105 and 150 minutes. Some briquettes were cured under O_2 at 473 K for 2 hours. For characterization, they used BET and impact resistance to find the optimum situation of granulation. The study shows that the BET would increase with temperature and contact time and slow heating rate a more significant amount of binders

and larger particle size. For impact resistance tests, the study shows that more binder with higher pressure would lead to a high strength briquette. The study also concludes that the granulation with grape must would cause the minimum decrease in the surface area compared with the non-briquettes situation (Deiana *et al.*, 2004).

Amaya et al. (2007) mixed wood and rice husk with "grape must" (fruit crush), to produce granular activated carbon. For granulation hydraulic pressure followed by steam activation for 2 hours was used. The effect of activation time (105 and 150min), activation temperature (880 and 920 °C), and steam flow (1.7 and 2.5g steam/g char) on BET surface area and mechanical strength were studied. The study shows activation at the higher temperature for more amount of time and a higher flow of steam, would result in better surface area but decreasing the mechanical stability a. Moreover, they realized that increasing time and steam flow at the lower temperature is more effective than increasing at the higher temperature (Amaya *et al.*, 2007)

Smith et al. (2012) used waste sewage sludge to produce granular activated carbon. In this study, several types of binders (polyvinyl alcohol (PVA), CMC, phenolic resin, calcium salt) were used to produce attrition-resistant GACs. For granulation, both extrusion and compaction were employed to assess the effectiveness. As a result, they found out that the choice of binder affects characterizations including hardness, surface chemistry, and methylene blue adsorption. They realized that by raising the concentration of hydroxyl groups, (PVA) on the surface would lead to more methylene blue adsorption. Ultimately, palletization, using hydraulic compaction, would result in a better BET surface area and

harder granules than extrusion. Also, using extrusion with most of the binders did not yield cohesive pellets (Smith *et al.*, 2012).

2.3 Factors Affecting Natural Organic Matter Removal by Activated Carbon and Design of Experiment

Different research groups studied factors affecting NOM adsorption from water using activated carbon. Characteristics of the adsorbent and adsorbate and solution chemistry such as contact time, pH, and temperature are some of the factors influencing NOM adsorption from water (Moreno-Castilla, 2004). These factors are briefly discussed in the following section.

2.3.1 Activated Carbon Properties

Activated carbon pore size distribution and surface charge are two important characteristics of carbon that would affect the adsorption of NOM (Moreno-Castilla, 2004). Micropores with a diameter less than 1 nm would get blocked with large molecules of NOM and are not efficient for NOM removal. On the other hand, mesoporous and macroporous carbon are suitable for NOM removal. A study by Velten et al. (2011) showed that GACs with the pore size distribution of 1-50 nm (mesopores and macropores) are capable of NOM removal while smaller pores are not efficient (Velten *et al.*, 2011).

NOM is generally divided into three different fractions: 1) Dissolved Organic Matter (DOM) which are soluble in water and consists of carbohydrates, fulvic acid, and proteins. 2) acid hydrolysis groups such as hemicellulose, cellulose, and fats. 3) non-hydrolysis group including lignin and humic acids (Kosobucki & Buszewski, 2014). Most NOM molecules have negative charges, and carbon surface charge (negative, positive, or neutral) can play an essential role in NOM removal efficiency (Bjelopavlic *et al.*, 1999).

2.3.2 NOM characteristics

Removal of NOM from water and its efficiency is strongly dependent on the size of NOM molecules and activated carbon's pore size distribution. NOM's molecules larger than carbon's pore would not be adsorbed to carbon or can block the carbon pores. On the other hand, as discussed in section 2.3.1, the charges and functional groups on NOM and carbon surfaces play a significant role in the NOM removal (Newcombe *et al.*, 2002). The study of Velten et al. (2011) showed that NOM with high molecular weight like biopolymers could not be adsorbed on GACs while small NOMs can irreversibly be removed from water (Velten et al., 2011).

2.3.3 Contact time

At the beginning of the adsorption process, a large number of vacant sites of adsorbent are available for the adsorbates. In this regard, adsorbates' uptake is swift at the early stage of the adsorption. However, after a lapse of time, vacant sites are unavailable

or occupied by adsorbates, and the adsorption rate would decrease. Moreover, repulsive forces between adsorbates on the surface of the adsorbent and adsorbates on the bulk phase is another reason for the decrease in the adsorption rate. This stage is known as equilibrium (Ho & McKay, 1998).

Influence of contact time can be distinguished by studying batch and column tests, simultaneously. Research of Schreiber et al. (2005) at 35 °C in batch and column tests show that the capacity of adsorption in batch experiments after 3000 minutes of contact time is much higher than in the column tests (Schreiber *et al.*, 2005).

2.3.4 Temperature

There are few researched regarding the effect of water temperature on NOM adsorption. Adsorption process in overall is considered as an exothermic process with an increase in the adsorption capacity by decreasing temperature (Radeke & Hartmann, 1991). El-Demerdash et al. (2015) used rice husk as raw material to remove NOM from water at the temperature range of 18-31°C and found out that increasing the temperature would decrease the adsorption because of the exothermic nature of physical adsorption (El-Demerdash *et al.*, 2015). On the other hand, the NOM adsorption increases by increasing the solution temperature. Schreiber et al. (2005) used GAC to remove NOM from water at the temperature of 5, 20, and 35 °C and they found that 35 °C is the most effective temperature to remove NOM from the water. They used a size exclusion chromatography and found out that increasing temperature would increase the adsorption of finer parts of

the dissolved organic matters (Ahmedna et al., 2000). Summers and Roberts (1988) removed humic substances within 1-41°C and found out that the increase in the water temperature would increase adsorption. They claimed that faster diffusion and hence, faster mass transfer at higher temperature led to better adsorption at the higher temperature (Summers & Roberts, 1988).

2.3.5 pH

The concentration and characterization of NOM in water are dependent on NOM source. Most of the NOM compounds in water carry negative charges due to the presence of carboxylic acid (Newcombe et al., 2002). Therefore, activated carbon with positive surface charge may favor the adsorption. pH is a factor that can control the adsorption process through electrostatic interaction between activated carbon and NOM. In the research of Catilla (2004), acidic pH was favored for phenol uptake due to better interaction between negatively charged phenol and positively charge activated carbon (Moreno-Castilla, 2004).

2.3.6 Experimental Design

A process is including of all methods, machines, resources, and factors that would transfer some input to output using response variables. While studying a process, experiments would take place to 1) determine the most influenced variables, 2) set the influenced variables to a fixed value to achieve the desired response, and 3) find a value of most effective factors in which a response would be maximized or minimized. Usually,

several factors would affect an experiment and depend on method, a different number of experiments should be done to find a desirable response (Montgomery, 2017).

One method to study a process is by using the one-factor-at-a-time (OFAT) approach. In the OFAT approach, a boundary or set of levels for each factor would be selected, and then each factor would vary while other factors are held constant. Interpretation for OFAT is straightforward and easy. However, OFAT approach has a disadvantage of being time-consuming and cost-intensive, as well as not considering the interaction between factors; Interaction of factors means that one factor would have opposite effects on response at the different level of another factor (Montgomery, 2017).

Response surface methodology (RSM) is a statistical technique that can be used to study the relationship between factors and responses. This method uses quantitative data from a set of experiments and determines regression model equations (Alam *et al.*, 2007). RSM is a technique for analysis of problems in which several variables would influence the response of interest, and this method can be used to optimize effective parameters (Sahu *et al.*, 2009, Vepsäläinen et al., 2009).

2.3.7 Analysis of Variances (ANOVA)

Analysis of variances (ANOVA) is a method to determine if a hypothesis of experiments with the specific response is acceptable. ANOVA is a valid analysis in experiments with more than two factors. ANOVA is a summary of test procedure which defines all the statistical models and differences of each factor used for analysis

(Montgomery, 2017). ANOVA divides a set of observation into distinct components which are summarized as follow. For comprehensive understanding, please refer to Design and analysis experiments by Douglas C. Montgomery.

- Sum of Squares: is a summation of all observations from their average point and it is calculated according to Equation (2.1), where y_{ij} is the ij$_{th}$ observation and $\bar{y}$ is an average value.

$\mathbf{SS= \sum_{i=1}^{a} \sum_{j=1}^{n} (y_{ij} - \bar{y})^2}$	**(2.1)**

- Mean Square: in statistic methods, a mean square is the average of squared errors.
- F Value: Mean Square for a term divided by Mean Square for the residuals is called F value and is a test to compare the variances of a term associated with variances of residuals.
- P Value (Prob>F): P value is a probability value and is associated with F value. This term determines the chance of getting a size of F value with no effect on a response. In general P value for a term smaller than 0.05 is considered as significant effect while P value of a factor greater than 0.1 is regarded as a not-effective factor (Montgomery, 2017).

2.4 Activated Carbon Regeneration

One major advantage of GACs over PACs is the feasibility of recycling and regeneration. During the adsorption process, adsorbate's molecules would block pores of activated carbon. As a result, to desorb these molecules in the spent GAC with high capacity, pore widening would be necessary. In this regard, regeneration of spent carbon is not necessarily desorption of adsorbed pores, but a restoration of activated carbon capacity. Thermal regeneration is the most common technique to regenerate activated carbon. This method includes thermal desorption of adsorbates following by steam or CO_2 reactivation (Guimont, 1980).

Three different parameters including adsorption capacity, hardness, and mass loss of regenerated carbon can be used to evaluate the efficiency of activated carbon. During regeneration, carbon burn-off would lead to mass loss, and fresh carbon would be added to make up the loss (Lambert *et al.*, 2002). To have regenerated carbon with high restored capacity, different regeneration conditions should be applied. Most effective factors in regeneration are time, temperature and gas flow (Zhang *et al.*, 2009). Duan et al. (2012), Xin-hui et al. (2014), and Cazetta et al. (2013) showed that increasing time, temperature, and gas flow would not necessarily obtain the best regenerated GAC with highest adsorption capacity since the structure of carbon at high level of regeneration would change (Duan et al., 2012, Xin-hui *et al.*, 2014, Cazetta *et al.*, 2013).

According to previous studies, it is obvious that using response surface methodology and design of experiments for NOM removal was hardly noticed. In addition,

using different binders and solvents specially bitumen and hexane for producing granular activated carbon was not used in previous researches. The key differences of current study with previous researches are the specific use of versatile binders for GAC production and DOE application for NOM removal. Moreover, treating drinking water of Pouch Cove community was another use of this study.

Chapter 3 Experimental Methods

In this chapter, experimental procedures and analytical techniques used for water treatment using granular activated carbon is discussed. The first section of the chapter is about sample collection, preservation and characterization while the second section deals with the development of adsorbents including cleaning, activation, and characterization. The third section covers experimental techniques, and the last section is on the adsorption study.

3.1 Water Collection and Characterization

3.1.1 Water Source

St. John's is the capital city of Newfoundland and Labrador, and according to Statistics Canada, the city has a population of 206,000 as of 2016 (Statistics Canada, 2016). The province has about several small communities, one of such communities is Pouch Cove covered in this study.

Pouch Cove is a community with about 2100 people. This community is located 27 km north of St. John's. In Figure 3-1, the locations of St. John's and Pouch Cove are shown. The main intake source for the drinking water in the Pouch Cove community is from North Three Island pond (Figure 3-2). The pond water pH before entering into the distribution systems is adjusted between 6.5 and 8.5 using Soda ash and then chlorinated. Since there is no treatment to reduce NOM concentration in water, DBPs in drinking water are high

(average of 206 µg/L of HAAs and 200 µg/L of THMs) while the Health Canada guideline is 80 µg/L for HAA and 100 µg/L for THM (Municipal Affairs and Environment-Government of Newfoundland and Labrador, 2018, March 13).

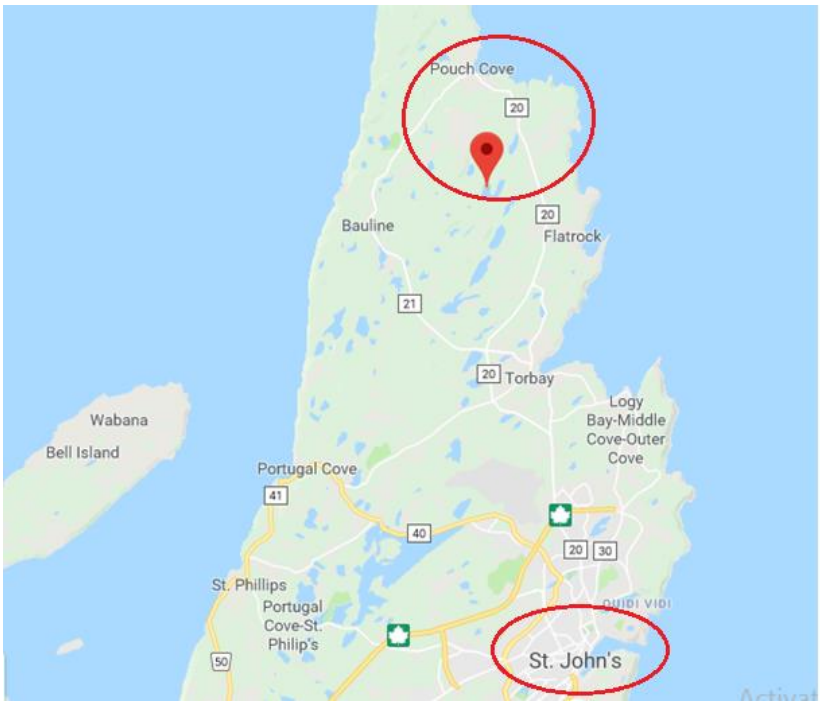

Figure 3-1: Location of St. John's and Pouch Cove

Figure 3-2: North Three Island Pond, Pouch Cove, NL

3.1.2 Water Characterization

Water samples, after being taken from the lake, were stored in a refrigerator under 4 °C. All bottles and lids were washed with detergent and rinsed with distilled water several times before water collection. Before water collection, 100 mg of ammonium chloride (NH_4Cl) per liter of sample water was added to remove residual chlorine (Kim *et al.*, 2003). For testing, the required amount of water was taken out of the refrigerator and before any action, the water was passed through a 0.45 µm membrane filter to remove suspended organic carbons. Organic molecules remaining in the water after passing through the membrane are called Dissolved Organic Matter (DOM) (Kolka *et al.*, 2008). Water samples were characterized regarding pH, initial TOC, and UV_{254}.

- **pH**

The Mettler Toledo pH meter, model EL20 was used for water sample pH determination. The buffer solution of pH 4.0, 7.0 and 10.0 have been used for calibration before pH measurement.

- **Total Organic Carbon (TOC)**

TOC was measured using TOC analyzer, TOC-L CPH/CPN model. In the analyzer, NPOC (non-purgeable organic carbon) measurement which is the most common method for environmental purposes was used. In this method, the water sample is acidified, and through a sparging process, inorganic and purgeable organic carbons are removed. Purified air is a carrier which leads the organic carbons to a combustion chamber at 680 °C where organic carbons are converted to CO_2 using platinum catalysts. Carbon dioxides generated under oxidation are detected using an infrared gas analyzer (Shimadzu, Mandel Scientific).

- **Ultraviolet Absorbance**

Ultraviolet (UV) visibility operates under Beer-Lambert law; when a beam of light passes through a transparent cell containing a liquid with absorbing particles, the intensity of light may reduce due to reflection, scattering or absorption. UV instruments measure the intensity of lights in the ultraviolet-visible region (Beckett & Stenlake, 1988). In the water treatment industry, to monitor the concentration of dissolved organic matter, light

absorbance at 254 nm is found to be useful (Morrow & Minear, 1987). For this study, Genesys 10S UV-Vis from Thermo-Scientific was used.

- **Elemental analysis**

One of the water characterization tests was to determine different elements existed in the water. For this, ICP-MS analyzer (Quadrupole Inductively Coupled Plasma Mass Spectrometer), model ELAN DRC II of Perkin Elmer manufacturer, was used. The ELAN DRC II analyzer uses reaction gases such as ammonia, methane, or oxygen to remove interference substances to improve the detection limits. After the reaction of substances with reaction gas in Dynamic Reaction Chamber (DRC), the ions beam would enter the mass analyzer for mass detection (Sample).

3.2 Adsorbents Preparation and Characterization

3.2.1 Carbon Source

Corner Brook Pulp and Paper (CBPP) mill located in the west coast of Newfoundland and Labrador was founded in 1927. This industry uses the thermal and mechanical pulping process to produce 700 metric tons of newsprint per day. CBPP plays a significant role in the economy of the western Newfoundland. This incorporation annually produces around 10,000 metric tons of boiler ash which is a valuable source for carbon (Levesque *et al.,* 2010). In this research, CBPP fly ash was used as the source of carbon to produce powder and granular activated carbon.

3.2.2 Powder Activated Carbon Production

- **CBPP pretreatment**

CBPP is a source of carbon with high carbon content. However, some impurities such as aluminum, magnesium, manganese, and calcium in low concentration exist in the source. The existence of impurities is not desired in the preparation of activated carbon due to obstruction of pore development (Yeganeh *et al.*, 2006). The pretreatment of ash should, therefore, be performed before activation.

Raw CBPP was sieved using a 30-mesh screen (U.S sieve series) to remove larger particles and then crushed in a Siebtecknik puck mill for 20 seconds. The ground sample was then washed with 5% HNO_3 at the ratio of 10 mL of acid per g of carbon at 80°C for 2-3 hours to remove volatile organic compounds (VOCs) and other impurities. In the end, the sample was repeatedly washed with distilled water until reaching neutral pH value. The cleaned sample was then dried at 110 °C overnight. The obtained product is called washed CBPP in this study.

- **CBPP activation**

In this study, the two-steps method as mentioned in section 2.2 for preparing activated carbon was used. Physical activation using the mixture of steam and CO_2 as oxidizing agents was considered for PAC preparation. Both carbonization and activation carried out in a vertical programmable furnace (Carbolite Gero Manufacturer model) with high control accuracy to reach critical temperatures.

For pyrolysis, 15 g of washed CBPP was placed in the furnace's tube. The temperature was then increased to 850 °C at the rate of 15 °C/min and held for 1 hour. Nitrogen gas flow was passed through the furnace at the rate of 500 cm^3/min to remove the air in the tube and organic matters of the sample. Then nitrogen flow switched to CO_2 and steam at the rate of 500 cm^3/min for 2 hours to develop the pore structure and carbon burn off. In the end, the tube cooled down to room temperature, and carbon was weighed. The obtained product of activation is called PAC in this study.

Carbon burn-off was calculated according to Equation (3.1).

$$\textbf{Burn off (\%)}=\frac{w_1-w_2}{w_1}\times 100 \quad (3.1)$$

Where:

W_1= weight of washed CBPP before activation

W_2= weight of PAC

3.2.3 Granular Activated Carbon Production

Raw CBPP, washed CBPP, and PAC were used to develop granular activated carbon. Five different binders including Carboxymethylcellulose (CMC), polyvinyl alcohol (PVA), Calcium sulfate (CS), sodium carboxymethylcellulose (S-CMC) and bitumen are commonly used to produce GAC. Mixing PAC with binders did not require heat treatment while using raw and washed CBPP, additional calcination step was needed (Machnikowski et al., 2010).

CMC, PVA, CS, and S-CMC were mixed with PAC, raw, and washed CBPP at the binder to carbon ratio of 10:90, 20:80, and 30:70. Then water was added to the mixture until a homogeneous paste was produced. The paste was then put in an extruder with 3mm diameter and extrudates were cut to 5-7 mm long. The extrudates were put in the oven (105 °C) to dry overnight. In case of using bitumen as a binder, hexane was used as the solvent and extrudates were put under the fume hood to dry.

Calcination and activation temperature, time, and heating rate would affect the chemical nature of the binder and quality of the produced GAC (Rubio et al., 1999). Besides these factors, the amount of binder would affect hardness and compressive resistance of the granules as well as its surface area and adsorption capacity. To study such effects, the different binder to carbon ratio were considered in this study (Rubio et al., 1999). Moreover, the steam temperature was considered as another factor to obtain high quality and efficient granular adsorbent. The range for each factor are summarized in Table 3-1. Literatures, different researches, and previous experiments have been applied to determine the range of the granulation process.

Table 3-1: Variables and their ranges for granulation study

Variable	Range
Activation and calcination temperature	750, 850, 950 °C
Activation time	1, 2, 3 hr
Heating rate	5, 10, 15 °C/min
Binder to carbon ratio	10:90, 20:80, 30:70
Steam temperature	60, 70, 80 °C

3.2.4 Adsorbent Characterization

Activated carbon is a common filtration media with high surface area and effective capacity to remove impurities from water. Source of raw carbon has a significant role in the characterization of the final product (DeSilva, 2000). Moreover, characterization of the final product has a great effect on the efficiency of water treatment. To assess the removal of impurities and get clean carbon of acceptable quality, different characterization tests were conducted on raw and washed CBPP, PAC, and GAC which are mentioned in follow.

- **pH**

ASTM D338-05 method was used to determine the pH of raw and washed CBPP, and PAC. For this, 10.0 g of the sample on a dry basis was used, and 100mL of boiled water was added to the carbon. The solution was boiled for 4minutes and filtered. The filtrate was cooled to 50 °C and pH was determined using a pH meter (Mettler Toledo, Education series EL20).

- **Moisture Content**

The moisture content of raw CBPP was determined according to ASTM D2867-09 (2014). According to the method, first, a dried crucible with lid was weighed. Then, 1-2 g of carbon was put into the crucible in such a way that its depth should not exceed 1.25 cm and then the filled crucible with lid was weighed and put in the oven with 110 °C for 3

hours. After cooling down in a desiccator, the dried sample, crucible and lid was weighed. The moisture content had been calculated by Equation (3.2).

$$\textbf{Moisture content, wt\%} = \frac{(\boldsymbol{C}-\boldsymbol{D})}{(\boldsymbol{C}-\boldsymbol{B})} \times \mathbf{100} \quad (3.2)$$

where,

C= weight of crucible + cover + original sample,

B= weight of crucible + cover,

D= weight of crucible + cover + dried sample.

- **Ash Content**

ASTM D2866-11 describes a procedure to determine the ash content of activated carbon. According to this method, an empty crucible was heated in a furnace at 650℃ for an hour to remove all impurities. After cooling down, around 2 g of dried raw CBPP, washed CBPP, and PAC samples were put in the crucible and burned in a furnace at 650°C for 16 hours. After cooling down in a desiccator, the crucible with the ash was weighed, and the ash content was calculated using the Equation (3.3).

$$\textbf{Ash content, wt\%} = \frac{(\boldsymbol{D}-\boldsymbol{B})}{(\boldsymbol{C}-\boldsymbol{B})} \times \mathbf{100} \quad (3.3)$$

where,

B= weight of dried crucible,

C= weight of crucible + original sample,

D= weight of crucible + ash

- **Iodine Number**

Amount of iodine that has been adsorbed by 1g of carbon is called iodine number. This number shows a rough estimation of the microporosity of carbon. According to ASTM D4607-11, to determine the iodine number, first required amount of carbon (raw CBPP, washed CBPP, PAC, and GAC) was weighed; in case of testing GAC, a representative sample was ground until 95% of the sample passed through a 100-mesh screen (U.S. sieve series). Then, 10 mL of 5% HCl was added, and the solution was boiled for 30s. In the next step, 15 mL of iodine solution was added to the mixture and stirred for 15 minutes at 200 rpm. In the end, the solution was filtered, and 10mL of the filtrate was titrated with Sodium thiosulfate. Starch was the indicator for the titration. Iodine number is then calculated using Equation (3.4).

$$\mathbf{IN}= \frac{[(\boldsymbol{C_0}\times\boldsymbol{V_0})-(\boldsymbol{C_1}\times\boldsymbol{V_1}\times\boldsymbol{DF})}{\boldsymbol{M_C}} \times \mathbf{126.9} \quad (3.4)$$

where,

IN= Iodine number, mg/(g of carbon)

C_0= Concentration of iodine solution, 0.1 N

V_0= Initial volume of iodine solution, 15 mL

C_1= Concentration of sodium thiosulfate, 0.1 N

V_1= Volume of sodium thiosulfate used for titration, mL

D_F= Dilution factor, 15/10

M_C= Weight of carbon, g

- **Methylene Blue Number**

Methylene blue, as an organic dye, has a diameter of more than 1 nm. In connection with this fact, mesoporous carbon is more advantageous to remove methylene blue from water than microporous carbon. In other word, methylene blue is an indicator of the activated carbon mesoporosity. Generally, activated carbon with methylene blue adsorption over 200 mg/g is considered an excellent mesopore carbon (Yan *et al.*, 2009).

In this study, GB/T 7702.6 (2008) method is used to determine the methylene blue number (MBN). According to this method, 15-20 mL of methylene blue stock solution was added to 0.1 g$\pm$0.001 of raw CBPP, washed CBPP and PAC and ground GAC. The mixture was shaken at 150 rpm for 30 minutes and then filtered using 10 µm filter paper. The filtrate was diluted for 200-500 times, and the adsorption was determined using UV spectrophotometer at 665 nm.

- **Elemental Analysis**

Elemental analysis was performed to determine the concentration of major elements in the raw and washed CBPP, PAC, and GAC. Microwave-assisted acid digestion followed by ICP-MS examination was used to trace elements concentrations, specifically heavy metals, in representative samples. In this regard, ICP-MS, model ELAN DRC II of Perkin Elmer manufacturer, was used.

- **Hardness**

The most important factor to define a good GAC is its hardness. There are several methods to determine the hardness for GAC. Ball pan hardness method (ASTM D3802-16) was used in this study. To determine the hardness number, 2 g of 40-mesh screened GAC was put in a beaker and 10 glass marbles (15mm diameter, 5 g each) was added. The beaker was capped with an aluminum foil and stirred at 200 rpm for 20 minutes. The obtained material was sieved using the same mesh-screen, and the retained material was weighed, and the hardness number was calculated using Equation (3.5) below (Ahmedna *et al.*, 1997).

$$\textbf{Hardness number} = \frac{(\boldsymbol{weight\ of\ carbon\ retained\ on\ the\ mesh-screen})}{\boldsymbol{initial\ sample\ weight}} \times \mathbf{100} \qquad (3.5)$$

- **BET surface area and pore size distribution**

Activated carbon's surface area and pore size distribution are two important properties that can determine the capacity of the adsorbent. Pore size distribution can determine what size and shape of a given pollutant can be adsorbed by activated carbon (Pelekani & Snoeyink, 2000). BET surface area and porosity of PAC and GAC were measured by N_2 adsorption at 77 K using 3Flex Surface Characterization Analyzer from Micromeritics Instrument Corporation. Equation (3.6) to Equation (3.10) have been used to determine the surface area (m^2/g).

$$\frac{\mathbf{1}}{\boldsymbol{v}(\frac{\boldsymbol{P_0}}{\boldsymbol{P}}-\mathbf{1})} = \frac{\mathbf{1}}{\boldsymbol{v_m c}} + (\frac{\boldsymbol{c}-\mathbf{1}}{\boldsymbol{v_m c}} \times \frac{\boldsymbol{P}}{\boldsymbol{P_0}}) \tag{3.6}$$

$$\boldsymbol{v_m} = \frac{\mathbf{1}}{\boldsymbol{S}+\mathbf{1}} \tag{3.7}$$

$$\boldsymbol{c} = \boldsymbol{a} + \frac{\boldsymbol{S}}{\boldsymbol{I}} \tag{3.8}$$

$$\boldsymbol{SA_{BET}} = \frac{\boldsymbol{v_m N A_{(N)}}}{\boldsymbol{v}} \tag{3.9}$$

$$\boldsymbol{S_{BET}} = \frac{\boldsymbol{SA_{BET}}}{\boldsymbol{a}} \tag{3.10}$$

Where:

v = volume of adsorbed N_2 gas at standard temperature and pressure (STP)

P and P_0 = the equilibrium and saturation pressures of the adsorbate

v_m = volume of gas required to form one monolayer (STP)

c = BET constant which is related to the energy of adsorption

N = Avogadro's number (6.02E+23)

$A_{(N)}$ = cross section of N_2 (0.162 nm^2),

SA_{BET} = total BET surface area (m^2)

a = mass of adsorbent (g)

S_{BET} = specific BET surface area (m^2/g)

By plotting $1 / v [(P_0 / P) - 1]$ on the y-axis and P/P_0 on the x-axis in the range of $0.05<P/P_0<0.35$, the BET surface was calculated. The slope (S) and the y-intercept (I) of the plot were used to calculate v_m and the BET constant c (Mofarrah, 2014).

3.3 NOM Adsorption in Batch and Column Tests

NOM adsorption was conducted in both batch and column tests. Batch tests are frequently used due to their simplicity and ease of operation. In batch tests, due to high shaking rate, the outer layer resistance is negligible, and the highest adsorption can be achieved. In this study, different conditions for batch adsorption have been considered. Batch tests were also used to determine the isotherm and kinetics of adsorption.

Column test is useful to predict the behavior of adsorption in a continuous flow. In this study, generated GAC were used in the column to determine the breakthrough curve of NOM adsorption.

3.3.1 NOM adsorption: Batch System

In this study, the RSM method was employed to optimize NOM adsorption conditions in the batch system as well as optimizing regeneration conditions for spent GACs in the continuous system. Different factors for each step are reported as follows. In section 2.3, that the effects of different factors including pH, temperature, characteristics of NOM, contact time, and carbon properties on the efficiency of NOM adsorption were discussed (Moreno-Castilla, 2004). In this section, the effect of carbon dose and contact time on adsorption kinetics and isotherm will be described for the experimental setup. Other factors include A: pH, B: temperature (°C), and, C: water volume (mL) were considered as RSM variables. Several runs of pretests were employed to determine the upper and lower levels of each variable. Table 3-2 shows levels of each factor for NOM adsorption in the batch system.

Table 3-2: Factors and levels of experiment

Variable	Lower level	Upper level
A: pH	4	7
B: Temperature (°C)	25	45
C: Water volume (mL)	50	800

The water sample was collected from Pouch Cove pond, transferred to the laboratory, and refrigerated at 4 °C. For NOM adsorption in the batch system, required volume of water passed through 0.45 μm vacuum filtration paper to remove large particles and living microorganism before UV and TOC analysis. Then 1 N HCl and 1 N NaOH, from Sigma Aldrich Canada, were prepared for pH adjustment. A heating plate with a

magnetic stirrer for experiments above 25 °C and mechanical shaker for experiments at 25 °C were used. Then, 0.1 g of produced PAC was mixed with water in a beaker at designed values and stirred for 5 hr at 250 rpm for a complete adsorption until equilibrium. At the end, NOM concentration in treated water were analyzed by TOC and UV analyzer. Adsorption capacity was calculated according to Equation (3.11).

$$\boldsymbol{q} = \frac{(\boldsymbol{C_0} - \boldsymbol{C_1}) \times \boldsymbol{V}}{\boldsymbol{M_C}} \tag{3.11}$$

Where,

q= adsorption, mg/g

C_0= Initial concentration, mg/L

C_1= Final concentration, mg/L

V= volume of water, L

M_C= Mass of carbon, g

3.3.2 NOM Adsorption: Column Test

Column test was designed using a column with a diameter of 2.5 cm and height of 15cm. A scheme of the experimental setup is shown in Figure 3-3. Column test was conducted using the same water as a batch test. 5 cm (8 g), 9 cm (12 g), and 12 cm (17 g) of the column was filled with produced GAC to study the effect of packing height. A flow of 6 mL/min of water samples passed through the column using a peristaltic pump (Fisher Scientific, Variable-Flow Peristaltic Pumps). The advantage of using the peristaltic pump

is that no further contamination would produce in the water sample since water would only pass through a tubing system and would not touch any mechanical part of the pump. Treated water was collected from the column and analyzed for concentration of NOM using TOC and UV analyzer. Table 3-3 shows time and amount of treated water for sample collection.

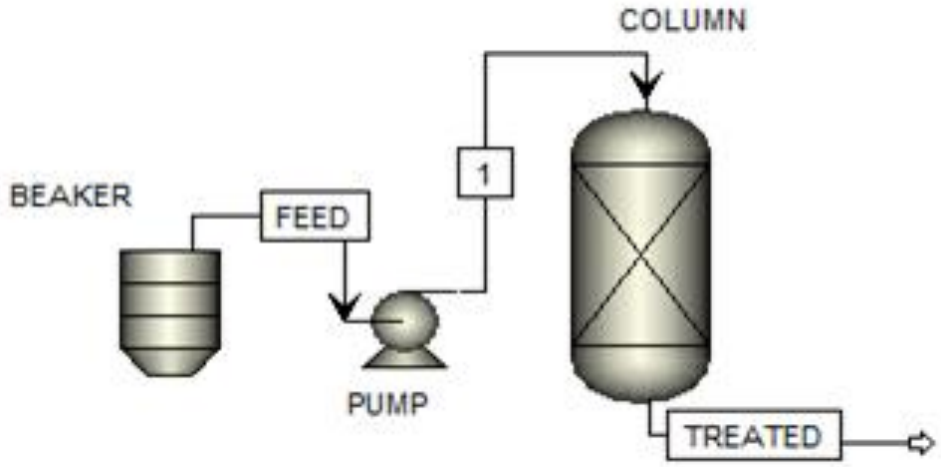

Figure 3-3: Experimental setup for column test

Table 3-3: Sample collection from column test

Time (min)	Treated water (mL)	Time (min)	Treated water (mL)
2	12	**720**	4320
15	90	**900**	5400
60	360	**1240**	7440
90	540	**1575**	9450
120	720	**1800**	10,800
180	1080	**2040**	12,400
360	2160	**2220**	13,320
480	2880	**2340**	14,040
660	3960	**2507**	15,040

3.3.3 Chlorination

Chlorination process is for the purpose of sterilizing and killing pathogenes existing in water. However, disinfectants would reacts with NOM and produce DBPs. DBPs formation in water depends on various factors including NOM and their characterization in water before adding disinfectant and contact time between NOM and disinfectant. In this study, the sample collected from column tests were chlorinated for different contact times to determine the THMs and HAAs formation potential. An attempt was made to maintain the residual chlorine between 0.04-2.0 mg/L in the distribution system according to Canadian guidelines (Health Canada, 2017). Table 3-4 shows the time and amount of treated water for sample collection. THMs and HAAs generated during the chlorination process were analyzed by liquid-liquid extraction, followed by a GC (HP-6890) coupled with a μ-ECD detector (EPA, 1995b, EPA, 1995a).

Table 3-4: Sample collection for chlorination

Time (min)	Treated water (mL)	Chlorination contact time (hr)
60	360	1, 8, 36
180	1080	1, 8, 36
480	2880	1, 8, 36
1300	7800	1, 8, 36
1800	10,800	1, 8, 36

- **HAAs Extraction Method**

To extract HAAs from the chlorinated sample, the following procedure was employed (Domino *et al.*, 2003).

1. Transfer 40 mL of the sample to a 60 mL vial
2. Add 1.5 mL of sulfuric acid (H_2SO_4) following by immediate sodium sulfate addition (16 g).
3. Add 4 mL of methyl tertiary-butyl ether (MTBE)
4. 15minutes shaking on a mechanical shaker at 200rpm
5. Leave for 5 minutes to develop two layers
6. Separate 3 mL of upper MTBE layer to a 15 mL centrifugal tube
7. Add 1mL of 10% of sulfuric acid and methanol solution
8. Place the centrifugal tube in 50 °C water bath for 2 hours
9. Leave the hot tube to adjust to room temperature
10. Add 4 mL of saturated sodium bicarbonate
11. Put the tube on a vortex for 2 minutes

12. Transfer 1 mL of the upper layer to a GC vial and analyze the samples as soon as possible

- **THMs Extraction Method**

To extract THMs from the chlorinated sample, the following procedure was employed (USEPA, 1995).

1. Transfer 40 mL of the sample to a 60 mL vial
2. Spike 3 µL of fluorobenzene into the sample, mix slowly by carefully inverting the vial two times
3. Add 3 mL of MTBE
4. Add 10 g of NaCl and shake the sample vigorously by hand for 4 minutes
5. Transfer 1 mL of upper layer to a GC vial

3.3.4 GAC Regeneration

In section 2.4, it was mentioned that one method for activated carbon regeneration is thermal regeneration which includes thermal desorption of adsorbed substances followed by steam reactivation (Guimont, 1980). Three factors: time of contact, temperature and amount of steam and CO_2 were selected for the RSM method to optimize regeneration conditions. To have a comprehensive study on regeneration, three different responses including MB number, IN number, and hardness of regenerated samples were considered. Several runs of pretests were employed to determine the upper and lower levels of each

variable; 5 different levels in Center Composite design were considered. Upper and lower levels of each variable are listed in Table 3-5.

Table 3-5: Factors and levels of experiment

Variable	Lower level	Upper level
A: time (minute)	30	120
B: Temperature (°C)	650	950
C: steam and CO_2 flow (mL/min)	200	500

3.4 Adsorption Study

The adsorption process is widely used in wastewater treatment because it is a simple, efficient, and economical technique (Largitte & Pasquier, 2016). By studying the adsorption kinetics and equilibrium, important information about designing and operating an adsorption plan would be achieved (Figaro *et al.*, 2009).

3.4.1 Adsorption Kinetic

The kinetic study determines the mechanism and rate of adsorption which is dependent on the concentration of the substance. By kinetic study, the rate of solute uptake would be established which can be used to determine the residence time for completing an adsorption process. Also, kinetic adsorption study can be used to calculate a scale of the adsorption apparatus (Qiu *et al.*, 2009). Adsorption models were developed to describe the kinetic data of an adsorption process (Banat *et al.*, 2003) using most applicable kinetic

models such as pseudo-first-order and pseudo-second-order models which are described below.

- **Pseudo-First-Order**

First order equation is the earliest kinetic model and describes the kinetic process of liquid-solid phase. This rate is based on adsorption capacity and is according to (3.12).

$$\frac{dq_t}{dt} = K_1(q_e - q_t) \quad \textbf{(3.12)}$$

Where q_e represents equilibrium adsorption (mg/g), q_t is adsorption at the time t (mg/g), and K_1 is the rate constant (min^{-1}).

Equation (3.12) can be rearranged to Equation (3.13) in a linear format. By plotting $\ln(q_e - q_t)$ versus (t), a linear plot would be provided in which slope and intercept will give K_1 and q_e, respectively (Figaro et al., 2009).

$$ln\,(q_e - q_t) = ln(q_e) - K_1 t \quad \textbf{(3.13)}$$

- **Pseudo-Second-Order**

  In various studies, this model has been successfully applied for the adsorption of organic compounds, heavy metals, dyes, and oils from aqueous solutions (Qiu et al., 2009).

Pseudo-second-order kinetic model is mathematically expressed in Equation (3.14). In Equation (3.14), t represents the time (minute), q_t is the adsorption at the time t (mg/g), K_2 is the model constant (g/mg.min) and q_e is the equilibrium adsorption (mg/g) and this

equation can be rearranged to linear format in Equation (3.15). By plotting $\frac{t}{q_t}$ versus t, slope and the intercept of the line will give q_e and K_2, respectively (Figaro et al., 2009).

$$\frac{dq_t}{dt} = K_2(q_e - q_t)^2 \quad \textbf{(3.14)}$$

$$\frac{t}{q_t} = \frac{1}{(K_2\, q_e^2)} + \frac{t}{q_e} \quad \textbf{(3.15)}$$

For kinetic study experiments, ten series of beakers with the same volume of water, pH, temperature and amount of carbon were used. The first sample was collected after 15 minutes, the second sample after 30 minutes and the rest after 45, 60, 120, 180, 300, 675, 1440, and 2700 minutes of filtration, and TOC was measured using TOC analyzer.

3.4.2 Adsorption Isotherm

Adsorption isotherm shows the equilibrium between concentration in the fluid phase and the solid phase at a constant temperature. Different typical isotherm shapes are shown in Figure 3-4. Isotherms that have downward concavity are called favorable since they have more capacity at lower fluid concentration. On the other hand, isotherms are convex downward are called unfavorable due to the low capacity of adsorption (McCabe

et al., 1993). Langmuir, Freundlich, and Temkin are favorable isotherms which will be discussed in follow.

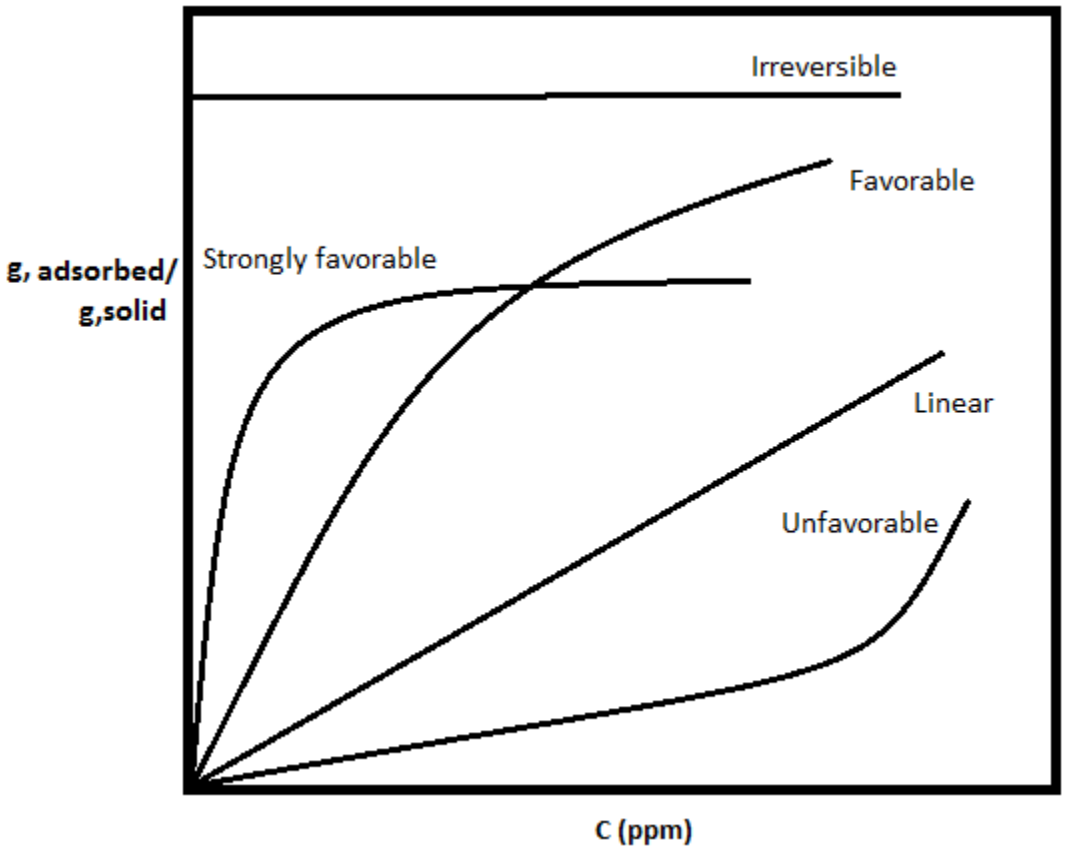

Figure 3-4: Adsorption Isotherms from (McCabe et al., 1993)

- **Langmuir Isotherm**

This model describes monolayer adsorption and can estimate the maximum adsorption capacity. Monolayer adsorption indicates that all adsorbates are in direct contact with adsorbent's surface.

The basic assumptions for this isotherm rather than monolayer adsorption, are constant adsorption potential on an adsorbent surface and no adsorbate existence on the adsorbent surface (Dada *et al.*, 2012). The general form of Langmuir isotherm is shown in Equation (3.16).

$$\boldsymbol{q_e = \frac{q_{max} K_L C_e}{1 + K_L C_e}} \quad \textbf{(3.16)}$$

In Equation (3.16), q_e is equilibrium adsorption (mg/g), q_{max} is the maximum capacity of adsorption (mg/g), K_L is Langmuir equilibrium constant (L/mg), and C_e is equilibrium concentration (mg/L). linear format of Equation (3.16) is according to Equation (3.17) and by plotting $\frac{C_e}{q_e}$ versus C_e, a line would be given. Maximum adsorption and Langmuir constant are slope and intercept of the line, respectively.

$$\boldsymbol{\frac{C_e}{q_e} = \frac{1}{q_{max} K_L} + \frac{C_e}{q_{max}}} \quad \textbf{(3.17)}$$

- **Freundlich Isotherm**

Freundlich isotherm is one of the most practical isotherms and describes adsorption systems with low adsorption capacities (Dada et al., 2012). The empirical equation for Freundlich isotherm is according to Equation (3.18), and its linear format is according to Equation (3.19). Plotting $\ln(q_e)$ versus $\ln(C_e)$ will give a line with K_F (Freundlich constant) as the intercept.

$$q_e = K_F \times C_e^{1/n} \quad \textbf{(3.18)}$$

$$ln(q_e) = ln(K_F) + \frac{1}{n} ln(C_e) \quad \textbf{(3.19)}$$

Where q_e is equilibrium adsorption, C_e is equilibrium concentration, KF and (n) are equilibrium constant. For adsorption from a liquid, n<1 is usually a better fit (McCabe et al., 1993).

- **Temkin Isotherm**

The basic assumption of the Temkin isotherm is a linear reduction in the heat of adsorption, and it implies as Equation (3.20) (Wang & Qin, 2005).

$$q_e = RTb \times ln(K_T C_e) \quad \textbf{(3.20)}$$

In Equation (3.20), R is the universal gas constant (8.314 J/(mol.K)), T is the temperature (K), b and K_T are isotherm constants. Rewriting Equation (3.20) and considering the first term as a constant B, will give a linear format as Equation (3.21) where B is a constant related to the heat of adsorption (J/mol). Plotting q_e versus ln (C_e) gives a line in which B and K_T are slthe ope and intercept, respectively.

$$q_e = Bln(K_T) + Bln(C_e) \quad \textbf{(3.21)}$$

Equilibrium adsorption was determined for six different carbon concentration with the same pH, temperature, and mixing time. The carbon concentration of 0.075, 0.1, 0.15,

0.25, 0.5, and 2 g/L of carbon have been used to determine the equilibrium. The samples were mixed for 5 hours and then filtered using 0.45 µm filter paper to prevent any carbon into the filtrate. The equilibrium concentration curves were developed using a TOC analyzer.

3.5 Quality control

To maintain the accuracy and reduce any errors to the minimum, some actions were taken which are as follow:

1. Water containers and lids were cleaned with laboratory detergents and washed with deionized water for sample collections.
2. In the laboratory, water samples were protected from light and refrigerated at 4°C.
3. Any dishes using for TOC removal were washed according to EPA method (552.2). Beakers, vials, and Erlenmeyer were washed with detergent and rinsed with tap water for 5-7 times followed by rinsing with distilled water seven times. After drying in an oven, all glassware except volumetric flasks were muffled at 400 °C for 1-2 hours. In the end, all dishes were sealed and stored in a clean environment to prevent entering any contaminations (Hodgeson *et al.*, 1995).

4. CBPP activation was done in duplicate, and characterization tests (methylene blue number, iodine number, pH, and ash content) were done in triplicate, and the reported results are the average number.
5. NOM removal tests in a batch system and continuous systems were done in duplicate, and the reported results are the average number.
6. Granulation tests were done in duplicate and reported results including methylene blue adsorption, iodine adsorption, and hardness are the average number.

3.6 Error Analysis

In order to verify the CBPP characterization tests, error analysis was applied on experimental data. For each test, standard deviation was calculated according to Equation (3.22). Standard deviation shows the precision of the measurement. Each data should be reported as mean ± standard deviation.

$$\boldsymbol{S = \pm \frac{\sqrt{\sum(x_i - \bar{x})^2}}{N - 1}} \qquad \textbf{(3.22)}$$

Where:

S = Standard deviation,

X_i = individual measurement,

$\bar{X}$ = mean or average data

$(X_i - \bar{X})$ = deviation from the mean,

N= number of measurements

Chapter 4 Results and Discussion

4.1 Adsorbents Characterization (Powder)

4.1.1 Moisture Content, Ash Content, pH, MB, and IN of CBPP

Table 4-1 shows pH, moisture content, ash content, methylene blue (MB) number, and iodine number for raw, washed, and activated CBPP. As mentioned in the previous chapter, results are the average of triplicate tests ± standard deviation.

Table 4-1: Raw, Washed, and Activated CBPP Characterization

	Carbon Type		
Parameter	**Raw CBPP**	**Washed CBPP**	**PAC**
pH	11.91±0.068	3.2±0.059	7.2±0.002
Moisture Content (%)	1.2±0.01	0.34±0.041	-
Ash Content (%)	11.26±0.032	3.15±0.057	3.4±0.021
MB Number (mg/g)	7±0.037	35.24±0.038	220.4±0.019
Iodine Number (mg/g)	796.11±0.074	925.6±0.069	1301.6±0.045

As listed in Table 4-1, raw CBPP has a basic pH while using nitric acid to remove impurities; the pH is reduced. During activation, all H^+ are separated from carbon, and as shown, the pH of PAC is neutral. Comparing washed CBPP with raw CBPP, it is clear that washing with nitric acid results in lower pH for washed CBPP but higher MB and IN. Due to high impurities in raw CBPP, ash content is relatively high (11%) while after acid washing, the

ash content for acid washed decreased to 3%. This matter leads to better MB and IN for washed CBPP rather than raw CBPP.

4.1.2 Elemental Analysis (major metal content)

To determine the concentration of various elements in raw and washed CBPP samples were weighed and burnt in a muffle furnace for 16 hours until only ash remained. ICP-MS examination with microwave assisted digestion was performed to determine the trace element concentrations. Table 4-2 shows different metals existed in raw and washed CBPP.

Table 4-2: Elemental analysis for raw and washed CBPP

Elements	Raw CBPP (ppm)	Washed CBPP (ppm)	Removal (%)	Elements	Raw CBPP (ppm)	Washed CBPP (ppm)	Removal (%)
Li	4.64	0.68	85.34	**Cu**	29.58	19.8	33.05
Be	0.053	0.013	75.27	**Zn**	74.10	13.76	81.43
B	26.2	2.89	88.97	**As**	0.93	0.18	80.61
Mg	2550.57	1018.66	60.06	**Rb**	23.13	0.93	96
Al	2220.38	743.53	66.51	**Sr**	92.74	25.1	72.94
P	1465.21	187.54	87.2	**Mo**	3.912	3.911	0.009
Ca	25432.69	3458.48	86.4	**Ag**	0.078	0.017	77.94
Ti	155.37	75.29	51.54	**Cd**	0.32	0.036	88.79
V	6.85	1.76	74.38	**Cs**	0.12	0.024	80.45
Cr	14.86	10.5	29.36	**Ba**	116.65	18.97	83.74
Mn	3471.06	758.26	78.15	**La**	2.54	0.43	83.23
Fe	2185.05	966.7	55.76	**Ce**	2.57	0.76	70.32
Co	12.42	0.6	95.2	**Pb**	4.048	0.79	80.6
Ni	8.36	3.84	54.08	**U**	0.17	0.1	39.59

The elemental analysis shows that raw CBPP contains mostly magnesium (Mg), aluminum (Al), phosphorous (P), calcium (Ca), manganese (Mn), and iron (Fe). However, after acid washing the raw CBPP, more than 60% of these elements were removed, and their concentration decreased significantly in the washed CBPP. Comparing the obtained results from Table 4-2 with Table 4-1 confirms the decrease in ash content for washed CBPP from 11.26% to 3.15% and significant improvement in IN and MB numbers.

4.1.3 BET Surface Area and Pore Size Distribution of PAC

BET surface area is an important index of an adsorbent and the higher surface area, the higher capacity an adsorbent has. A test to determine the BET surface area of PAC have been done according to section 3.2.4 and the isotherm curves for adsorption and desorption of N_2 into PAC is according to Figure 4-1. According to IUPAC classification, the isotherm of PAC is a combination of type I and type IV isotherms which is concave to the p/p° axis and approaches a limiting value as p/p° approaches to 1. Type I isotherms shows majorly microporous solids with relatively small external surfaces such as activated carbons and zeolites and Type IV isotherms shows mesoporosity (Harris *et al.*, 1998). Applying Equation (3.6) to Equation (3.10), obtained that the BET surface area of PAC is 565 m^2/g. 3FLEX share software (version 4.04) was used for BET surface area calculations. Also, micropore volume and mesopore volume are 0.28 and 0.169 cm^3/g, respectively.

Density functional theory (DFT) method is used to analyze the pore size distribution of PAC into micropore and mesopore ranges. The model conditions were set to analyze the pore size distribution, and the result is shown in Figure 4-2. According to the figure, it can be seen that the major pore size for PAC was micropores (less than 1nm, 10Å) while some mesopores have been developed as well. The result for PAC size distribution agrees with MB and IN tests (Table 4-1). The detailed information and data about the porosity and BET surface area of these samples are presented in appendix A.

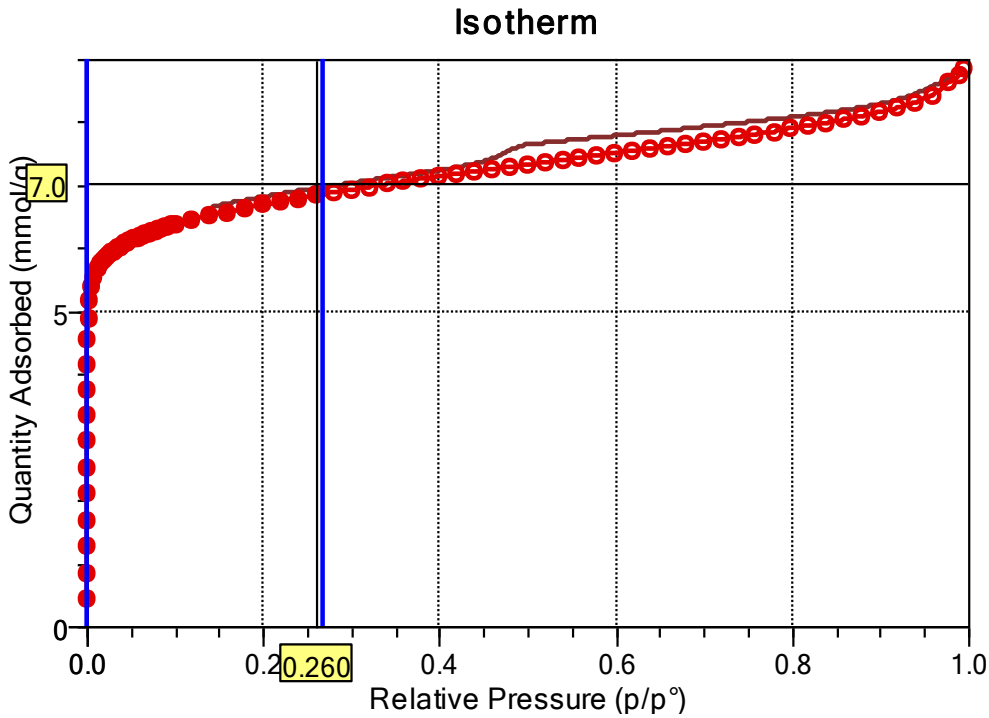

Figure 4-1: Isotherm plot of PAC

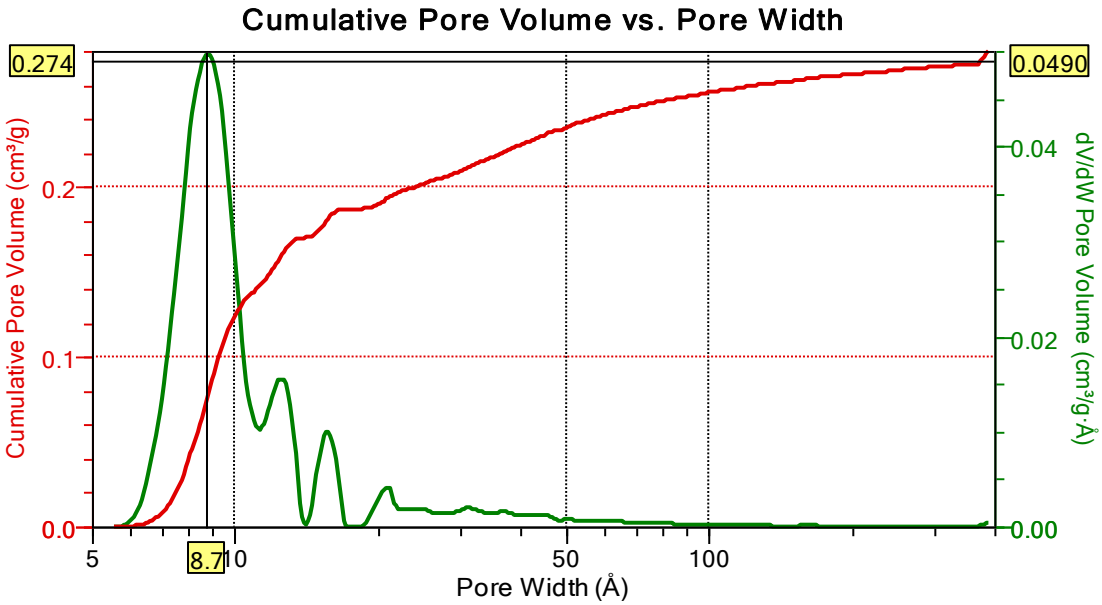

Figure 4-2: Pore Size Distribution for of PAC

4.2 GAC Generation with Raw CBPP and PAC

Apart from bitumen, it was found that none of the other binders were able to produce cohesive granules. Using raw or PAC did not change the result. Moreover, mixing bitumen with PAC produced fragile and fragmented GACs. Also, granules produced by using raw CBPP mixed with bitumen produced hard calcinated granules, however, activating the resulted granules produced a high content of ash and soft granules.

In the following section, characterization of granules produced from mixing bitumen with washed CBPP is reported.

4.3 GAC Generation by Washed CBPP and Bitumen

Bitumen is a black and highly viscous form of petroleum. In different studies, heating of bitumen at 140 °C was used to soften the bitumen (Ahmedna et al., 2000, Pendyal et al., 1999a, Pendyal et al., 1999b). To avoid the emission of harmful vapors from heated bitumen, it was dissolved in hexane and mixed with the carbon. Effects of calcination and activation temperature, activation time, heating rate, amount of binder, and steam temperature were studied to determine optimum condition for GAC production. This section covers the findings to determine the optimum conditions to make granulated carbon using bitumen as a binder.

4.3.1 Calcination temperature

To determine the effective calcination temperature, granules with the different binder to carbon ratios (10:19, 20:80, and 30:70 by weight) were produced. Each sample was calcinated at three different temperature (750, 850, and 950 °C) with 15 °C /min for 1 hour. Each case has been characterized by burn-off, MB adsorption, and Iodine number tests. Results for characterizations are according to Table 4-3 and Figure 4-3.

- Burn-off rate: As listed in Table 4-3, by increasing binder-to-carbon ratio the burn-off would increase at a given temperature. However, increasing the temperature for each binder-to-carbon ratio has no specific effect on the burn-off rate (Figure 4-3a) which means that all the binders have been evaporated and carbons have been bonded at 750 °C.
- MB Adsorption: Calcinated granules have been ground for MB tests, and the results are shown in Figure 4-3b. It is obvious that by increasing temperature, the opening of the pores increased which led to increasing the MB adsorption values, but the rate of increase is not affected significantly.
- Iodine number: As shown in Figure 4-3, the increase in the temperature would decrease iodine number for the binder to carbon ratios of 30:70 and 20:80 and has no specific effect on the binder which has carbon ratio of 10:90. This shows that the calcination temperature of 750 °C is the ideal temperature for calcination. A decrease in the Iodine number may be due to pore widening from micropores to mesopores.

Table 4-3: Characterization for the effect of calcination temperature on different carbon-to-binder ratios

Temperature (°C)	Ratio	Burn-off (%)	MB (mg/g)	IN (mg/g)
750	**10:90**	14.56	12.49	988.35
850	**10:90**	14.25	15.55	987.33
950	**10:90**	14.28	17.35	987.21
750	**20:80**	21.76	7.64	969.93
850	**20:80**	20.55	12.5	934.07
950	**20:80**	21.97	16.28	921.32
750	**30:70**	27.75	5.98	953.45
850	**30:70**	27.14	8.12	900.09
950	**30:70**	27.28	14.12	898.7

a)

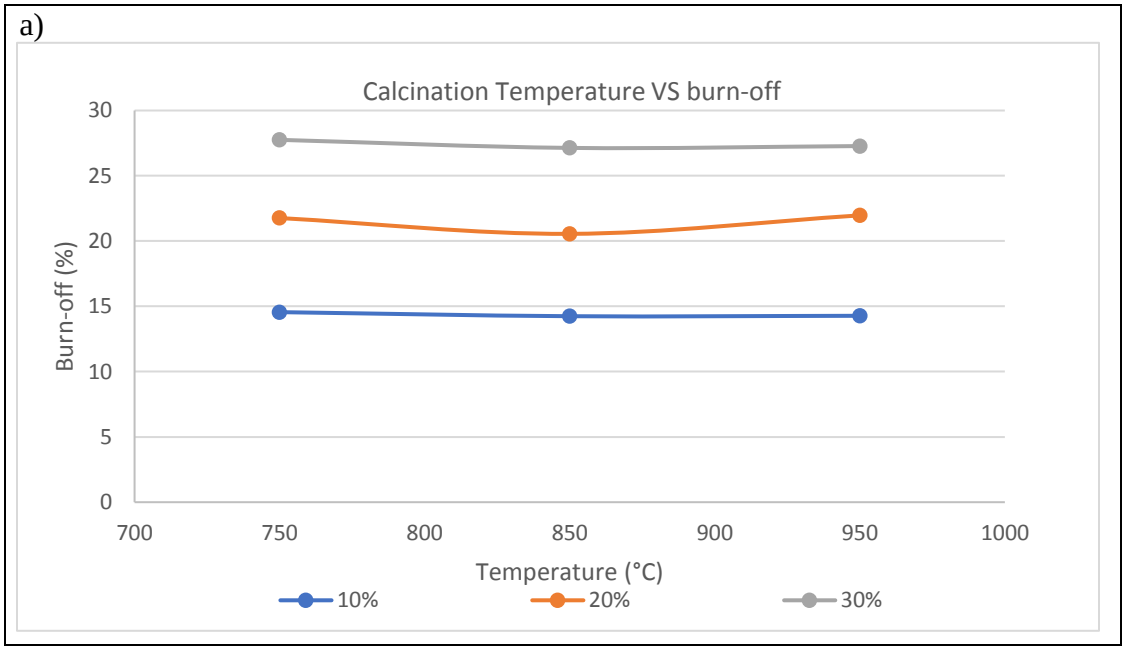

b)

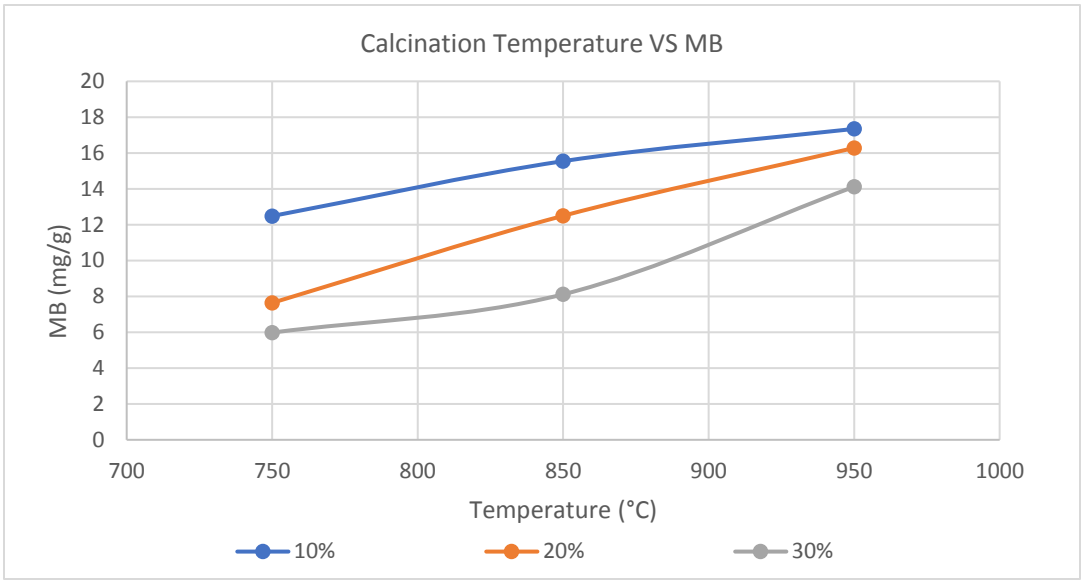

c)

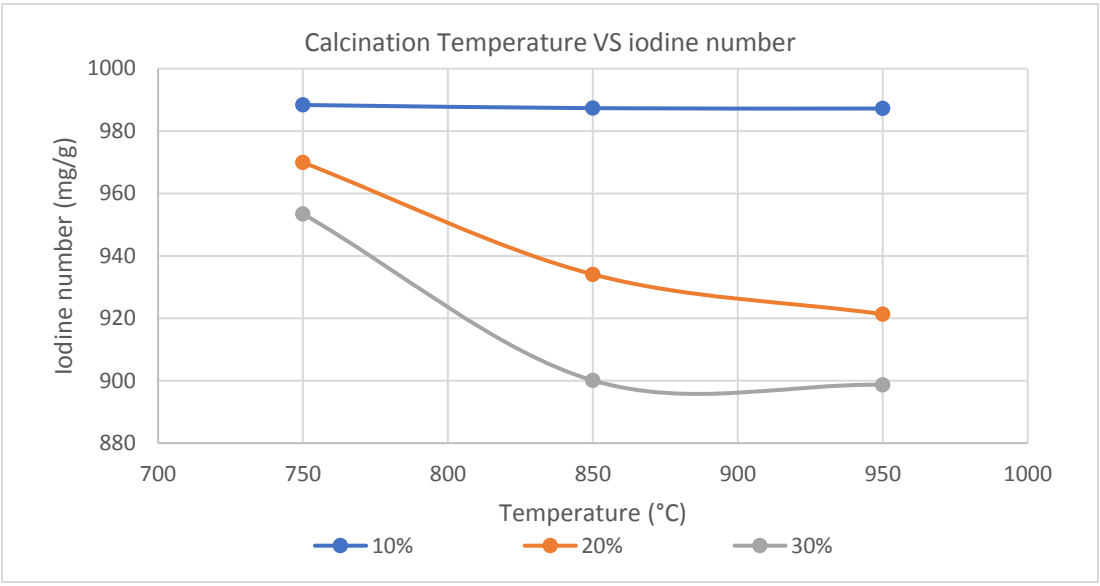

Figure 4-3: Characterizations for the effect of calcination temperature on different carbon-to-binder ratios; a) Burn-off, b) MB, c) IN

4.3.2 Activation Temperature

To determine the best temperature for activation, CO_2 activation at 750, 850, and 950 °C for 2 hours for the binder to carbon ratios of 10:90, 20:80, and 30:70 has been considered. In this case, the calcinated granules at 750 °C for 1 hour at 15 °C /min temperature increase rate was used. Burn-off rate, MB adsorption, Iodine number, and hardness tests were considered as characterization tests. The results are listed in Table 4-4 and plotted in Figure 4-4.

- Burn-off rate: Figure 4-4a and Table 4-4 show that increasing the activation temperature would increase the burn-off rate with increase in carbon loss. It is also concluded that increasing temperature for the lower binder to carbon ratio would lead to higher burn-off rate. This matter is for weak binding of carbons and leads to the high potential of carbon loss.
- MB Adsorption: As shown in Figure 4-4b, increasing the temperature from 750 °C to 850 °C does not show any significant increase in MB adsorption values. However, at 950 °C, MB adsorption has increased to a higher level showing a better activation at 950 °C.
- Iodine number: increasing activation temperature from 750 °C to 850 °C would lead to a better porosity development with higher iodine number (Figure 4-4c). However, above 850 °C, iodine number s decreased due to micro-pores widening to produce more mesopores with a significant increase in the MB adsorption values (Figure 4-4b). Moreover, lower binder to carbon ratio had higher MB number rather than higher binder to carbon

ratio due to weaker binding and more carbon burn-off. It is important to mention that although the decrease in the IN above 850 °C can be considered as a negative point for activation, iodine adsorption is still high (above 1000 mg/g) at a higher temperature (i.e., 950 °C).

- Hardness: Higher porosity would lead to lower hardness, especially, for the lower binder to carbon ratio as shown Figure 4-4d. It is obvious that increasing the activation temperature for the binder to carbon ratio of 10:90 and 20:80, would lead to extremely soft granules.

In summary, it can be concluded that calcination at 750 °C, activation at 950 °C, and binder to carbon ratio of 30:70 are the optimized conditions for the granulation.

Table 4-4: Characterization for the effect of activation temperature on different carbon-to-binder ratios

Temperature(°C)	Ratio	Burn-off (%)	MB (mg/g)	IN (mg/g)	Hardness (%)
750	**10**	6.47	17.36	1014.73	0.51
850	**10**	7.7	18.35	1004.82	0
950	**10**	8.59	60.55	990.22	0
750	**20**	5.17	9.82	1006.78	61.38
850	**20**	7.057	17.29	1061.13	18.44
950	**20**	7.98	55.15	1045.22	11.26
750	**30**	3.94	10.33	988.35	88.14
850	**30**	6.71	16.22	1064.78	86.6
950	**30**	7.67	49.26	1041.64	85.35

a)

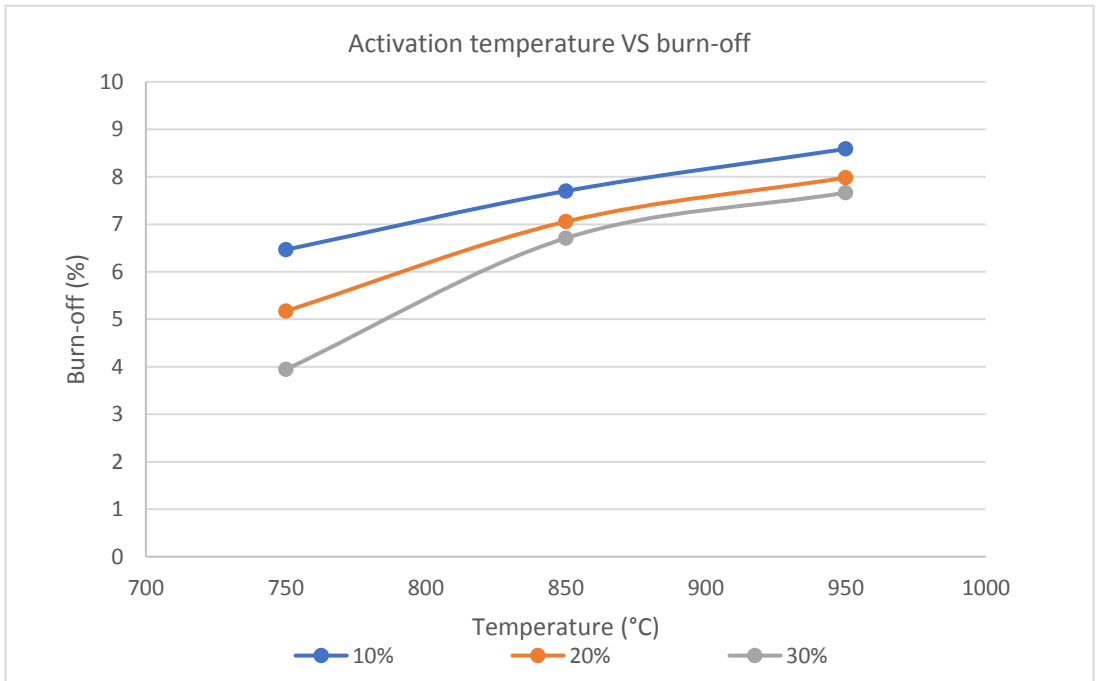

b)

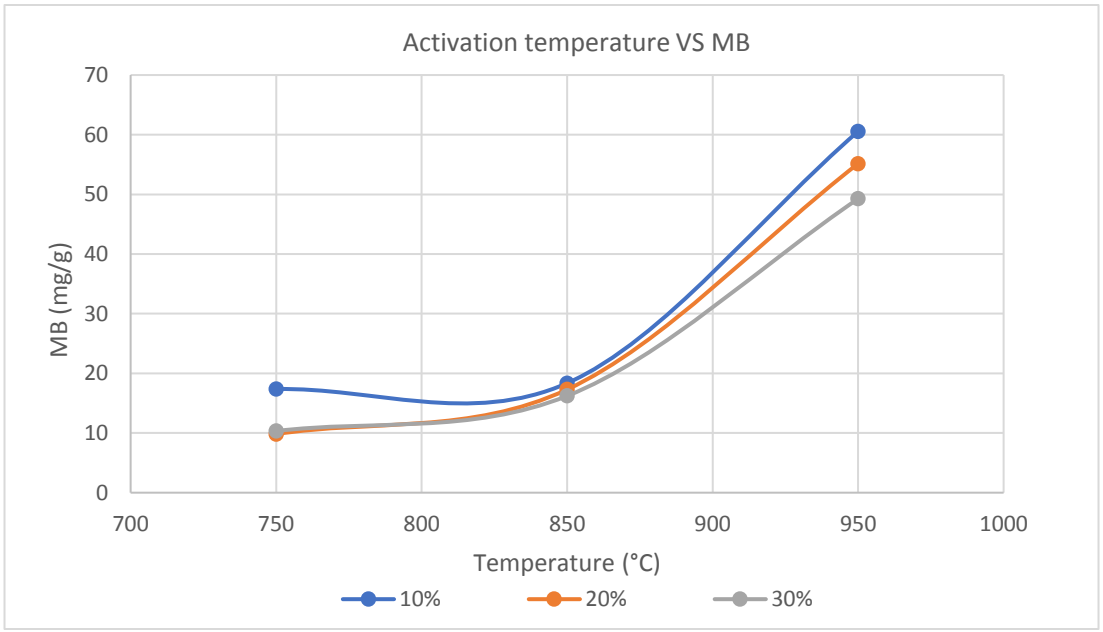
Activation temperature VS MB
MB (mg/g)
70
60
50
40
30
20
10
0
700
750
800
850
900
950
1000
Temperature (°C)
10%
20%
30%

c)

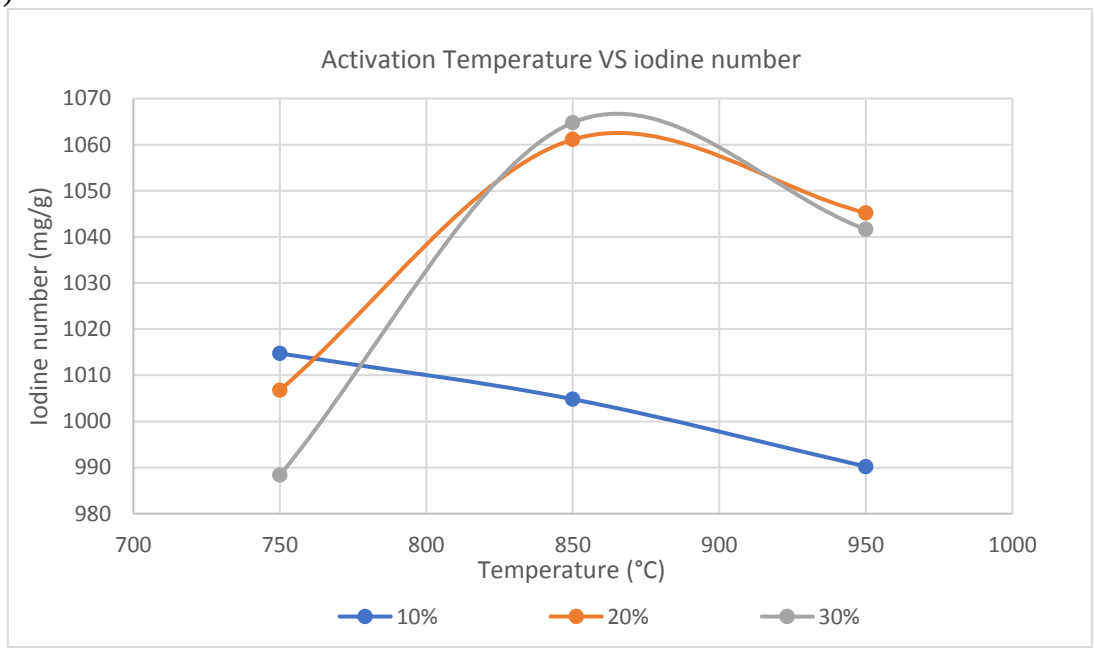
Activation Temperature VS iodine number
Iodine number (mg/g)
1070
1060
1050
1040
1030
1020
1010
1000
990
980
700
750
800
850
900
950
1000
Temperature (°C)
10%
20%
30%

d)

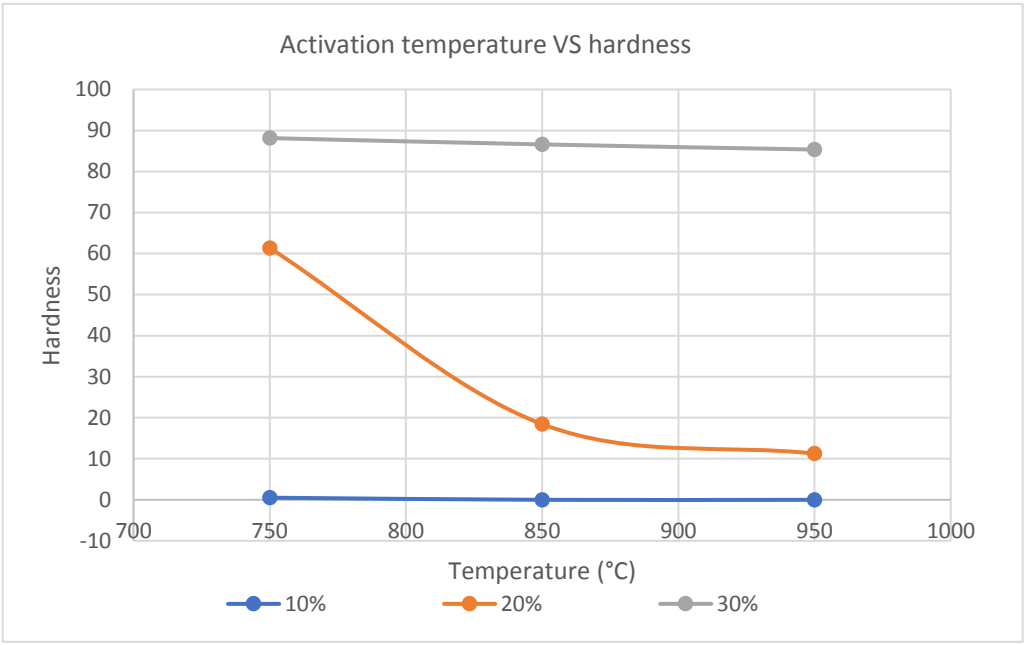

Figure 4-4: Characterizations for the effect of activation temperature on different carbon-to-binder ratios; a) Burn-off, b) MB, c) IN, d) Hardness

4.3.3 Calcination temperature increasing rate

In the previous section, it was concluded that the calcination at 750 °C is the optimum temperature and binder to carbon ratio of 30:70 as an optimum ratio. To determine the best temperature increasing rate for calcination, 30% binder and calcination at 750 °C with temperature increasing rate of 5 °C/min, 10 °C/min and 15 °C/min were tested, and the findings are summarized in Figure 4-5 and Table 4-5.

It is obvious from the Table and plots that at slower temperature increase rate, the burn-off rate and Iodine number was decreased but MB adsorption was increased, and more

mesopores was formed. However, the increase in the MB is not very significant. Therefore, the calcination should be done at 750 °C with 15 °C/min temperature increase.

Table 4-5: Characterization for the effect of calcination temperature increasing rate on 30% binder granules

Temperature increasing rate(°C/min)	Burn-off	MB (mg/g)	IN (mg/g)
15	27.75	5.98	953.45
10	25.37	10.34	944.95
5	24.98	11.42	943.97

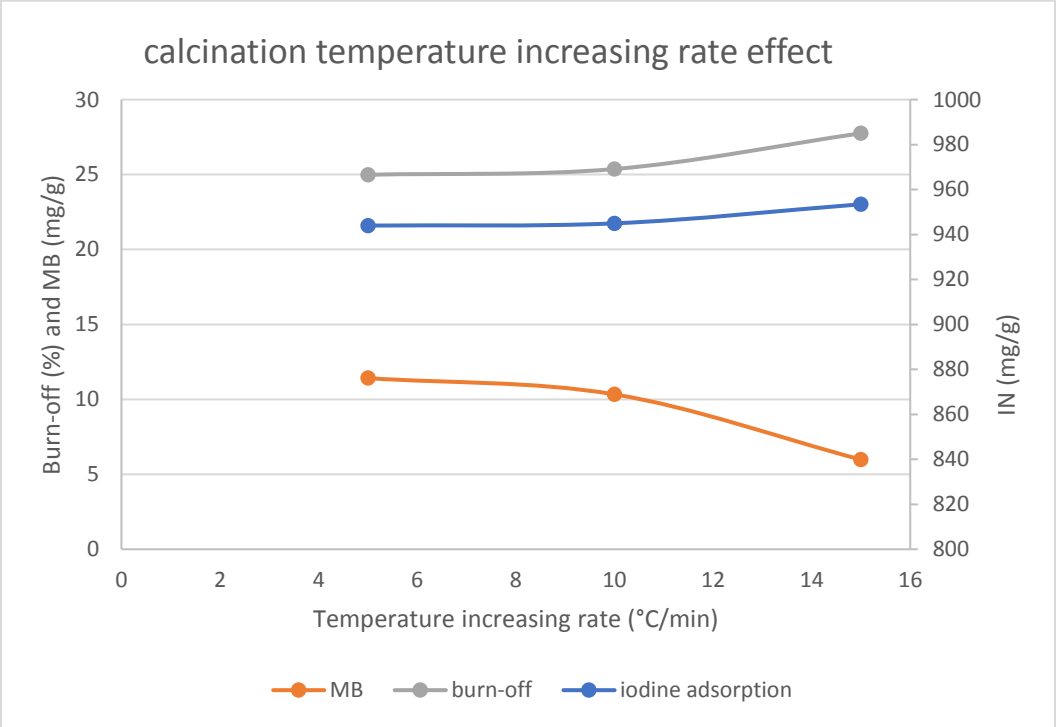

Figure 4-5: Characterization for the effect of activation temperature increasing rate on 30% binder granules

4.3.4 Activation temperature increasing rate

As concluded in the previous section, the calcinated granules at 750 °C with 15 °C/min heating rate, and binder to carbon ratio as 30:70 are the optimized parameters for calcination while the activation temperature of 950 °C is considered as the most effective temperature for activation. The findings on activation temperature increasing rate are presented in Figure 4-6 and Table 4-6.

Based on the analysis, it is clear that decreasing the temperature increasing rate was resulted in a better MB and Iodine adsorption values. However, the hardness decreased to near 80%. Although there are no well-defined guidelines on the limit for GAC's hardness, for this study a hardness below 85%, is considered to be soft.

Table 4-6: Characterization for the effect of activation temperature increasing rate on 30% binder-to-carbon granules

Temperature increasing rate (°C/min)	Burn-off (%)	MB (mg/g)	IN (mg/g)	Hardness (%)
15	7.67	49.26	1041.64	85.35
10	8.76	50.8	1050.59	85.60
5	8.9	55.15	1094.29	81.63

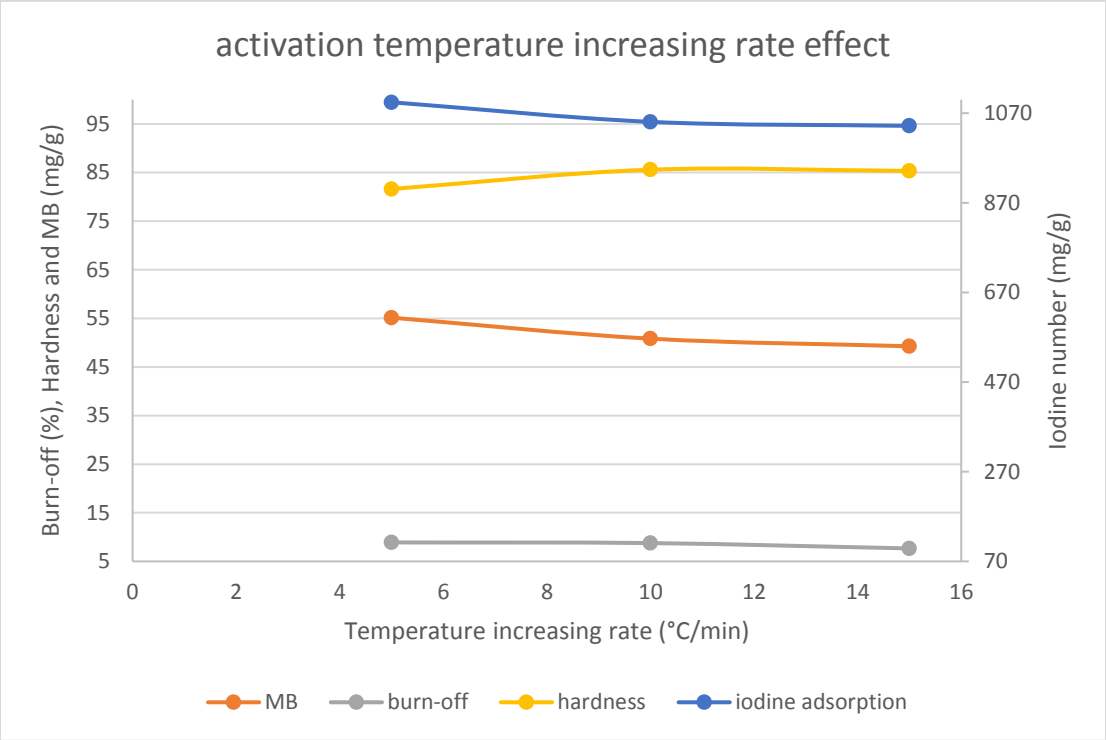

Figure 4-6: Characterization for the effect of activation temperature increasing rate on 30% binder granules

4.3.5 Steam Activation, Steam Temperature

By finding the optimum calcination temperature, calcination temperature increasing rate, binder to carbon ratio, activation temperature, and activation temperature increasing rate, the effect of steam activation has been tested. One important factor in steam activation is the steam temperature. For this, 30% calcinated granules were activated at 950 °C with the steam temperature of 60, 70, and 80 °C. The findings are summarized in Table 4-7 and trend shown in Figure 4-7.

- Burn-off rate: The burn-off rate increases with the increasing temperature with higher carbon loss although it helps in producing GAC with higher porosity and better adsorbent.
- MB adsorption: by increasing the steam temperature, more mesopores are formed with a better adsorbent. Comparing Table 4-7 with Table 4-6 (at 15 °C/min), it is obvious that the steam temperature at 60 °C has low MB and IN compared to CO_2 activation at the same temperature and temperature increasing rate. This is due to the low flow of steam and CO_2 into the furnace. On the other hand, by increasing the steam temperature to 80 °C, a well-formed GAC with high MB adsorption is obtained.
- Iodine number: Increasing the steam temperature from 60 °C to 80 °C, would cause widening of the pores and forming new micro-pores.
- Hardness: A better result in the steam activation at 80 °C is achieved. Although the high burn-off rate is observed, the pores are well formed in the GAC while developed GAC has relatively high hardness.

In summary, the activation temperature at 950 °C and keeping the steam temperature at 80 °C are optimized conditions.

Table 4-7: Effect of steam temperature on GAC's generation

Steam temperature (°C)	Burn-off (%)	MB (mg/g)	IN (mg/g)	Hardness (%)
60	7.83	31.86	1245.86	89.29
70	10.26	51.4	1259.98	86.68
80	21.1	220.15	1332.68	86.59

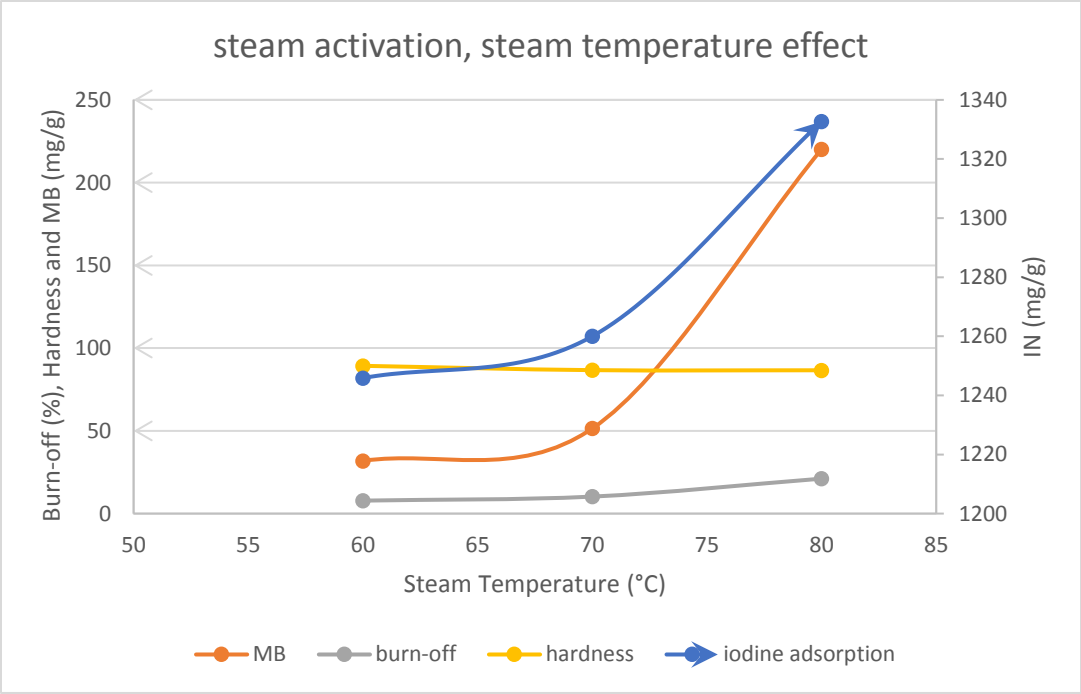

Figure 4-7: Effect of steam temperature on GAC's generation

4.3.6 Steam Activation time

To determine the effect of activation time on GAC production, 30% granules have been calcinated at 750 °C with 15 °C/min for 1 hour. Then, steam activation at 950°C with 15 °C /min and the steam at a temperature of 80 °C was used for 1,2, and 3 hours. The

results are listed in Table 4-8 and From Figure 4-8 and Table 4-8, it can be concluded that increasing the time from 1 hour to 3 hours would result in better MB and Iodine numbers with acceptable hardness. Therefore, 3 hours of activation have been chosen to produce GAC.

Table 4-8: Effect of activation time on GAC's characterizations

activation time (hr)	Burn-off (%)	MB (mg/g)	IN (mg/g)	Hardness (%)
1	12.33	77.97	1295.68	87.09
2	21.1	220.15	1332.68	86.59
3	23.44	240.71	1420.56	84.94

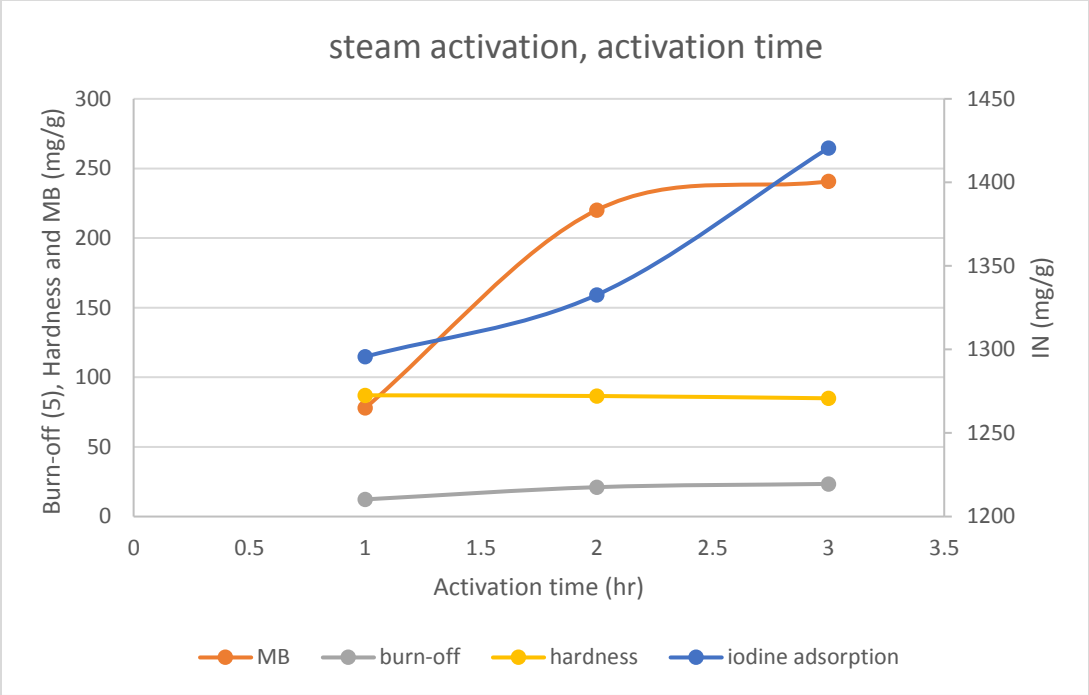

Figure 4-8: Effect of activation time on GAC's characterizations

Summary

In conclusion, to produce GAC, 30:70 binder to carbon ratio of granules have been calcinated at 750 °C with 15 °C/min of the heating rate for 1 hour. Then, calcinated granules have been activated at 950 °C with 15 °C/min using steam at 80 °C for 3 hours.

4.4 GAC Characterization

4.4.1 Elemental Analysis for produced GAC

Table 4-9 shows different metals existed in PAC and GAC. The result for tracing different elements in raw CBPP is also reported again for comparison purposes. Based on the results, it is observed that during cleaning and production of PAC, all the elements were removed considerably from raw CBPP. However, a high concentration of Vanadium and Nickle in produced GAC in comparison with raw CBPP and PAC, it may be as a result of using untreated bitumen as a binder.

Table 4-9: Elemental analysis for PAC and GAC

Elements	Raw CBPP (ppm)	PAC (ppm)	GAC (ppm)	Elements	Raw CBPP (ppm)	PAC (ppm)	GAC (ppm)
Li	4.64	0.78	0.54	**Cu**	29.58	17.98	11.31
Be	0.053	0.017	0.006	**Zn**	74.10	1.74	0.42
B	26.20	6.69	0.84	**As**	0.93	0.19	0.16
Mg	2550.57	1154.15	841.88	**Rb**	23.128	1.68	0.64
Al	2220.38	709.33	274.31	**Sr**	92.74	26.34	19.22
P	1465.21	214.37	193.35	**Mo**	3.91	4.26	2.88
Ca	25432.69	3794.94	3182.35	**Ag**	0.07	0.01	0.01
Ti	155.37	98.08	35.41	**Cd**	0.31	0.019	0.02
V	6.85	2.7	48.6	**Cs**	0.12	0.02	0.018
Cr	14.86	10.83	8.58	**Ba**	116.65	27.55	0.74
Mn	3471.06	791.63	625.05	**La**	2.54	0.45	0.2
Fe	2185.04	1217.69	993.77	**Ce**	2.57	0.79	0.36
Co	12.42	0.77	0.93	**Pb**	4.048	0.14	0.059
Ni	8.36	5.01	19.3	**U**	0.17	0.11	0.056

4.4.2 BET Surface Area and Pore Size Distribution of GAC

N_2 adsorption and desorption into GAC at 77 K resulted in isotherm curves and pore size distribution of GAC that are shown in Figure 4-9 and Figure 4-10, respectively. Isotherm for GAC is a combination of type I and type IV isotherms according to IUPAC classifications which are attributed to an adsorbent with both micropores mesopores. Considering Figure 4-10 and comparing it with Figure 4-2 shows that microporosity of

PAC and GAC is almost the same while PAC has more mesopores rather than GAC. Applying Equation (3.6) to Equation (3.10), obtained that the BET surface area of GAC is 588 m^2/g. Also, micropore volume and mesopore volume are 0.276, 0.017 cm^3/g, respectively. 3FLEX share software (version 4.04) was used for BET surface area calculations. The detailed information and data about the porosity and BET surface area of these samples are presented in appendix B.

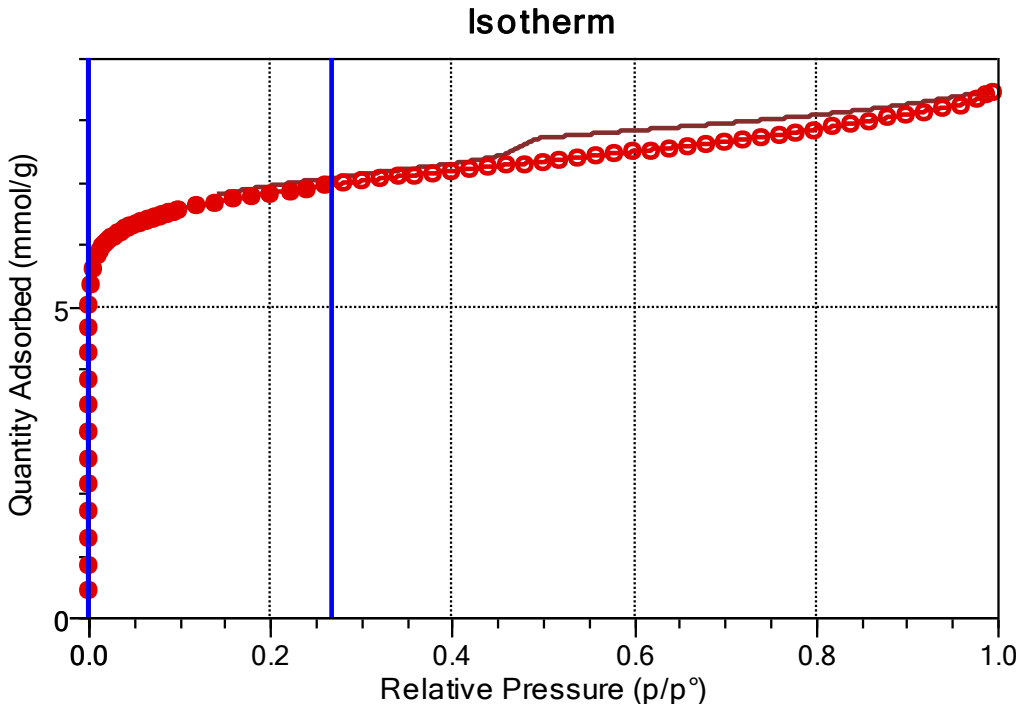

Figure 4-9: Isotherm plot of GAC

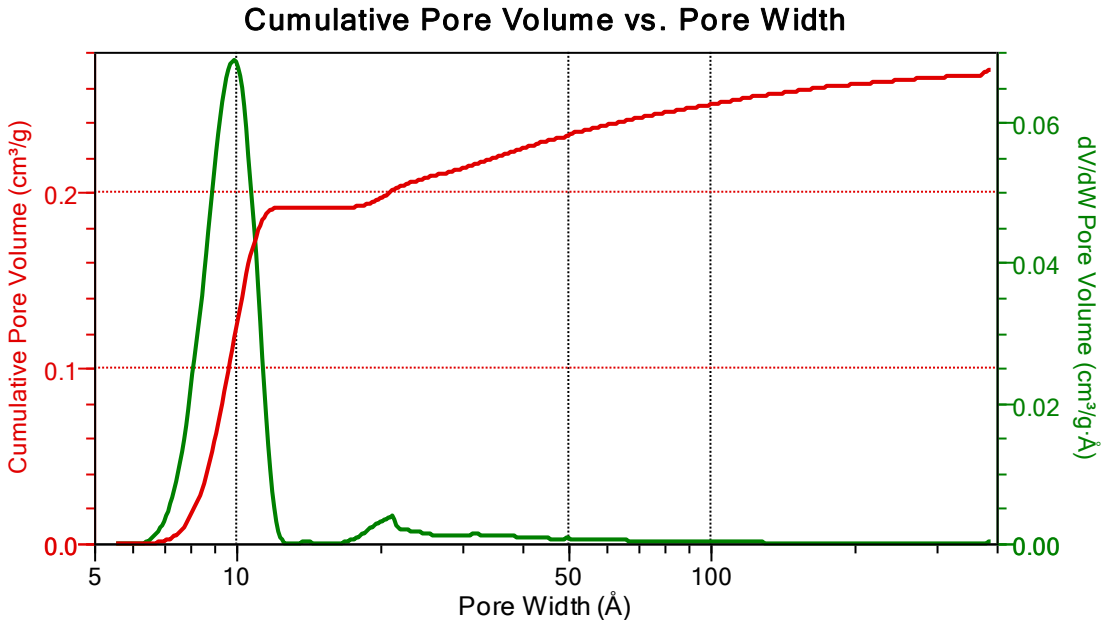

Figure 4-10: Pore Size Distribution for GAC

Chapter 5 NOM Removal by Generated Adsorbents

5.1 Water Sample Characterization

As mentioned in the previous chapter, water samples were characterized based on its initial pH, TOC concentration, UV_{254}, and elemental analysis. The results for the first three parameters are listed in Table 5-1, and for elemental analysis, the results are tabulated in Table 5-2.

Table 5-1: Water sample characterization

Parameter	Result
pH	6.74
Initial TOC concentration (mg/L)	6.95
UV_{254}	0.242

Table 5-2: Pouch Cove Water Elemental Analysis

Element	Concentration (ppb)	Detection limit (ppb)	Element	Concentration (ppb)	Detection limit (DL) (ppb)
Li	0.253	0.106	**Br**	54.8	5.4043
Be	< DL	0.06922	**Se**	< DL	1.2825
Mg	1068.403	0.805457	**Rb**	0.319	0.0325
Al	47.7	0.294	**Sr**	7.50	0.0072
P	< DL	23.437	**Mo**	0.0551	0.0286
Cl	11161.09	1,043.707	**Ag**	< DL	0.3790
Ca	2060.115	45.5177	**Cd**	< DL	0.0094
Ti	0.541	0.1491	**Sn**	< DL	0.0361
V	< DL	1.411	**I**	< DL	24.2065
Cr	< DL	0.138	**Cs**	< DL	0.0118
Mn	2.82	0.031	**Ba**	2.59	0.0276
Fe	154	7.2785	**La**	0.0482	0.0099
Co	0.0276	0.0116	**Ce**	0.0491	0.0094
Ni	0.275	0.0690	**Tl**	< DL	0.0269
Cu	1.41	0.1005	**Pb**	0.0809	0.0175
Zn	< DL	2.5879	**Bi**	< DL	0.0110
As	< DL	0.16	**U**	< DL	0.0134

5.2 NOM adsorption: Batch System

As discussed in section 3.3.1, the effect of water pH, temperature, and volume on NOM adsorption were studied. 20 different experiments were considered using the design of experiment (Table 5-3). For each experiment, the required volume of water passed

through 0.45 μm vacuum filtration paper to remove large particles and living microorganism before UV and TOC analysis. Then 1N HCl and 1N NaOH, from Sigma Aldrich Canada, were prepared for pH adjustment. A heating plate with a magnetic stirrer for experiments above 25 °C and mechanical shaker for experiments at 25 °C were used. Then, 0.1 g of produced PAC was mixed with water in a beaker at designed values and stirred for 5 hr at 250 rpm for a complete adsorption until equilibrium. At the end, NOM concentration in treated water were analyzed by TOC and UV analyzer. Adsorption capacity was calculated according to Equation (3.11).

Table 5-3 lists the results of NOM adsorption at a different temperature, pH, and water volume. The analysis indicates that the water volume and pH are the significant factors for NOM adsorption and temperature has little or no significant effect on adsorption.

Table 5-4 shows the results for analysis of variances (ANOVA) for NOM removal. Analysis of Variance (ANOVA) is a summary of the test procedure in which all the statistical models and differences of each factor is reported and used for analysis. ANOVA table is used to determine the eligibility of the analysis (Montgomery, 2017). As mentioned in section 2.3.7, when the Probe>F value is smaller than 0.05, the model or the effect is significant and, in this study, the Prob>F value for the model is significant. Analysis also shows that water volume, pH, and their interaction are significantly effective for NOM adsorption.

pH can be an important factor in the NOM adsorption process by its effect on a surface charge of activated carbon and the charge of NOM. NOM have negative charges when the pH value is higher than 4 (Bjelopavlic et al., 1999). Meanwhile, if activated carbon also has a negative surface charge, it repels NOM, and thus it reduces the adsorption capability. At lower pH, activated carbon contains positive charge with maximum NOM adsorption at pH = 4. The negative effect of pH on NOM adsorption can be seen in Equation (5.1) which indicates the final equation of NOM adsorption. The equation is used to predict a final answer using actual units. The validity of the equation can be determined using prediction-R squared which is determined in the following section.

(ads.) = -4.15+0.077*(water volume) + 0.809*pH - 9.17E-3*(water volume) *(pH) **(5.1)**

Table 5-3: Results for NOM adsorption in batch system

run	Temperature (°C)	Water Volume (mL)	pH	Adsorption (mg/L)
1	35	425	5.5	14.59
2	25	800	4	31.62
3	45	425	5.5	13.72
4	25	425	5.5	10.89
5	45	50	7	1.29
6	35	425	5.5	11.84
7	25	800	7	11.58
8	25	50	7	1.39
9	35	425	4	18.70
10	35	425	5.5	9.93
11	35	425	5.5	12.05
12	35	800	5.5	17.32
13	35	425	5.5	13.05
14	45	800	4	33.64
15	45	50	4	1.028
16	45	800	7	13.14
17	35	425	7	13.18
18	35	425	5.5	9.87
19	25	50	4	0.97
20	35	50	5.5	1.17

Table 5-4: Analysis of Variance (ANOVA)

Source	Sum of Squares	df	Mean Square	F Value	p-value Prob > F
Model	1566.04	3	522.01	93.20	< 0.0001
B-Water volume	1110.95	1	1110.95	198.35	< 0.0001
C-pH	231.40	1	231.40	41.31	< 0.0001
BC	234.07	1	234.07	41.79	< 0.0001
Residual	95.21	17	5.60		
Lack of Fit	64.85	11	5.90	1.16	0.4471
Pure Error	30.37	6	5.06		
Cor Total	1661.25	20			

5.2.1 R-Squared Interpretation

Table 5-5 shows that R^2 is 0.9427; adjusting R-squared for the number of parameters and points of design would dive Adj-R^2 which is 0.9326 and shows that the model is strong. Pred-R^2 is a measure to determine how well the model predicts a response value and is 0.9229 and shows the reasonable agreement with Adj-R^2 since it is within 20% of Adj-R^2. Adeq-Precision shows signal to noise ratio, and the value greater than 4 is desirable; 29.64 is adequately greater than 4.

Table 5-5: R-Squared

Std. Dev.	2.37	**R-Squared**	0.9427
Mean	11.29	**Adj R-Squared**	0.9326
C.V. %	20.96	**Pred R-Squared**	0.9229
PRESS	128.16	**Adeq Precision**	29.640

5.2.2 Model Adequacy

In the design of experiments, the residual is the difference between the observed and the predicted response. In practice, it is unwise to solely rely on R-squared analysis to determine the adequacy of design. Examination of residuals is part of the ANOVA assumption and is an essential step in an investigation about the adequacy of a model. The residual examination should be structureless with no specific patterns in an adequate model. Model diagnostic is a graphical analysis for residuals (Montgomery, 2017). Diagnostic curves for NOM adsorption are shown in Figure 5-1. Normal plot of residuals is shown in Figure 5-1a.

Normal probability plot is a useful procedure and determines whether residuals have normal error distribution. A straight line resembles a normal distribution, and this matter can be seen in Figure 5-1a.

In an adequate model with satisfied assumptions, residuals should not have any relation with other variables including the predicted response. In nonconstant variances case, residuals versus predicted plot would shape like an outward funnel. Figure 5-1b shows no funnel-shaped residuals.

In the design of experiment, the order of experiments should be randomized so the residuals would not correlate with each other. Figure 5-1c shows that residuals are independent and do not have a trend by a run. As a result, all the ANOVA assumptions are met, the model is adequate and a good predictor.

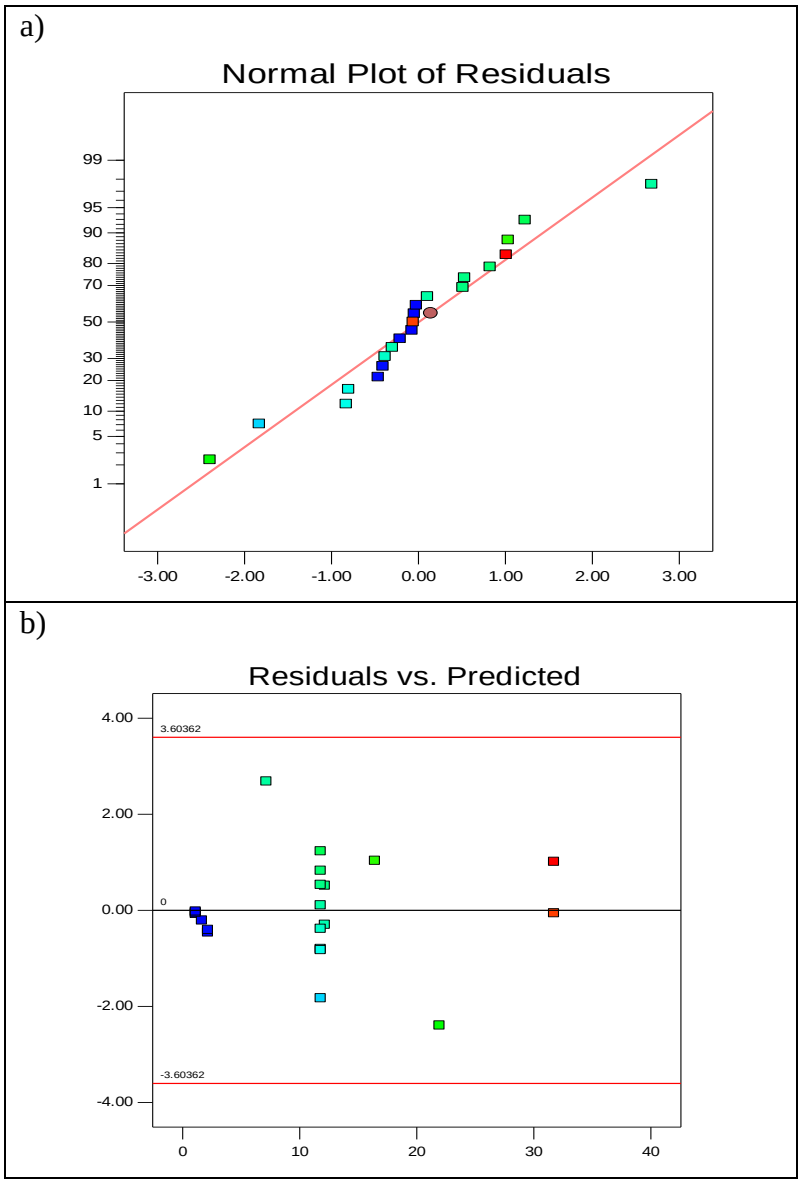

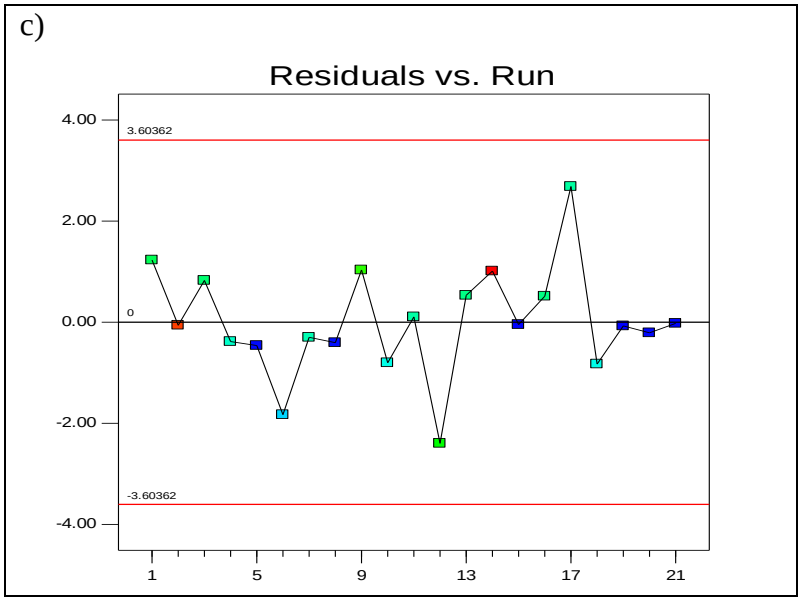

Figure 5-1: Diagnostics curves for NOM adsorption

5.2.3 Important Factors of Adsorption and Interactions

Figure 5-2 shows the contour graph and 3D surface graph for effective factors for NOM adsorption; water volume and pH. According to the figure, at lower pH and higher water volume, the adsorption is maximum. Figure 5-3 shows the interaction between pH and water volume. It is obvious that at higher pH, increasing water volume increased the adsorption. However, this increase is at a higher rate at lower pH. As a result, to have a better adsorption pH should be minimized and water volume should be at its highest value.

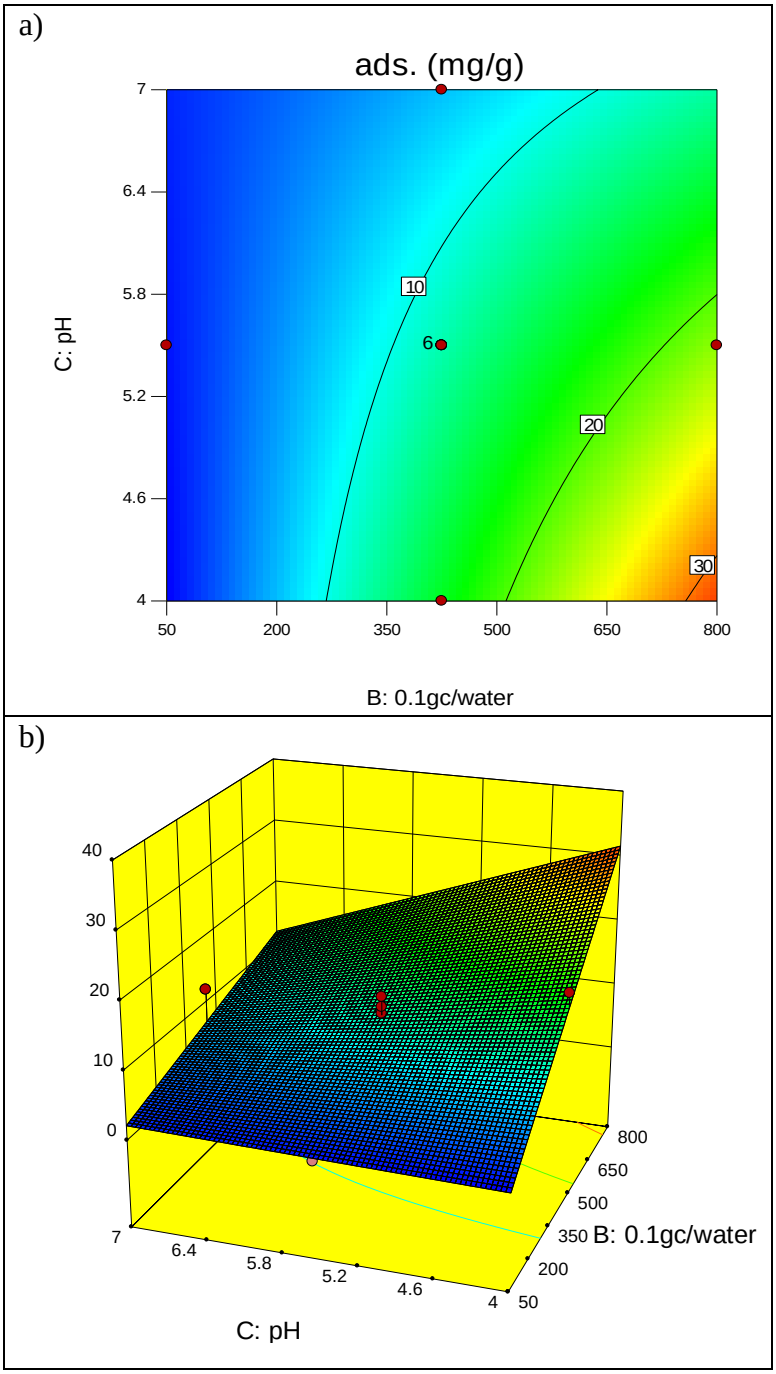

Figure 5-2: Model Graphs; a) Contour Graph for water volume and pH b) 3D Surface Graph for water volume and pH

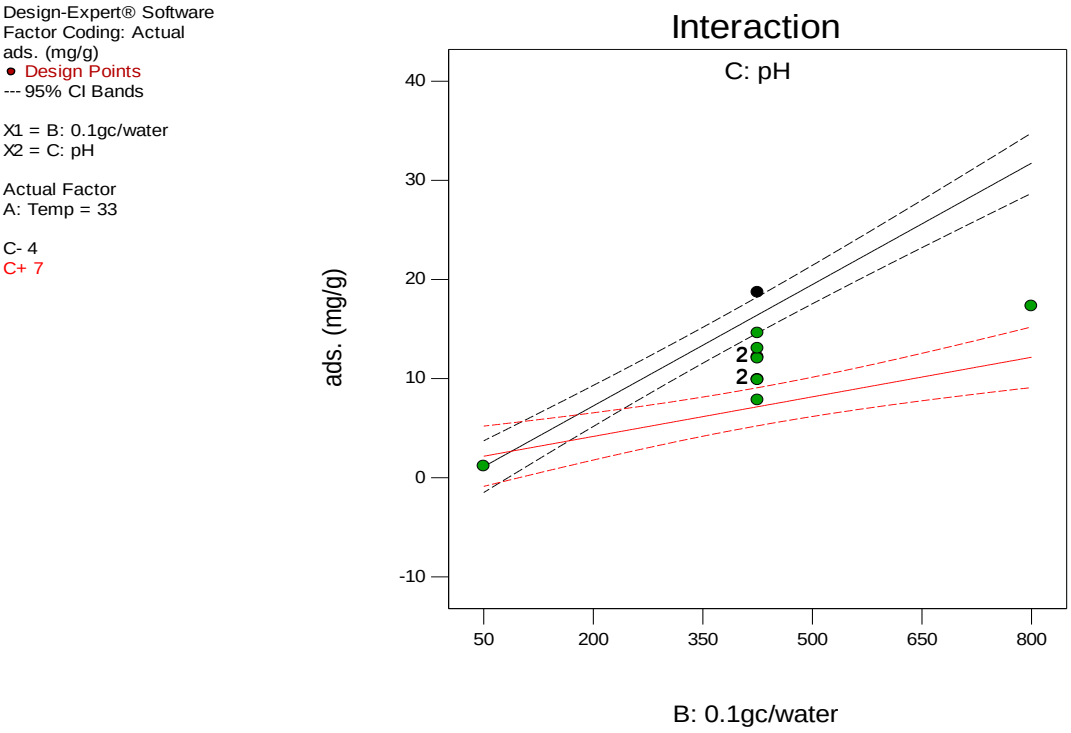

Figure 5-3: interaction of water volume and pH

5.2.4 Model Validation

Point prediction of Design-Expert software was used to validate the model. Three different untested conditions were chosen to validate the model. The adsorption results and predicted 95% Confidence Interval are shown in Table 5-6. The results of the tested conditions for model validation indicate that the adsorption is stable and can fall into predicted 95% confidence intervals. Most of the validation experiment results are very close to the mean of predicted points. This model is relatively accurate and can be applied in the real experiment prediction.

Table 5-6: Validation of the model

Temperature (°C)	Water volume (mL)	pH	Adsorption (mg/g)	Mean	95% predicted intervals
30	600	4.5	26.324	21.2266	(15.92, 26.53)
27	100	6.5	3.766	2.89279	(-2.6, 8.39)
40	400	5.3	9.714	11.6926	(6.58, 16.81)

5.2.5 Adsorption Study: Kinetic Study

The kinetic study determines the mechanism and rate of adsorption which is dependent on substances concentration. Studying kinetic of adsorption can help to determine the retention time for an adsorption process to achieve equilibrium; in another world, the kinetic study shows how dependent an adsorption process is to retention time. NOM adsorption onto activated CBPP have been studied, and optimum condition was determined. To study the kinetic of adsorption, 10 samples with 800 mL mixed with 0.1 g of PAC at pH 4 were alternatively were filtered after 15, 30 45, 60, 120, 180, 300, 675, 1440, 2700 minutes. After filtration using 0.45µm filter paper, TOC was determined using a TOC analyzer instrument (TOC-L CPH/CPN model). The result is according to Figure 5-4. It is obvious that after 300 minutes, the adsorption was decreasing due to desorption. Therefore, the required time for NOM adsorption to reach equilibrium point was considered 300 minutes.

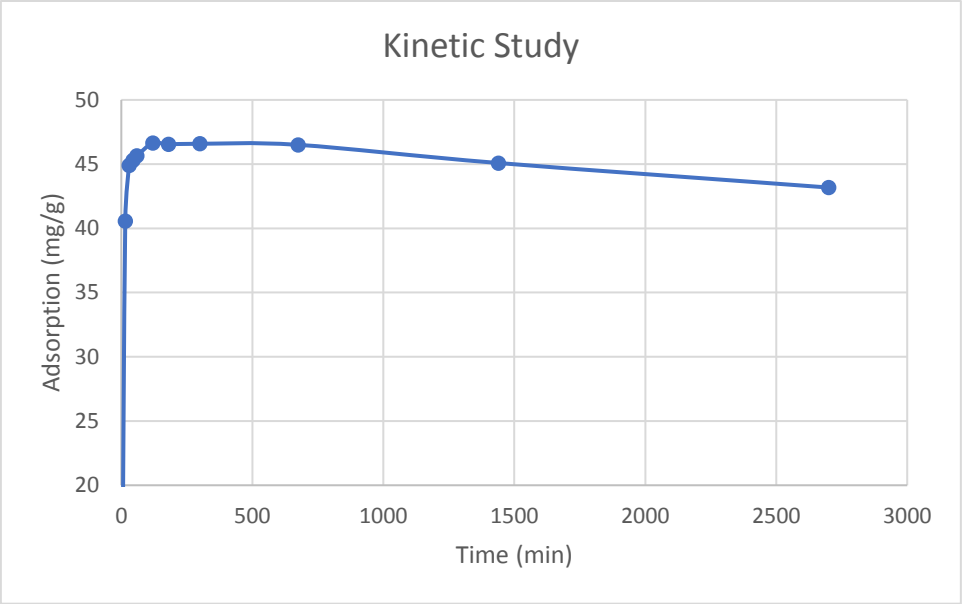

Figure 5-4: NOM Adsorption Kinetic Study

As discussed in section 3.4.1, pseudo-first-order and pseudo-second-order kinetic models (Equation (5.2) and Equation (5.3)) were used to describe the kinetic data of an adsorption process. Each term of Equation (5.2) and Equation (5.3) are described in section 3.4.1. Figure 5-5 shows pseudo-first-order and pseudo-second-order models for kinetic study. Parameters for both models are shown in Table 5-7. It is obvious that pseudo-second-order is the better model for understanding kinetic of NOM adsorption onto activated CBPP since kinetic data had better fitting this model. The q_e provided by this model is close to real equilibrium adsorption (46.5 mg/g).

$$\boldsymbol{ln\,(q_e - q_t) = ln(q_e) - K_1 t} \tag{5.2}$$

$$\frac{\boldsymbol{t}}{\boldsymbol{q_t}} = \frac{\boldsymbol{1}}{(\boldsymbol{K_2\, q_e^2})} + \frac{\boldsymbol{t}}{\boldsymbol{q_e}} \tag{5.3}$$

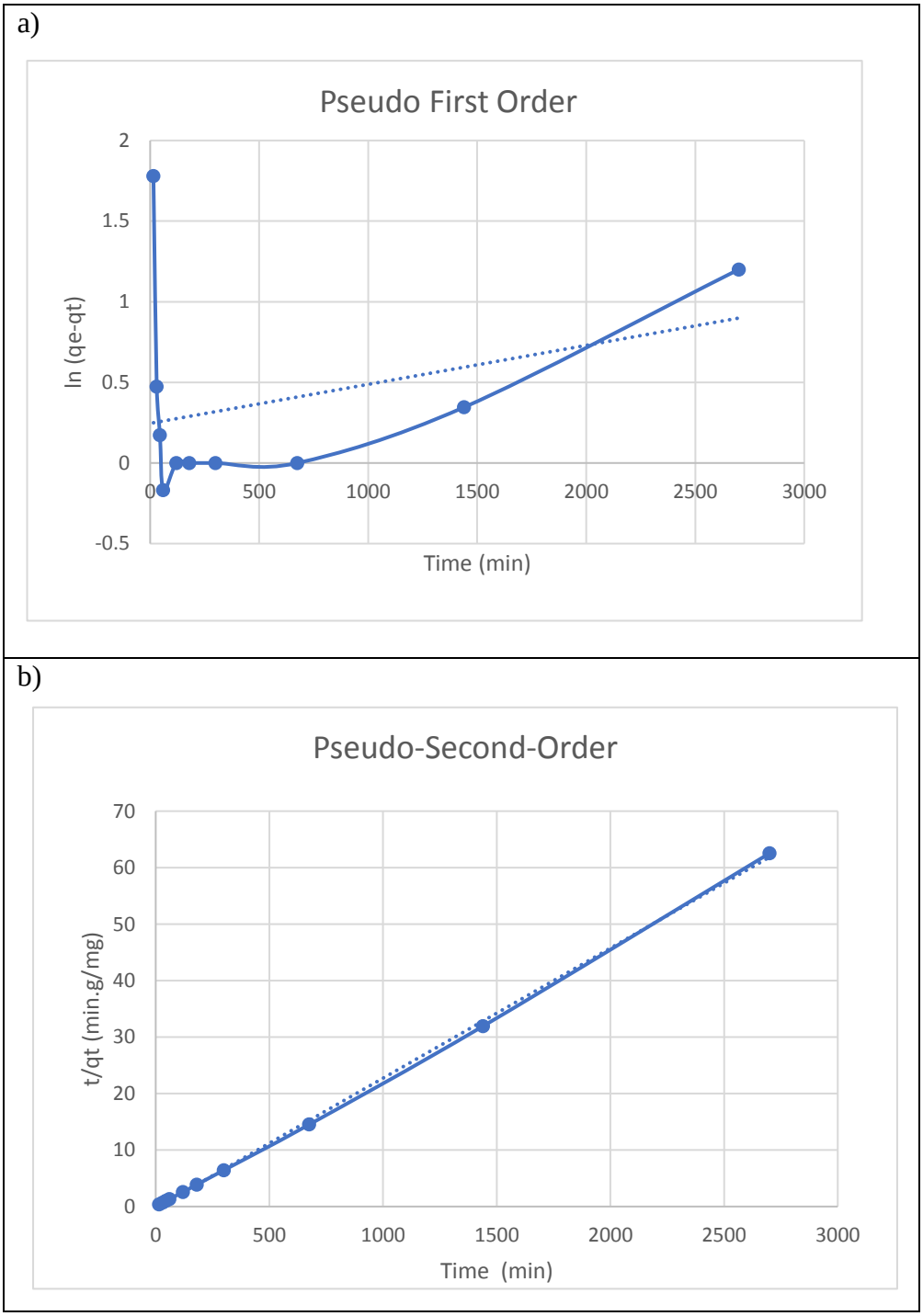

Figure 5-5: NOM Adsorption Kinetic models: a) pseudo-first-order, b)pseudo-second-order

Table 5-7: Kinetic Models Parameters for NOM Adsorption

Model	R^2	q_e (mg/g)	K
Pseudo-first order	0.1127	1.28	-0.0002 (min)
Pseudo-second order	0.9994	43.48	-0.002 (g/mg.min)

If an adsorption process follows pseudo-first-order kinetics, the plot of $\ln(q_e-q_t)$ versus time would be a straight line. Through different adsorption process studies, pseudo-first order kinetics was found to be valid for initial interaction time (20-30 minutes). Pseudo-first-order's constant (K_1) depends on the initial concentration of adsorbate and can be determined from the slope of the plot (McKay *et al.*, 1999). A linear plot of t/q_t versus time would determine that an adsorption process is following the pseudo-second-order kinetic model. This model can describe a whole range of contacting time in an adsorption process. The model constant (K_2) can be determined according to the plot intercepts and depends on operating conditions including pH, temperature, and concentration (Azizian, 2004).

5.2.6 Adsorption Study: Equilibrium Study

Studying equilibrium or isotherms are essential to understanding the mechanism of the adsorption process. Adsorption isotherms determine a relation between equilibrium concentration of adsorbate in the liquid phase and in solid phase which in here is activated CBPP. The results for adsorption of NOM using different carbon concentration are shown in Figure 5-6. It is obvious that decreasing carbon concentration is increasing the

adsorption and equilibrium concentration. As discussed in 3.4.2, three common isotherm models, Langmuir, Freundlich, and Temkin isotherms have been used to study the mechanism of NOM adsorption with different carbon concentration. Fitting equilibrium data with three different isotherm models (Langmuir, Freundlich, and Temkin) is shown in Figure 5-7 and parameters for each model is according to Table 5-8. According to the R-squared of each model, it is obvious that Temkin model is a better fit for NOM adsorption equilibrium study.

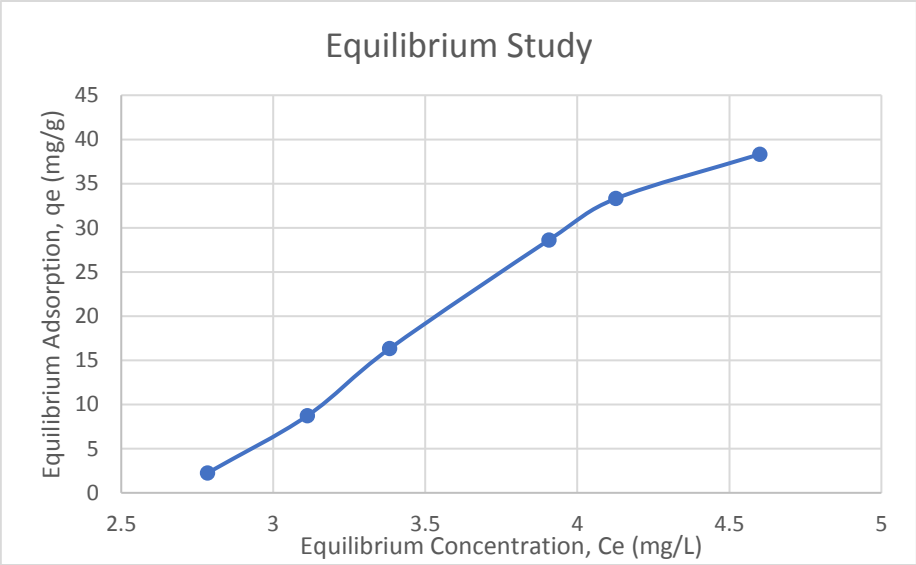

Figure 5-6: NOM Adsorption Isotherm, Equilibrium Study

a)

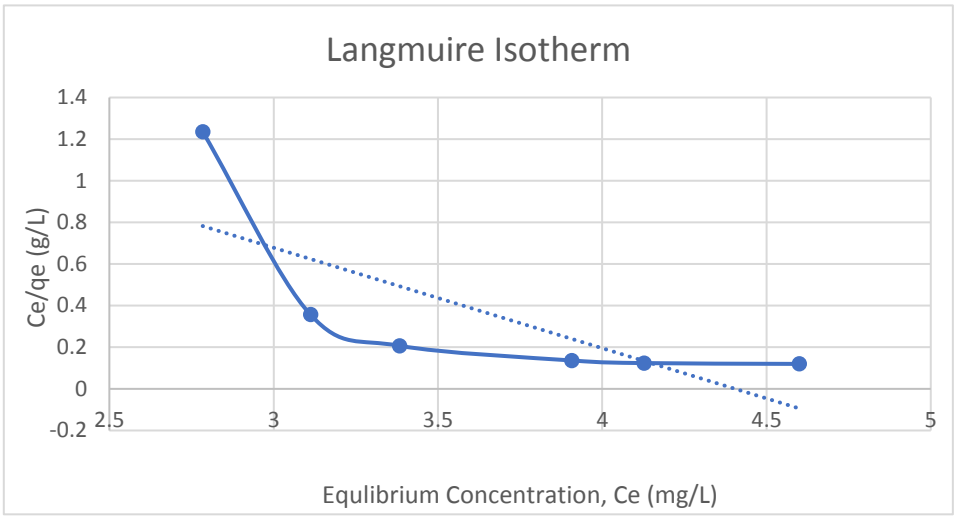
Langmuire Isotherm
Ce/qe (g/L)
1.4
1.2
1
0.8
0.6
0.4
0.2
0
-0.2
2.5
3
3.5
4
4.5
5
Equlibrium Concentration, Ce (mg/L)

b)

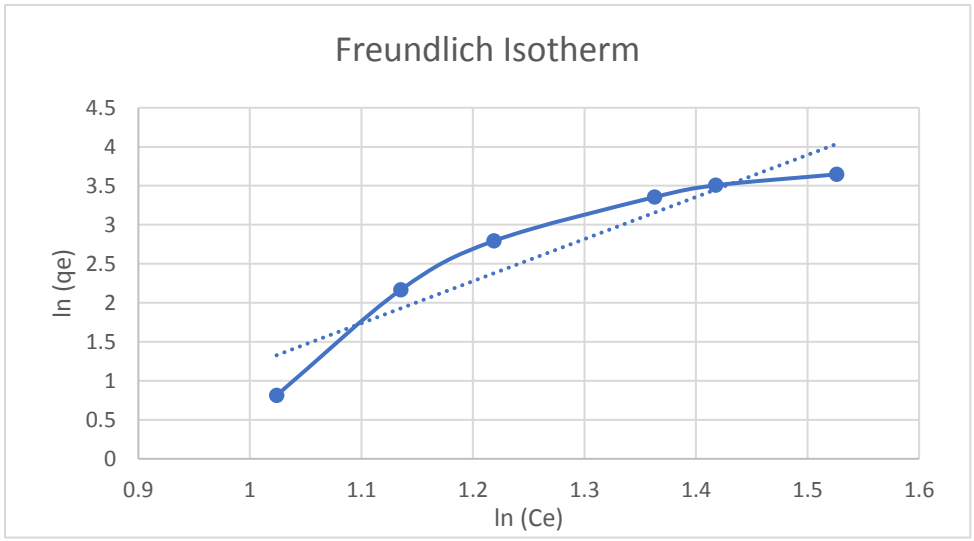
Freundlich Isotherm
ln (qe)
4.5
4
3.5
3
2.5
2
1.5
1
0.5
0
0.9
1
1.1
1.2
1.3
1.4
1.5
1.6
ln (Ce)

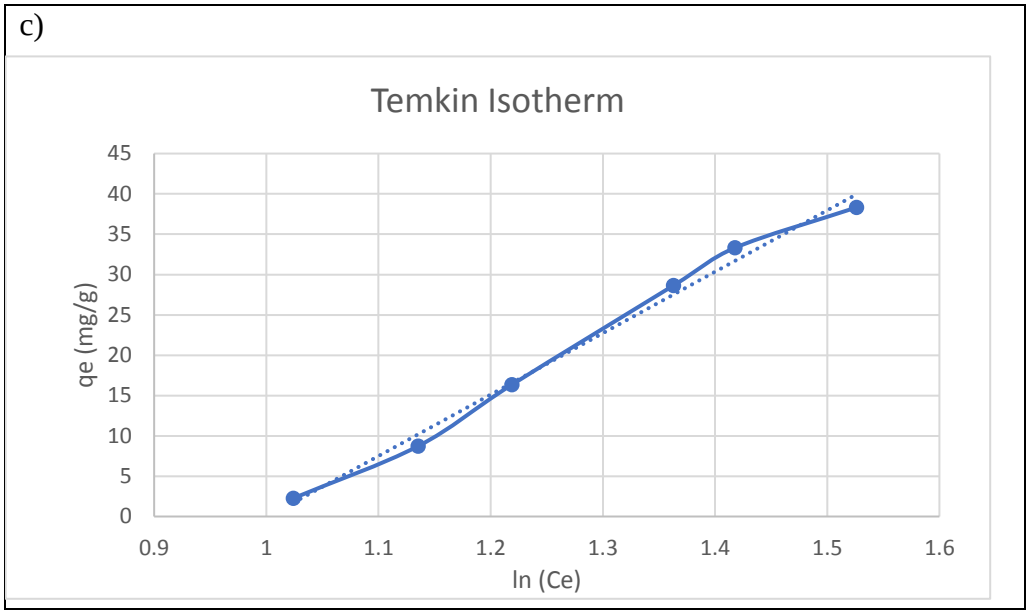

Figure 5-7: NOM Adsorption Isotherm models: a) Langmuir, b) Freundlich, c) Temkin

Table 5-8: Isotherm Models Parameters for NOM Adsorption

Langmuir Isotherm	**R^2**	**K_L**	**q_{max}**
	0.5641	-4.41	0.47
Freundlich Isotherm	**R^2**	**K_F**	**n**
	0.8819	0.015	0.19
Temkin Isotherm	**R^2**	**K_T**	**B**
	0.9913	0	0.013

5.3 NOM Adsorption: Column Test

A breakthrough curve in an adsorption system is a curve of adsorptive concentration versus time (McCabe et al., 1993). Breakthrough curve for NOM adsorption using GAC was provided for bed length of 5, 9, and 12 cm. The results are according to Figure 5-8. It is clear that by increasing the length of bed from 5 cm by using 8 g of GAC

to 12 cm (17 g of GAC), the adsorption at the beginning and required time for saturation has increased. The breakthrough curves using UV analyzer is provided in Figure 5-8b which also shows the same trend.

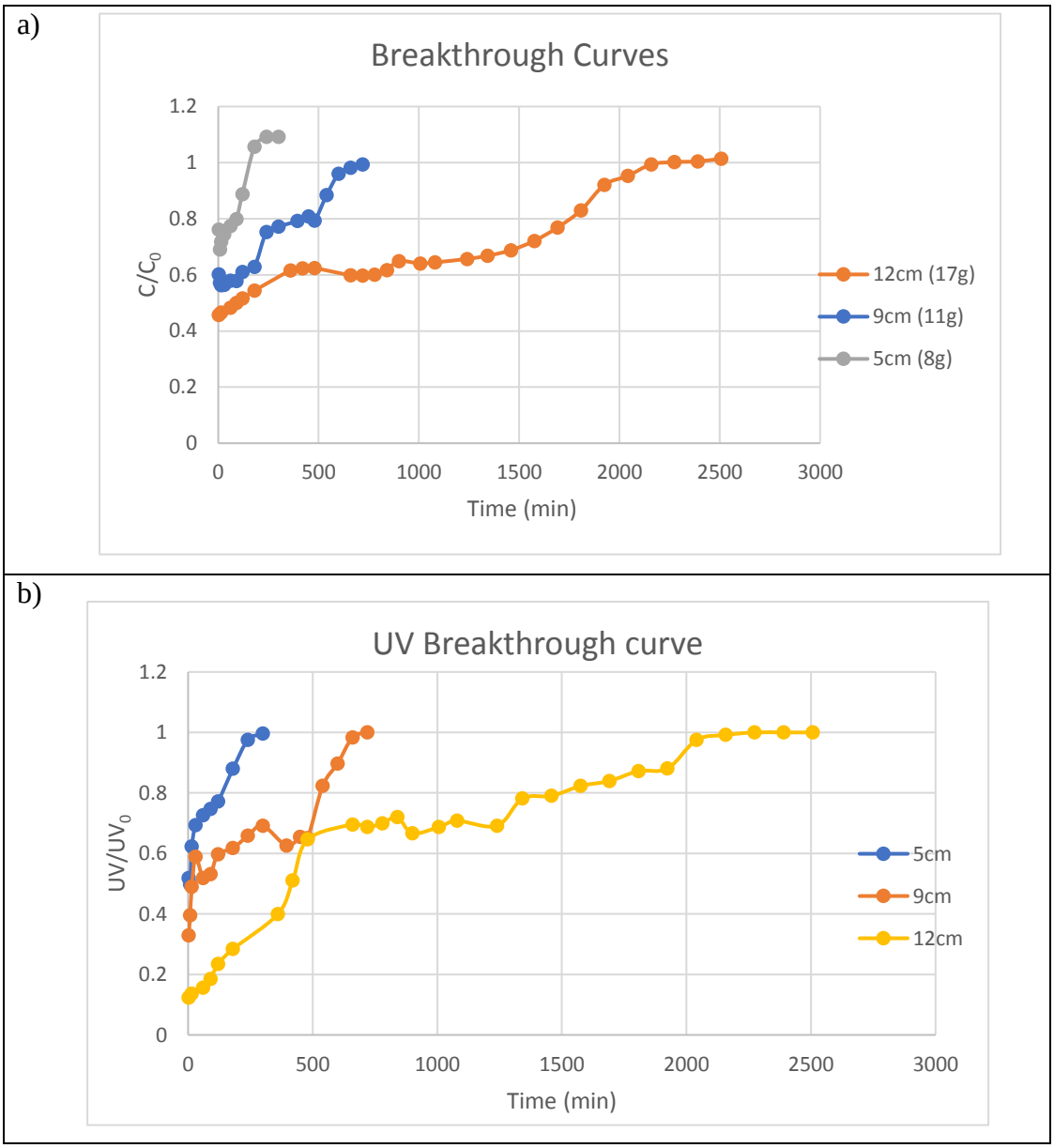

Figure 5-8: Breakthrough Cuves for NOM adsorption a)Concentration b)UV

5.3.1 Elemental Analysis for Treated water

Elemental analysis of raw and treated water is reported in Table 5-9, and it can be concluded that hazardous elements including cadmium, chromium, lead, arsenic, barium, and uranium were leached to the water from GAC (see Table 4-9). However, according to Canadian guideline, the concentration of mentioned elements are lower than the maximum allowable concentrations of each element in drinking water which are 0.005, 0.05, 0.01, 0.01, 1, and 0.02 ppm, respectively (Water & Organization, 2000).

Table 5-9: Elemental analysis for treated water

Element	Raw water (ppb)	Treated water (ppb)	Maximum allowable concentration (ppm)	Detection limit (DL) (ppb)
Li	0.253	4.02	-	0.106
Mg	1068.403	2054.989	-	0.805457
Al	47.7	37	-	0.294
P	< DL	43.5	-	23.437
Cl	11161.09	10557.22	2.0	1,043.707
Ca	2060.115	7037.178	-	45.5177
Ti	0.541	0.416	-	0.1491
V	< DL	49.6	-	1.411
Cr	< DL	0.193	0.05	0.138
Mn	2.82	6.94	-	0.031
Fe	154	115	-	7.2785
Co	0.0276	0.0128	-	0.0116
Ni	0.275	0.257	-	0.0690
Cu	1.41	0.851	-	0.1005
As	< DL	0.214	0.01	0.16
Br	54.8	30.5	-	5.4043
Rb	0.319	5.13	-	0.0325
Sr	7.5	41.7	5	0.0072
Mo	0.0551	6.01	-	0.0286
Cd	< DL	0.0222	0.005	0.0094
Cs	< DL	0.157	10 (Bq/L)	0.0118
Ba	2.59	63.4	1	0.0276
La	0.0482	0.0387	-	0.0099
Ce	0.0491	0.0302	-	0.0094
Pb	0.0809	0.101	0.01	0.0175
U	< DL	0.0286	0.02	0.0134

5.4 Chlorination

NOM and their characterization in water before adding disinfectant and contact time between NOM and disinfectant have a significant effect on DBPs formation. In this

study, treated water collected from column test at 60, 180, 480, 1300, and 1800 minutes were chlorinated for 1, 8, and 36 hours contact time to determine the formation potential of THMs and HAAs in the chlorinated water. Chlorination dose was controlled, so the concentration of free chlorine was maintained in a range of 0.04-2.0 mg/L, according to Canadian guideline (Health Canada, 2017). Table 5-10 shows the time and amount of treated water for sample collection. TOC level of the treated sample is also shown in the table.

Table 5-10: Sample collection for chlorination

Time (min)	Treated water (mL)	TOC level (mg/L)
60	360	3.631
180	1080	4.087
480	2880	4.689
1300	7800	5.02
1800	10,800	6.24

As discussed before, due to potential carcinogenic DBPs, drinking water regulations across the world needs proper monitoring for the concentration of DBPs. There are more than 600 DBPs due to the reaction of NOM with chlorine, and it is difficult to track all of them. Two groups of DBPs, Trihalomethanes (THMs) and Haloacetic acids (HAAs) have attracted much attention due to high formation potential (Zhang *et al.*, 2017). In the following sections, the effect of TOC removal on the THM and HAA formation will be discussed.

5.4.1 THMs Analysis After Chlorination

The THMs group includes four compounds: Chloroform ($CHCl_3$), Bromodichloromethane ($CHCl_2Br$), Dibromochloromethane ($CHClBr_2$), and Bromoform ($CHBr_3$). Figure 5-9 and Table 5-11 show the results for total THMs formation and their compounds, respectively.

Figure 5-9 displays the total THM concentrations for raw and treated water during chlorination. As shown in Figure 5-9, the total THM concentration is increasing with chlorination contact time. For raw water, 40% of all THMs are formed within the first hour of chlorination. THMs concentrations are gradually increasing for treated water, and the increasing rate is at a lower rate rather than raw water. Raw water has a THM concentration of 2270 ppb after 36hr of chlorination, while the THM concentrations of 36hr chlorination for the column 60, 180, 480, 1330, and 1800 minutes treated samples are 852 ppb, 868 ppb, 1059 ppb, 1120 ppb, and 1132 ppb, respectively. This matter indicates that the column filtration is effective and can significantly reduce THMs levels in Pouch Cove drinking water (more than 50%). From Table 5-11, it is clear that the chloroform ($CHCl_3$) is a dominant compound in total THM concentration. Moreover, comparing Dibromochloromethane ($CHClBr_2$), and Bromoform ($CHBr_3$) concentration in raw and treated water, it is obvious mentioned compounds are only forming in raw water and that the potential for the formation of these compounds is eliminated after treating.

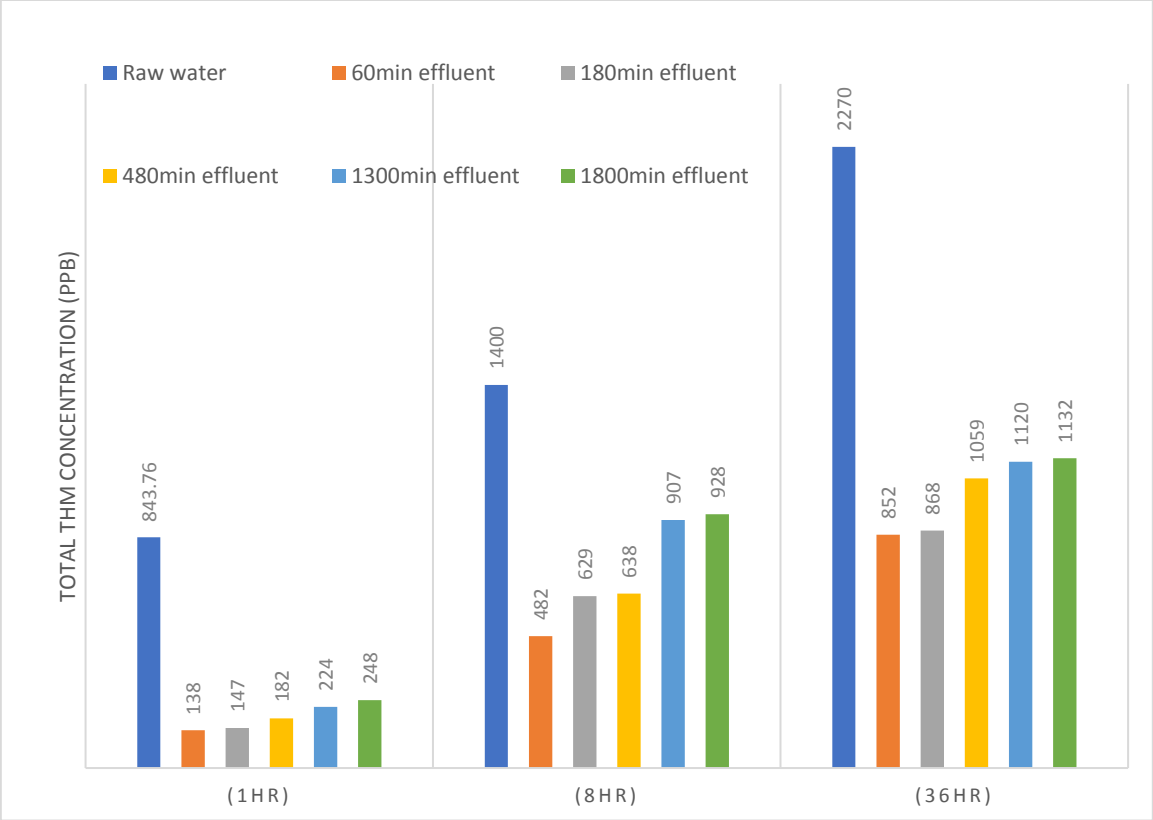

Figure 5-9: Total THMs in raw and Treated samples after chlorination

Table 5-11: THM compounds in raw and treated water

THMs	Raw Water (ppb)			50min effluent (ppb)			180min effluent (ppb)		
Chlorination time (hr)	**1**	**8**	**36**	**1**	**8**	**36**	**1**	**8**	**36**
$CHCl_3$	780.82	1350.3	2148.3	119.5	420.7	774.7	130.9	552.9	776.2
$CHCl_2Br$	46.78	29.2	84.1	18.1	61.1	77.5	15.7	75.6	91.7
$CHClBr_2$	3.20	5.5	12.6	0	0	0	0	0	0
$CHBr_3$	12.96	15	25	0	0	0	0	0	0
Total THMs	843.76	1400	2270	137.6	481.8	852.2	146.6	628.5	867.9
	480min effluent (ppb)			**1300min effluent (ppb)**			**1800min effluent (ppb)**		
Chlorination time (hr)	**1**	**8**	**36**	**1**	**8**	**36**	**1**	**8**	**36**
$CHCl_3$	149.33	577.3	955.52	193.1	825.6	1028	206.5	821.4	1047.4
$CHCl_2Br$	32.64	60.64	103.28	30.7	81.1	92.0	41.5	106.4	84.4
$CHClBr_2$	0	0	0	0	0	0	0	0	0
$CHBr_3$	0	0	0	0	0	0	0	0	0
Total THMs	181.97	637.94	1058.8	223.8	906.7	1120	248	927.8	1131.8

5.4.2 HAAs Analysis After Chlorination

The HAAs group includes nine compounds of Monochloroacetic acid (MCAA), Monobromoacetic acid (MBAA), Dichloroacetic acid (DCAA), Trichloroacetic acid (TCAA), Bromochloroacetic acid (BCAA), Bromodichloroacetic acid (BDCAA), Dibromoacetic acid (DBAA), Dibromochloroacetic acid (DBCAA), and Tribromoacetic

acid (TBAA). Figure 5-10 and Table 5-12 shows the results for total HAAs formation and their individual compounds, respectively.

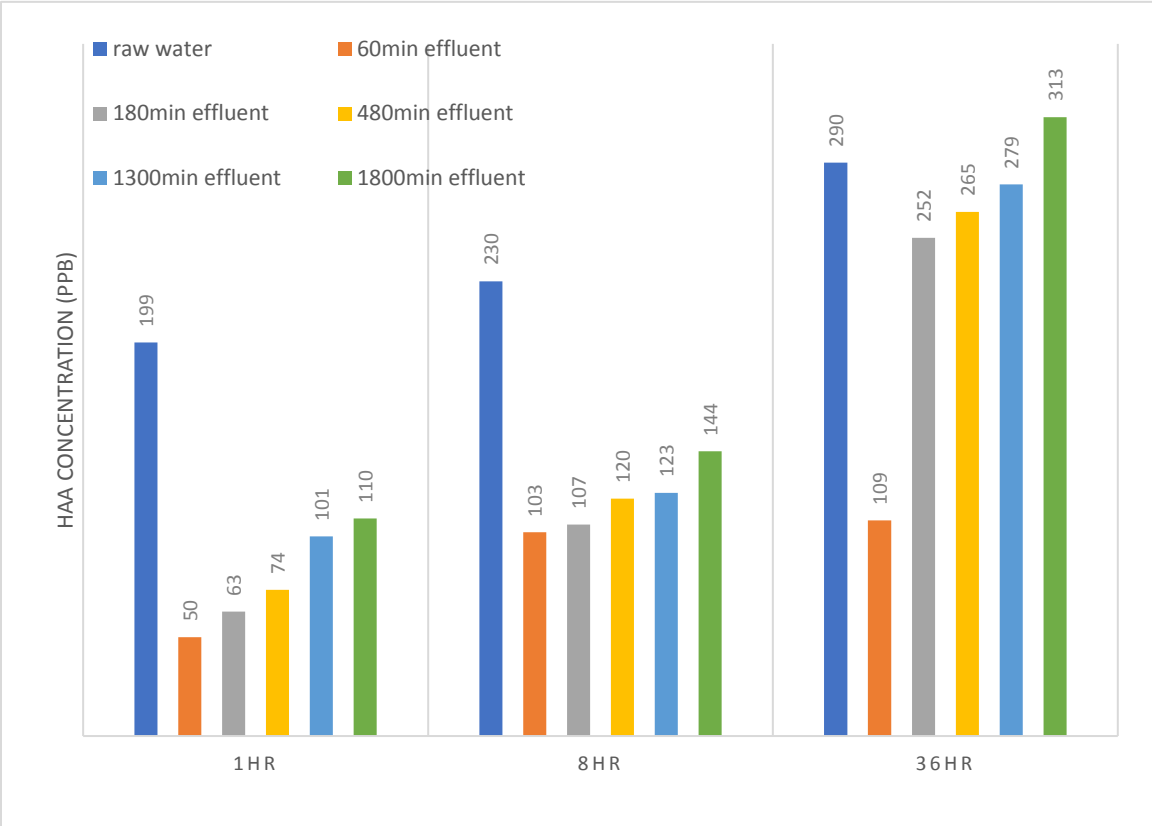

Figure 5-10: Total HAAs in raw and Treated samples after chlorination

Table 5-12: HAA compounds in raw and treated water

HAAs	Raw water (ppb)			60min effluent (ppb)			180min effluent (ppb)		
Chlorination time (hr)	1	8	36	1	8	36	1	8	36
MCAA	0.05	0.05	0.05	0	0	0	0	0	77.17
MBAA	1.68	2.86	3.2	0	0	0	0	0	0.05
DCAA	147.9	175.5	227.1	18.40	58.06	58.75	26.78	61.39	112.67
TCAA	32.7	33.59	35.03	10.97	16.12	29.54	10.92	17.74	36.10
BCAA	9.54	10.01	13.7	6.57	10.04	8.84	8.22	10.56	16.37
BDCAA	0.95	0.9	0.9	1.15	1.29	1.81	1.0793	1.3625	2.61
DBAA	0	0	0	0	2.56	2.55	4.31	0	2.89
CDBAA	6.6	7	9	12.87	14.99	7.31	12.06	15.56	4.62
TBAA	0	0	0	0	0	0	0	0	0
Total HAAs	199.42	229.91	289.98	49.96	103.06	108.8	63.38	106.61	252.48
	48 min effluent (ppb)			1300min effluent (ppb)			1800min effluent (ppb)		
Chlorination time (hr)	1	8	36	1	8	36	1	8	36
MCAA	0	0	5.19	0	0	0	0	0	75.05
MBAA	0	0	1.36	0	0	0	0	0	2.389
DCAA	33.06	66.08	150.27	52.2	66.91	161.9	58.9	86.21	144.45
TCAA	12.9	25.2	77.96	20.58	21.95	85.44	30.62	28.82	60.55
BCAA	9.05	11	17.64	11.01	11.03	19.01	8.8	13.56	17.93
BDCAA	1.16	1.92	4.37	1.61	1.67	4.76	1.61	1.8977	3.76
DBAA	5.32	2.59	2.75	2.58	2.71	2.83	2.55	2.67	3.04
CDBAA	12.63	13.24	5.49	13.17	18.39	4.89	7.68	10.77	5.88
TBAA	0	0	0	0	0	0	0	0	0
Total HAAs	74.12	120.03	265.03	101.15	122.66	278.83	110.16	143.93	313.05

Figure 5-10 shows the total HAA concentration of raw and column treated water for a different period of chlorination. Similar to THM results as listed in Figure 5-9, concentrations of HAAs in all samples are increasing by increasing the chlorination contact time. Except for 36hr of chlorination for 1800minute effluent sample, HAA concentration of all samples is lower than raw water samples which prove that carbon filtration can remove precursors causing the formation of HAAs in the water. All column filtered samples show that at the beginning of water treatment, fresh GACs were more capable of reducing HAA concentration; the HAA concentration in treated water is slightly different from the concentration of HAA in raw water near the end of the adsorption process. Also, because using GAC for water treatment would result in a lower concentration of DBPs, comparing the results of HAA removal with THM, shows that THM formation was reduced at a higher level than HAA formation. It is therefore revealed that the column test is more efficient regarding the reduction of THM formation than HAA.

The concentration of each compound of HAA compounds is listed in Table 5-12. For all chlorinated samples, DCAA is the dominant compound among all HAA compounds. TCAA and BCAA are also important formed components after DCAA in the total HAAs concentration. The concentration of BDCAA, DBAA, CDBAA, and TBAA during the chlorination process are very limited in both raw and treated water. In some treated samples, the concentration of MCAA is decreasing for 1hour and 8hours of chlorination while after 36 hours of chlorination, the concentration of MCAA is even higher than the raw sample. This matter can be due to the leaching of substances from adsorbent to the water as discussed in section 5.3.1.

5.5 GAC Regeneration

As discussed in section 3.3.4, the effects of regeneration temperature, time, and steam flow on regeneration efficiency were studied. 13 different experiments were considered using the design of experiment (Table 5-13). For each experiment, spent GACs loaded with adsorbed NOM were washed with deionized water several times to remove impurities. The washed spent GAC were dried in an oven at 105°C. The regeneration process was carried out by placing the 2 g of spent GAC in a tubular furnace. The target temperature according to Table 5-13 was set along with nitrogen flow of designed value. Upon reaching the designed temperature, nitrogen was replaced with CO_2 and steam at the designed flow rate. The regeneration time was according to designed value and spent GAC was left in the reactor until the end of the time.

Table 5-13 lists the results of MB, IN, and hardness of regenerated GAC at a different temperature, time, and gas flow. Three responses have been considered to determine the optimum condition in which the MB, IN, and hardness of regenerated GAC are at the maximum level, simultaneously. Third response was considered (1-hardness) to signify the difference between each experiment.

ANOVA table for MB adsorption, IN adsorption, and hardness are reported in Table 5-14, Table 5-15, and Table 5-16 respectively. Probe>F value for all responses are less than 0.05 which shows that all three models are significant. Moreover, regeneration temperature and gas flow are significant factors and affect MB, IN, and hardness of

regenerated carbon according to Probe>F value of less than 0.05. Also, time of regeneration process has a significant factor on MB and hardness.

The Pred R-Squared of MB adsorption of 0.9343 is in reasonable agreement with the Adj R-Squared of 0.8874. The Adeq Precision of 15.417 indicates an adequate signal. The Pred R-Squared of IN of 0.9554 is in reasonable agreement with the Adj R-Squared of 0.9108. Adeq Precision of IN of 12.887 indicates an adequate signal. Also, the Pred R-Squared for (1-Hardness) is 0.8522 which is in reasonable agreement with the Adj R-Squared of 0.8029. The Adeq Precision of 12.487 indicates an adequate signal.

Increasing regeneration temperature, time, and gas flow would increase the MB adsorption and decrease the hardness. This matter is due to pore widening and reactivation. However, for IN adsorption, increasing the temperature and gas flow to would reduce due to pore widening from micropores to mesopores. Final equation for MB adsorption, IN, and (1-hardness) for regeneration is according to Equation (5.4), Equation (5.5), and Equation (5.6), respectively. The equation is used to predict a final answer using actual units. Since the pred-R^2 for all responses are close to 1, the equations can be used to predict the responses in different conditions without experiments.

Table 5-13: Results of thermal regeneration

Time (min)	Temperature (°C)	Flow (mL/min)	Response 1: MB	Response 2: IN	Response 3: 1-Hardness
75	800	350	218.96	1223.9	19.36
30	800	350	208.99	1195.76	9.48
120	800	350	300.91	1223.9	22.17
45	690	250	196.3	1157.54	8.62
75	800	200	243.04	1102.7	14.98
75	800	350	252.02	1212.49	15.58
75	800	500	281.86	1217.8	20.56
75	950	350	345.65	1208.86	21.51
75	650	350	174.39	1156.39	11.51
75	800	350	245.14	1227.97	16.05
105	690	450	244.03	1214.92	18.37
105	905	250	264.93	1140.77	16.94
45	905	450	315.01	1211.28	16.94

Table 5-14: ANOVA for MB adsorption

Source	Sum of Squares	df	Mean Square	F Value	p-value Prob > F
Model	26566.34	5	5313.27	19.92	0.0005
A-Time	4189.27	1	4189.27	15.70	0.0054
B-Temp	14639.08	1	14639.08	54.87	0.0001
C-Flow/H	2969.62	1	2969.62	11.13	0.0125
AC	1375.40	1	1375.40	5.16	0.0574
BC	2028.86	1	2028.86	7.60	0.0282
Residual	1867.54	7	266.79		
Lack of Fit	1258.90	5	251.78	0.83	0.6269
Pure Error	608.64	2	304.32	Pure Error	608.64
Cor Total	28433.88	12		Cor Total	28433.88

Table 5-15: ANOVA for IN adsorption

Source	Sum of Squares	df	Mean Square	F Value	p-value Prob > F
Model	17832.76	6	2972.13	21.41	0.0008
A-Time	99.56	1	99.56	0.72	0.4295
B-Temp	1363.90	1	1363.90	9.83	0.0202
C-Flow/H	10626.94	1	10626.94	76.56	0.0001
AC	1188.06	1	1188.06	8.56	0.0264
B^2	1609.03	1	1609.03	11.59	0.0144
C^2	4685.18	1	4685.18	33.75	0.0011
Residual	832.80	6	138.80		
Lack of Fit	704.05	4	176.01	2.73	0.2853
Pure Error	128.75	2	64.37		
Cor Total	18665.56	12			

Table 5-16: ANOVA for Hardness

Source	Sum of Squares	df	Mean Square	F Value	p-value Prob > F
Model	191.74	3	63.91	17.30	0.0004
A-Time	97.54	1	97.54	26.39	0.0006
B-Temp	55.58	1	55.58	15.04	0.0037
C-Flow/H	38.63	1	38.63	10.45	0.0103
Residual	33.26	9	3.70		
Lack of Fit	24.79	7	3.54	0.84	0.6424
Pure Error	8.47	2	4.23		
Cor Total	225.00	12			

MB=692.7-2.06*time-0.4372*temperature-13.8793*flow +0.04*time*flow+ 0.014*temperature*flow **(5.4)**

IN=7.63-2.75*time+2.33*temperature+6.98*flow+ 0.04*time*flow - 0.001*temperature2-0.06*flow2 **(5.5)**

1-hardness= -19.3 + .11*time + 0.02*temperature+ 0.1*flow **(5.6)**

5.5.1 Regeneration Optimization

The model was optimized by numerical optimization of Design-Expert software. By setting the goal of maximum MB, maximum IN, and minimum (1-hardness), conditions according to Table 5-17 was achieved. Applying the conditions was concluded in IN of 1150 mg/g, MB of 280 mg/g, and hardness of 85% (1-hardness of 15%). Higher MB of regenerated GAC rather than original GAC is a sign for pore widening and release of some NOM from pores. On the other hand, lower IN for regenerated GAC rather than original GAC is showing that regeneration was not able to remove all adsorbed NOM from used GAC.

Table 5-17: Optimum Condition for GAC regeneration

Time (min)	Temperature (°C)	Flow (mL/min)	MB (mg/g)	IN (mg/g)	Hardness (%)
43.180	916.613	350	286.585	1214.770	15.516

5.6 NOM Adsorption: Column Test, Regenerated carbon

Regeneration was optimized according to section 5.5. To find the regeneration efficiency, used GAC as discussed in section 5.3, were regenerated and the same steps were applied to find the breakthrough curves for NOM adsorption using regenerated GAC. Three runs of column tests for NOM adsorption were applied and between each step, used GAC was regenerated according to section 5.5.1. The results are according to Figure 5-11.

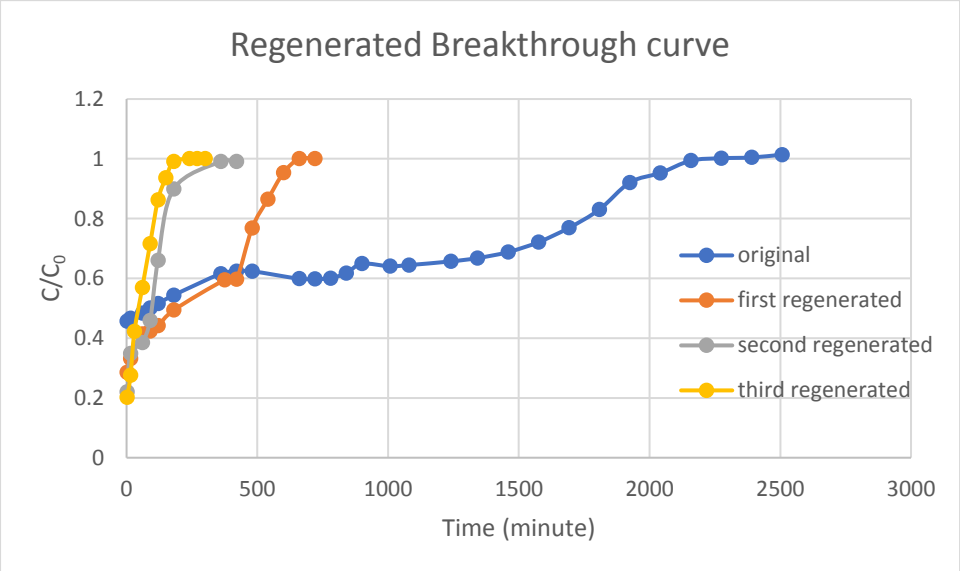

Figure 5-11: Breakthrough Curves for NOM adsorption using regenerated GAC

Comparing the results for NOM adsorption using regenerated GAC and comparing MB and IN of original GAC and regenerated GAC, the higher NOM adsorption in the beginning and fast saturation of regenerated GAC can be justified. Unfortunately, fast saturation of regenerated GAC shows that the regeneration was not successful. It is necessary to mention that increasing time, flow and temperature of regeneration would decrease the hardness for regenerated GAC to lower than 85%.

Chapter 6 Conclusions and Recommendations

6.1 Conclusions

In this research, two forms of activated carbon (PAC and GAC) were used to remove NOM from drinking water. The water sample was collected from North Three Island pond which is a source of drinking water for Pouch Cove, Newfoundland. Raw materials for the activated carbon was obtained from Corner Brook Pulp and Paper (CBPP) mill ash which contains above 80% carbon. The carbon was extracted from ash, and it was cleaned and activated with and without a binder to make GAC and PAC for research.

To provide a comprehensive study, chemical and physical characterizations were applied to both adsorbents. Ash content, moisture content, pH, IN, MB, elemental analysis, BET surface area, and pore size distribution analysis were applied to characterize PAC and GAC. Since the same raw materials were used to produce PAC and GAC, the final characterizations of adsorbents were close, and both adsorbents showed high surface area and microporous structures.

PAC was used in batch tests to reduce NOM from Pouch Cove water. Response surface methodology was applied to study the effect of temperature, pH, and water volume on TOC removal using PAC. The study shows that the water volume and pH can have a significant effect on TOC removal. Adjusting pH to the acidic condition can greatly help for TOC removal. The adsorption kinetics and isotherm of NOM removal using PAC carried out in a batch experimental system. The results showed that the adsorption strongly

depends on initial PAC dose and Temkin isotherm was a better fit to equilibrium data. Also, the rate of NOM adsorption follows the pseudo-second-order model.

Raw CBPP washed CBPP, and PAC was mixed with different binders including CMC, S-CMC, CS, PVA, and bitumen to produce GAC. Apart from bitumen, it was found that none of the other binders were able to produce cohesive granules. In results, GAC was produced using a mixture of hexane, washed CBPP, and bitumen. Produced extrudates at different binder to carbon ratio were calcinated and activated at a different temperature, temperature increasing rate, and activation time to determine the ideal condition for granulation. Different techniques including MB, IN, and hardness were applied to determine the efficiency of GAC production.

The following conclusions are drawn from this study on GAC experiment:

1. Extrudates of 30:70 binder to carbon ratio calcinated temperature at 750 °C for 1hr, activated at 950 °C with 80 °C steam for 3 hours under 15 °C/min heating rate was found optimum for best adsorption capacity and mechanical strength
2. MB, IN, and hardness of optimized GAC were approximately 241mg/g, 1420 mg/g, and 85%, respectively.
3. The study showed that produced GAC has a high potential for efficiently removal of NOM from raw water.
4. The packed column of 12 cm height and 2.5 cm diameter GAC removed more than 60% of NOM from water for over 36 hours (17 L of raw water).

Chlorination was carried out on both treated and raw water for 1, 8, and 36 hours of contact time. The result showed that chlorination of treated water for 36hours would result in 80% lower THMs concentrations rather than raw water. Also, dibromochloromethane and bromoform would not form by chlorination of treated water. Also, the concentration of HAAs in treated water reduced by 50% in comparison with raw water. The formation of DCAA compound in treated water reduced significantly and MCAA, MBAA, and TBAA did not form after the chlorination of treated water.

Spent GAC in column test were regenerated at different temperature (650-950 °C), time (30-120 minutes), and steam flow rate (200-500 cm^3/min) using response surface methodology. MB, IN, and hardness were considered as response variables, and the regeneration optimization was based on all three responses, simultaneously.

When GAC was used for removal of THM and HAA, the following conclusions are drawn:

1. Regeneration for 43 minutes at 916 °C under 350 cm^3/min of steam flow rate was found optimal, and the regenerated GAC was effective to remove NOM for around 12 hours (4.5L of water).
2. Original and regenerated GAC removed more than 80% of total THM and 50% of total HAA.

6.2 Major Research Contributions

Environment-friendly and low-cost methods to reduce NOM from Pouch Cove, a small community near St. John's, were developed in this thesis. Major contributions of the research are listed in the following:

1. The optimum condition for NOM removal was obtained through maximizing capacity of the adsorbent (PAC) and minimizing DBPs formation.
2. The optimum condition for producing GAC was determined using a low-cost binder to provide a potential affordable water treatment system in small communities.
3. Results of the study shows significant performance regarding NOM adsorption and hence, high THMs and HAAs reduction
4. The optimum condition for GAC regeneration was obtained to reduce operational costs for water treatment.

6.3 Recommendations and Future Works

The following recommendations are made for future studies:

1. The analysis on NOM adsorption was based on only one community in this study. To have a comprehensive study on GAC and to assess its effectiveness to remove NOM, water samples from different locations and season should be analyzed.
2. Surface modification on generated GAC would help to improve its capacity regarding NOM removal.

3. Studying the effects of produced GAC regarding heavy metal removal would help to improve the practical performance of generated GAC in different aspects of water treatment.
4. According to some pretests, using two columns in series in a way that effluent of the first column can be considered as feed for the second column can improve the NOM adsorption to more than 80% removal.
5. Optimization for second and third regeneration can be another recommendation to improve reusing GAC and increasing its adsorption capacity.

References

.

Ahmadpour, A. and D. Do, 1996: The preparation of active carbons from coal by chemical and physical activation. *Carbon,* **34,** 471-479.

Ahmedna, M., M. Johns, S. Clarke, W. Marshall and R. Rao, 1997: Potential of agricultural by‐product‐based activated carbons for use in raw sugar decolourisation. *Journal of the Science of Food and Agriculture,* **75,** 117-124.

Ahmedna, M., W. Marshall and R. Rao, 2000: Surface properties of granular activated carbons from agricultural by-products and their effects on raw sugar decolorization. *Bioresource technology,* **71,** 103-112.

Al Bahri, M., L. Calvo, M. Gilarranz and J. J. Rodríguez, 2012: Activated carbon from grape seeds upon chemical activation with phosphoric acid: Application to the adsorption of diuron from water. *Chemical Engineering Journal,* **203,** 348-356.

Alam, M. Z., S. A. Muyibi and J. Toramae, 2007: Statistical optimization of adsorption processes for removal of 2, 4-dichlorophenol by activated carbon derived from oil palm empty fruit bunches. *Journal of Environmental Sciences(China),* **19,** 674-677.

Amaya, A., N. Medero, N. Tancredi, H. Silva and C. Deiana, 2007: Activated carbon briquettes from biomass materials. *Bioresource Technology,* **98,** 1635-1641.

Amy, G., R. Bull, G. F. Craun, R. Pegram, M. Siddiqui and W. H. Organization, 2000: Disinfectants and disinfectant by-products.

Azizian, S., 2004: Kinetic models of sorption: a theoretical analysis. *Journal of colloid and Interface Science,* **276,** 47-52.

Baccar, R., J. Bouzid, M. Feki and A. Montiel, 2009: Preparation of activated carbon from Tunisian olive-waste cakes and its application for adsorption of heavy metal ions. *Journal of Hazardous Materials,* **162,** 1522-1529.

Balathanigaimani, M., W.-G. Shim, J.-W. Lee and H. Moon, 2009: Adsorption of methane on novel corn grain-based carbon monoliths. *Microporous and Mesoporous Materials,* **119,** 47-52.

Banat, F., S. Al-Asheh and L. Makhadmeh, 2003: Preparation and examination of activated carbons from date pits impregnated with potassium hydroxide for the removal of methylene blue from aqueous solutions. *Adsorption Science & Technology,* **21,** 597-606.

Beckett, A. H. and J. B. Stenlake, 1988: *Practical Pharmaceutical Chemistry: Part II Fourth Edition*. A&C Black.

Bellar, T. A., J. J. Lichtenberg and R. C. Kroner, 1974: The occurrence of organohalides in chlorinated drinking waters. *Journal‐American Water Works Association,* **66,** 703-706.

Bjelopavlic, M., G. Newcombe and R. Hayes, 1999: Adsorption of NOM onto activated carbon: effect of surface charge, ionic strength, and pore volume distribution. *Journal of colloid and interface science,* **210,** 271-280.

Carvalho, A., A. Mestre, J. Pires, M. Pinto and M. E. Rosa, 2006: Granular activated carbons from powdered samples using clays as binders for the adsorption of organic vapours. *Microporous and Mesoporous Materials,* **93,** 226-231.

Cazetta, A. L., O. P. Junior, A. M. Vargas, A. P. Da Silva, X. Zou, T. Asefa and V. C. Almeida, 2013: Thermal regeneration study of high surface area activated carbon obtained from coconut shell: Characterization and application of response surface methodology. *Journal of analytical and applied pyrolysis,* **101,** 53-60.

Chaulk, M. and G. Sheppard, 2011: Study on Characteristics and Removal of Natural Organic Mater in Drinking Water Systems in Newfoundland and Labrador. Newfoundland Labrador Department of Environment and Conservation Division WM; 2011 August 2011. Report No. *Contract*.

Chow, C. W., R. Fabris, J. v. Leeuwen, D. Wang and M. Drikas, 2008: Assessing natural organic matter treatability using high performance size exclusion chromatography. *Environmental science & technology,* **42,** 6683-6689.

Clark, R. M. and B. K. Boutin, 2001: *Controlling disinfection by-products and microbial contaminants in drinking water*. National Risk Management Research Laboratory, Office of Research and Development, US Environmental Protection Agency.

Clarke, D. E. and H. Marsh, 1989: Factors influencing properties of coal briquettes. *Fuel*, **68,** 1031-1038.

Dąbrowski, A., 2001: Adsorption—from theory to practice. *Advances in colloid and interface science*, **93,** 135-224.

Dada, A., A. Olalekan, A. Olatunya and O. Dada, 2012: Langmuir, Freundlich, Temkin and Dubinin–Radushkevich isotherms studies of equilibrium sorption of Zn2+ unto phosphoric acid modified rice husk. *IOSR Journal of Applied Chemistry,* **3,** 38-45.

DeGroot, W. F. and G. Richards, 1989: Relative rates of carbon gasification in oxygen, steam and carbon dioxide. *Carbon,* **27,** 247-252.

Deiana, A., D. Granados, L. Petkovic, M. Sardella and H. Silva, 2004: Use of grape must as a binder to obtain activated carbon briquettes. *Brazilian Journal of Chemical Engineering,* **21,** 585-591.

DeSilva, F. J., 2000: Activated carbon filtration. *Water quality products***,** 16.

Din, M. I., S. Ashraf and A. Intisar, 2017: Comparative study of different activation treatments for the preparation of activated carbon: a mini-review. *Science Progress,* **100,** 299-312.

Domino, M., B. Pepich, D. Munch, P. Fair and Y. Xie, 2003: EPA Method 552.3, Revision 1.0: Determination of haloacetic acids and Dalapon in drinking water by liquid-liquid microextraction, derivatization, and gas chromatography with electron capture detection. EPA/815/B-03/002.

Drikas, M., M. Dixon and J. Morran, 2011: Long term case study of MIEX pre-treatment in drinking water; understanding NOM removal. *Water research,* **45,** 1539-1548.

Duan, X. H., C. Srinivasa Kannan, W. W. Qu, X. Wang, J. H. Peng, L. B. Zhang and H. Y. Xia, 2012: Thermal regeneration of spent coal‐based activated carbon using carbon dioxide: process optimisation, Methylene Blue decolorisation isotherms and kinetics. *Coloration Technology*, **128,** 464-472.

El-Demerdash, F., A. Abdullah and D. Ibrahim, 2015: Removal of Trihalo methanes using activated carbon prepared from agricultural solid wastes. *Hydrology: Current Research*, **6,** 1.

Everett, D., 1972: IUPAC manual of symbols and terminology for physicochemical quantities and units. App. II, Part I. *Pure Appl. Chem*, **21,** 584-594.

Fabris, R., C. W. Chow, M. Drikas and B. Eikebrokk, 2008: Comparison of NOM character in selected Australian and Norwegian drinking waters. *Water research*, **42,** 4188-4196.

Figaro, S., J. Avril, F. Brouers, A. Ouensanga and S. Gaspard, 2009: Adsorption studies of molasse's wastewaters on activated carbon: Modelling with a new fractal kinetic equation and evaluation of kinetic models. *Journal of hazardous materials*, **161,** 649-656.

GAN, Q., X. ZHOU, B. ZHAO and K. HU, 2006: The Advance of Research on Formed Activated Carbon Preparation [J]. *Materials Review*, **1,** 018.

Goi, D., F. Tubaro, F. Barbone, G. Dolcetti and G. Bontempell, 2005: Evaluation of Chlorinated By‐Products in Drinking Waters of Clentral Friuli (Italy). *Annali di chimica*, **95,** 617-627.

Guimont, F., 1980: The effect of capital and operation costs on GAC adsorption system design, Activated carbon adsorption of organics from the aqueous hase. *Annabor Science, Ann Abrbor, MI*, **1,** 980.

Harris, R. K., J. Kowalewski and S. C. de Menezes, 1998: International Union of Pure and Applied Chemistry Physical Chemistry Division Commission on Molecular Structure and Spectroscopy. Parameters and symbols for use in nuclear magnetic resonance (IUPAC recommendations 1997). *Magnetic Resonance in Chemistry*, **36,** 145-149.

Health Canada, 2017: *Guidelines for Canadian Drinking Water Quality*. Canadian Government Publishing.

Hesas, R. H., W. M. A. W. Daud, J. Sahu and A. Arami-Niya, 2013: The effects of a microwave heating method on the production of activated carbon from agricultural waste: a review. *Journal of Analytical and Applied Pyrolysis*, **100,** 1-11.

Ho, Y. and G. McKay, 1998: The kinetics of sorption of basic dyes from aqueous solution by sphagnum moss peat. *The Canadian Journal of Chemical Engineering*, **76,** 822-827.

Hodgeson, J., J. Collins, R. Barth, D. Munch, J. Munch and A. Pawlecki, 1995: METHOD 552.2 Determination of haloacetic acids and dalapon in drinking water by liquid-liquid extraction, derivatization and gas chromatography with electron capture detection. *Methods for the Determination of Organic Compounds in Drinking Water, Supplement III, US Environmental Protection Agency, Cincinnati, OH*, **45268**.

Humbert, H., H. Gallard, H. Suty and J.-P. Croué, 2008: Natural organic matter (NOM) and pesticides removal using a combination of ion exchange resin and powdered activated carbon (PAC). *Water Research*, **42,** 1635-1643.

Ioannidou, O. and A. Zabaniotou, 2007: Agricultural residues as precursors for activated carbon production—a review. *Renewable and sustainable energy reviews,* **11,** 1966-2005.

Jahan, M. I., M. A. Motin, M. Moniuzzaman and M. Asadullah, 2008: Arsenic removal from water using activated carbon obtained from chemical activation of jute stick.

Johns, M. M., W. E. Marshall and C. A. Toles, 1998: Agricultural by‐products as granular activated carbons for adsorbing dissolved metals and organics. *Journal of Chemical Technology & Biotechnology: International Research in Process, Environmental AND Clean Technology,* **71,** 131-140.

Kandiyoti, R., J. I. Lazaridis, B. Dyrvold and C. R. Weerasinghe, 1984: Pyrolysis of a ZnCI2-impregnated coal in an inert atmosphere. *Fuel,* **63,** 1583-1587.

Kerwick, M. I., S. M. Reddy, A. H. L. Chamberlain and D. M. Holt, 2005: Electrochemical disinfection, an environmentally acceptable method of drinking water disinfection? *Electrochimica Acta,* **50,** 5270-5277.

Kim, J., 2009: Fate of THMs and HAAs in low TOC surface water. *Environmental research,* **109,** 158-165.

Kim, J., Y. Chung, D. Shin, M. Kim, Y. Lee, Y. Lim and D. Lee, 2003: Chlorination by-products in surface water treatment process. *Desalination,* **151,** 1-9.

Kolka, R., P. Weishampel and M. Fröberg, 2008: Measurement and importance of dissolved organic carbon. *Field measurements for forest carbon monitoring.* Springer.

Korotta-Gamage, S. M. and A. Sathasivan, 2017: A review: Potential and challenges of biologically activated carbon to remove natural organic matter in drinking water purification process. *Chemosphere,* **167,** 120-138.

Kosobucki, P. and B. Buszewski, 2014: Natural organic matter in ecosystems-A review. *Nova Biotechnologica et Chimica,* **13,** 109-129.

Krasner, S., 1999: Chemistry of disinfection by-product formation. *Formation and control of disinfection by-products in drinking water***,** 27-52.

Kühl, H., M. Kashani-Motlagh, H.-J. Mühlen and K. Van Heek, 1992: Controlled gasification of different carbon materials and development of pore structure. *Fuel,* **71,** 879-882.

Lambert, S. D., G. S. Miguel and N. J. Graham, 2002: Deleterious effects of inorganic compounds during thermal regeneration of GAC: a review. *Journal‐American Water Works Association,* **94,** 109-119.

Largitte, L. and R. Pasquier, 2016: A review of the kinetics adsorption models and their application to the adsorption of lead by an activated carbon. *Chemical Engineering Research and Design,* **109,** 495-504.

Levesque, M., E. Kelly, N. Novakowski, O. Parpia, K. Hancock, S. Ganz, T. Philpott, G. Curtis and S. Pottle, 2010: Response to Corner Brook Pulp & Paper Tire Derived Fuel (TDF) Co-Firing Trial Project Proponent: Corner Brook Pulp & Paper Ltd.(Reg. 1539).

Li, M.-s., S. C. Wu, Y.-H. Peng and Y.-h. Shih, 2016: Adsorption of volatile organic vapors by activated carbon derived from rice husk under various humidity

conditions and its statistical evaluation by linear solvation energy relationships. *Separation and Purification Technology,* **170,** 102-108.

Liang, S., N. Ye, Y. Hu, Y. Shi, W. Zhang, W. Yu, X. Wu and J. Yang, 2016: Lead adsorption from aqueous solutions by a granular adsorbent prepared from phoenix tree leaves. *RSC Advances,* **6,** 25393-25400.

Liu, L., H. Ai, Y. Lin, Y. Liu and Q. He, 2014a: Adsorption of Methylene Blue on Sewage Sludge Based Granular Activated Carbon. *Asian Journal of Chemistry,* **26**.

Liu, L., Y. Lin, Y. Liu and Q. He, 2014b: Effect of Binders on Porous Properties, Surface Chemical Properties and Adsorption Characteristics of Granular Adsorbents from Sewage Sludge. *Materials Science,* **20,** 488-492.

Liu, W., S. Andrews, J. Bolton, K. Linden, C. Sharpless and M. Stefan, 2002: Comparison of disinfection byproduct (DBP) formation from different UV technologies at bench scale. *Water Science and Technology: Water Supply,* **2,** 515-521.

Lozano-Castello, D., D. Cazorla-Amoros, A. Linares-Solano and D. Quinn, 2002: Influence of pore size distribution on methane storage at relatively low pressure: preparation of activated carbon with optimum pore size. *Carbon,* **40,** 989-1002.

Lozano-Castelló, D., D. Cazorla-Amorós, A. Linares-Solano and D. Quinn, 2002: Activated carbon monoliths for methane storage: influence of binder. *Carbon,* **40,** 2817-2825.

Lu, G. and D. Do, 1992: A kinetic study of coal reject-derived char activation with CO2, H2O, and air. *Carbon,* **30,** 21-29.

Ma, X., H. Yang, L. Yu, Y. Chen and Y. Li, 2014: Preparation, surface and pore structure of high surface area activated carbon fibers from bamboo by steam activation. *Materials,* **7,** 4431-4441.

Machnikowski, J., K. Kierzek, K. Lis, H. Machnikowska and L. Czepirski, 2010: Tailoring porosity development in monolithic adsorbents made of KOH-activated pitch coke and furfuryl alcohol binder for methane storage. *Energy & Fuels,* **24,** 3410-3414.

Machnikowski, J., K. Kierzek and K. Torchała, 2012: Adsorption capacity enhancement by activation with CO2 of monolithic adsorbents made of KOH-activated carbon and polymer-derived binder. *Energy & Fuels,* **26,** 3697-3702.

Maciá-Agulló, J., B. Moore, D. Cazorla-Amorós and A. Linares-Solano, 2004: Activation of coal tar pitch carbon fibres: Physical activation vs. chemical activation. *Carbon,* **42,** 1367-1370.

Malik, P. K., 2003: Use of activated carbons prepared from sawdust and rice-husk for adsorption of acid dyes: a case study of Acid Yellow 36. *Dyes and pigments,* **56,** 239-249.

Manocha, S. M., 2003: Porous carbons. *Sadhana,* **28,** 335-348.

Markets, A. C., 1994: Report No. 612. The Freedonia Group. *Inc. Cleveland, OH,* **161**.

McCabe, W. L., J. C. Smith and P. Harriott, 1993: *Unit operations of chemical engineering*. McGraw-hill New York.

McKay, G., Y. Ho and J. Ng, 1999: Biosorption of copper from waste waters: a review. *Separation and Purification Methods,* **28,** 87-125.
Menya, E., P. Olupot, H. Storz, M. Lubwama and Y. Kiros, 2017: Production and performance of activated carbon from rice husks for removal of natural organic matter from water: A review. *Chemical Engineering Research and Design*.
Metsämuuronen, S., M. Sillanpää, A. Bhatnagar and M. Mänttäri, 2014: Natural organic matter removal from drinking water by membrane technology. *Separation & Purification Reviews,* **43,** 1-61.
Mofarrah, A., 2014: Environmental management and potential use of heavy oil fly ash. Memorial University of Newfoundland.
Mofarrah, A., T. Husain and C. Bottaro, 2014: Characterization of activated carbon obtained from Saudi Arabian fly ash. *International Journal of Environmental Science and Technology,* **11,** 159-168.
Montgomery, D. C., 2017: *Design and analysis of experiments*. John wiley & sons.
Moreno-Castilla, C., 2004: Adsorption of organic molecules from aqueous solutions on carbon materials. *Carbon,* **42,** 83-94.
Morrow, C. M. and R. A. Minear, 1987: Use of regression models to link raw water characteristics to trihalomethane concentrations in drinking water. *Water Research,* **21,** 41-48.
Municipal Affairs and Environment-Government of Newfoundland and Labrador, 2018, March 13: Thms Summary for Public Water Supplies in Newfoundland and Labrador.
Newcombe, G., J. Morrison, C. Hepplewhite and D. Knappe, 2002: Simultaneous adsorption of MIB and NOM onto activated carbon: II. Competitive effects. *Carbon,* **40,** 2147-2156.
Nieuwenhuijsen, M. J., M. B. Toledano, N. E. Eaton, J. Fawell and P. Elliott, 2000: Chlorination disinfection byproducts in water and their association with adverse reproductive outcomes: a review. *Occupational and environmental medicine,* **57,** 73-85.
Olorundare, O., T. Msagati, R. Krause, J. Okonkwo and B. Mamba, 2014: Steam activation, characterisation and adsorption studies of activated carbon from maize tassels. *Chemistry and Ecology,* **30,** 473-490.
Patnukao, P. and P. Pavasant, 2008: Activated carbon from Eucalyptus camaldulensis Dehn bark using phosphoric acid activation. *Bioresource technology,* **99,** 8540-8543.
Pelekani, C. and V. L. Snoeyink, 2000: Competitive adsorption between atrazine and methylene blue on activated carbon: the importance of pore size distribution. *Carbon,* **38,** 1423-1436.
Pendyal, B., M. Johns, W. Marshall, M. Ahmedna and R. Rao, 1999a: The effect of binders and agricultural by-products on physical and chemical properties of granular activated carbons. *Bioresource Technology,* **68,** 247-254.
Pendyal, B., M. Johns, W. Marshall, M. Ahmedna and R. Rao, 1999b: Removal of sugar colorants by granular activated carbons made from binders and agricultural by-products. *Bioresource Technology,* **69,** 45-51.

Qiu, H., L. Lv, B.-c. Pan, Q.-j. Zhang, W.-m. Zhang and Q.-x. Zhang, 2009: Critical review in adsorption kinetic models. *Journal of Zhejiang University-Science A,* **10,** 716-724.

Radeke, K. and G. Hartmann, 1991: On the temperature dependence of adsorption of organic materials from aqueous solution. *Adsorption Science & Technology*, **8,** 153-156.

Rahman, M., M. Awang, B. Mohosina, B. Kamaruzzaman, W. W. Nik and C. Adnan, 2012: Waste palm shell converted to high efficient activated carbon by chemical activation method and its adsorption capacity tested by water filtration. *APCBEE Procedia*, **1,** 293-298.

Rao, P., I. M. Lo, K. Yin and S. C. Tang, 2011: Removal of natural organic matter by cationic hydrogel with magnetic properties. *Journal of environmental management*, **92,** 1690-1695.

Richardson, S. D., M. J. Plewa, E. D. Wagner, R. Schoeny and D. M. DeMarini, 2007: Occurrence, genotoxicity, and carcinogenicity of regulated and emerging disinfection by-products in drinking water: a review and roadmap for research. *Mutation Research/Reviews in Mutation Research,* **636,** 178-242.

Rubio, B., M. Izquierdo and E. Segura, 1999: Effect of binder addition on the mechanical and physicochemical properties of low rank coal char briquettes. *Carbon,* **37,** 1833-1841.

Sahu, J., J. Acharya and B. Meikap, 2009: Response surface modeling and optimization of chromium (VI) removal from aqueous solution using Tamarind wood activated carbon in batch process. *Journal of hazardous materials,* **172,** 818-825.

Saka, C., 2012: BET, TG–DTG, FT-IR, SEM, iodine number analysis and preparation of activated carbon from acorn shell by chemical activation with ZnCl2. *Journal of Analytical and Applied Pyrolysis,* **95,** 21-24.

Sample, A.-q., the ultimatetool.

Schreiber, B., T. Brinkmann, V. Schmalz and E. Worch, 2005: Adsorption of dissolved organic matter onto activated carbon—the influence of temperature, absorption wavelength, and molecular size. *Water Research,* **39,** 3449-3456.

Shen, X., Z. Shao, Q. Xian, H. Zou, S. Gao and J. Zhang, 2010: Detection method and toxicity study of a new disinfection by-product, 2, 2, 4-trichloro-5-methoxycyclopenta-4-ene-1, 3-dione (TCMCD), in chlorinated drinking water. *Water research,* **44,** 974-980.

Simay, Į., L. G. Nagy and A. Bóta, 1984: Preparation of activated carbon from the by-products of agricultural industry. *Periodica Polytechnica Chemical Engineering,* **28,** 293-297.

Singer, P. C., 1999: Humic substances as precursors for potentially harmful disinfection by-products. *Water Science and Technology*, **40,** 25-30.

Smith, K., G. Fowler, S. Pullket and N. Graham, 2012: The production of attrition resistant, sewage–sludge derived, granular activated carbon. *Separation and purification technology*, **98,** 240-248.

Statistics Canada, 2016: Census profile, 2016 census. Statistics Canada Ottawa.

Summers, R. S. and P. V. Roberts, 1988: Activated carbon adsorption of humic substances: II. Size exclusion and electrostatic interactions. *Journal of Colloid and Interface Science,* **122,** 382-397.

Sun, J., T. A. Brady, M. J. Rood, C. M. Lehmann, M. Rostam-Abadi and A. A. Lizzio, 1997: Adsorbed natural gas storage with activated carbons made from Illinois coals and scrap tires. *Energy & fuels,* **11,** 316-322.

Świetlik, J., A. Dąbrowska, U. Raczyk-Stanisławiak and J. Nawrocki, 2004: Reactivity of natural organic matter fractions with chlorine dioxide and ozone. *Water research,* **38,** 547-558.

Szymczycha, B., A. Winogradow, K. Kuliński, K. Koziorowska and J. Pempkowiak, 2017: Diurnal and seasonal DOC and POC variability in the land-locked sea. *Oceanologia,* **59,** 379-388.

Tancredi, N., N. Medero, F. Möller, J. Píriz, C. Plada and T. Cordero, 2004: Phenol adsorption onto powdered and granular activated carbon, prepared from Eucalyptus wood. *Journal of colloid and interface science,* **279,** 357-363.

Tibbetts, J., 1995: What's in the water: the disinfectant dilemma. *Environmental health perspectives,* **103,** 30.

Tubić, A., J. Agbaba, B. Dalmacija, J. Molnar, S. Maletić, M. Watson and S. U. Perović, 2013: Insight into changes during coagulation in NOM reactivity for trihalomethanes and haloacetic acids formation. *Journal of environmental management,* **118,** 153-160.

USEPA, 1995: Method 551.1. Determination of Chlorination Disinfection Byproducts, Chlorinated Solvents, and Halogenated Pesticides/Herbicides in Drinking Water by Liquid‐‐Liquid Extraction and Gas Chromatography with Electron‐Capture Detection (Revision 1.0). *Methods for the Determination of Organic Compounds in Drinking Water*.

Van Leeuwen, F., 2000: Safe drinking water: the toxicologist's approach. *Food and Chemical Toxicology,* **38,** S51-S58.

Velten, S., D. R. Knappe, J. Traber, H.-P. Kaiser, U. Von Gunten, M. Boller and S. Meylan, 2011: Characterization of natural organic matter adsorption in granular activated carbon adsorbers. *Water Research,* **45,** 3951-3959.

Vepsäläinen, M., M. Ghiasvand, J. Selin, J. Pienimaa, E. Repo, M. Pulliainen and M. Sillanpää, 2009: Investigations of the effects of temperature and initial sample pH on natural organic matter (NOM) removal with electrocoagulation using response surface method (RSM). *Separation and Purification Technology,* **69,** 255-261.

Villanueva, C. M., K. P. Cantor, J. O. Grimalt, N. Malats, D. Silverman, A. Tardon, R. Garcia-Closas, C. Serra, A. Carrato and G. Castano-Vinyals, 2006: Bladder cancer and exposure to water disinfection by-products through ingestion, bathing, showering, and swimming in pools. *American journal of epidemiology,* **165,** 148-156.

Wang, X.-s. and Y. Qin, 2005: Equilibrium sorption isotherms for of Cu2+ on rice bran. *Process Biochemistry,* **40,** 677-680.

Water, S. and W. H. Organization, 2000: WHO guidelines for drinking water quality: training pack.

WHO, 2000: WHO guidelines for drinking water quality: training pack. *WHO guidelines for drinking water quality: training pack.*

Xin-hui, D., C. Srinivasakannan and L. Jin-sheng, 2014: Process optimization of thermal regeneration of spent coal based activated carbon using steam and application to methylene blue dye adsorption. *Journal of the Taiwan Institute of chemical engineers,* **45,** 1618-1627.

Yan, C., C. Wang, J. Yao, L. Zhang and X. Liu, 2009: Adsorption of methylene blue on mesoporous carbons prepared using acid-and alkaline-treated zeolite X as the template. *Colloids and Surfaces A: Physicochemical and Engineering Aspects,* **333,** 115-119.

Yeganeh, M. M., T. Kaghazchi and M. Soleimani, 2006: Effect of raw materials on properties of activated carbons. *Chemical Engineering & Technology: Industrial Chemistry‐Plant Equipment‐Process Engineering‐Biotechnology,* **29,** 1247-1251.

Zhang, H., H. Tafvizi, T. Husain and Y. Chen, 2017: Affordable Water Filtration Technology for Small Rural Communities.

Zhang, Z., J. Peng, W. Qu, L. Zhang, Z. Zhang, W. Li and R. Wan, 2009: Regeneration of high-performance activated carbon from spent catalyst: optimization using response surface methodology. *Journal of the Taiwan Institute of Chemical Engineers,* **40,** 541-548.

Appendixes

Appendix A

BET surface area and porosity analysis report of the PAC

micromeritics®

3Flex Share 4.04 | 3Flex Version 4.04 Serial # 652 Unit 1 Port 1 | Page 1

Sample: PAC
Operator: Victoria
Submitter: Victoria
File: D:\000-355.SMP

Started:	11/8/2018 2:09:07 PM	Analysis adsorptive:	N2
Completed:	11/9/2018 9:00:59 AM	Analysis bath temp.:	77.781 K
Report time:	12/11/2018 7:12:53 PM	Thermal correction:	No
Sample mass:	0.0481 g	Ambient free space:	10.4134 cm³ Measured
Analysis free space:	31.2961 cm³	Equilibration interval:	10 to 30 s
Low pressure dose:	0.44615 mmol/g	Sample density:	1.000 g/cm³
Automatic degas:	No		

Summary Report

Surface Area

Single point surface area at p/p° = 0.025020038: 561.0305 m²/g

BET Surface Area: 564.8773 m²/g

Pore Volume

Single point adsorption total pore volume of pores less than 3,133.887 Å width at p/p° = 0.993860258: 0.308421 cm³/g

Single point desorption total pore volume of pores less than 1,934.646 Å width at p/p° = 0.990000000: 0.307171 cm³/g

Pore Size

Adsorption average pore diameter (4V/A by BET): 21.840 Å

Desorption average pore diameter (4V/A by BET): 21.751 Å

Isotherm Tabular Report

Relative Pressure (p/p°)	Absolute Pressure (mmHg)	Quantity Adsorbed (cm³/g STP)	Elapsed Time (h:min)	Saturation Pressure (mmHg)
			01:16	784.656311
1.42066E-06	0.001117265	9.543736446	01:42	786.4431152
2.17518E-06	0.001712488	19.15197846	01:51	787.2866211
4.39609E-06	0.003463988	28.72264198	01:58	787.9702759
6.65549E-06	0.005249207	38.27891185	02:06	788.7027588

1.05294E-05	0.008309115	47.85315963	02:15	789.1328125
1.59889E-05	0.012622598	57.37765107	02:24	789.4580688
2.27173E-05	0.017939249	66.86502997	02:34	789.6711426
3.23794E-05	0.025571965	76.38333886	02:47	789.7583618
5.63664E-05	0.04452822	85.88041974	03:00	789.9771729
0.000129545	0.102339506	95.25456298	03:11	789.9926147
0.000358575	0.283417135	104.3592822	03:29	790.3980103
0.001007012	0.796598971	112.7963875	04:02	791.0521851
0.002514236	1.991883874	120.1727845	05:10	792.2423096
0.005414627	4.294655323	126.1477178	06:42	793.1581421
0.009866967	7.84414959	130.7116359	08:23	794.9909668
0.012385056	9.84533596	132.2162339	08:30	794.9367065
0.015338439	12.19380474	133.6132732	08:38	794.9833984
0.01723411	13.70259094	134.4050301	08:43	795.0855103
0.019852571	15.7848053	135.342127	08:49	795.1013184
0.022302244	17.73200035	136.1299261	08:54	795.0769653
0.024804269	19.72268677	136.8458749	09:00	795.1327515
0.027351117	21.74752045	137.5027234	09:05	795.1236572
0.029809154	23.70267105	138.0889516	09:10	795.1473999
0.032323414	25.70327759	138.6360507	09:15	795.1906738
0.034841007	27.70306206	139.1506879	09:19	795.1280518
0.037492552	29.81283951	139.6544814	09:24	795.1669922
0.039796644	31.64817429	140.0705433	09:28	795.2473145
0.04233146	33.67246246	140.5110924	09:32	795.4476929
0.044902562	35.71635437	140.9275963	09:36	795.4190674
0.047381813	37.69270325	141.2985041	09:40	795.5099487
0.052714906	41.9351387	142.0212565	09:44	795.5081787
0.054669503	43.49573898	142.2984663	09:48	795.6124878
0.057322761	45.60535049	142.6438369	09:51	795.5888672
0.059887825	47.65699387	142.9766335	09:55	795.7709961
0.062413245	49.6649971	143.2807405	09:58	795.7445068
0.064847009	51.61701965	143.558351	10:02	795.9815063
0.067302395	53.57209396	143.8266603	10:05	795.9909058
0.069982721	55.70770264	144.1119487	10:08	796.020813
0.072253757	57.51875305	144.3548698	10:11	796.065918
0.074944896	59.66412354	144.6392819	10:14	796.1065674
0.077349528	61.58333969	144.8818382	10:17	796.1695557
0.079884652	63.59097672	145.1180657	10:20	796.0349731
0.082305492	65.52306366	145.3434558	10:23	796.0958862

0.084886417	67.58415222	145.591305	10:26	796.1715698
0.087281874	69.48571014	145.8151311	10:29	796.1069946
0.089845106	71.53794861	146.0445728	10:32	796.2364502
0.092320954	73.5	146.2676094	10:34	796.1358643
0.094692848	75.40407562	146.4737832	10:37	796.3016968
0.09727513	77.46437073	146.6936976	10:40	796.3430176
0.099689107	79.39431763	146.8945711	10:43	796.4191895
0.119832682	95.45697784	148.3030207	10:47	796.5855103
0.139894579	111.4513321	149.5603246	10:51	796.6808472
0.160025024	127.4879532	150.7129466	10:55	796.6746216
0.180279447	143.6376495	151.8098689	10:58	796.75
0.200454444	159.6787262	152.826962	11:02	796.5836182
0.220998596	176.0176392	153.8125271	11:05	796.4649658
0.241120286	192.0775909	154.7449487	11:08	796.6048584
0.260882495	207.8390045	155.6253229	11:11	796.6766968
0.28069115	223.6487427	156.4630195	11:14	796.7787476
0.300613356	239.5368652	157.2775857	11:17	796.8270874
0.320738368	255.5718842	158.06882	11:20	796.8235474
0.340738897	271.5205688	158.8508808	11:23	796.8581543
0.359183249	286.1941833	159.5625602	11:26	796.7915649
0.379231702	302.2167664	160.2929164	11:29	796.9185181
0.398701234	317.7714539	160.9930619	11:31	797.0164795
0.418815651	333.7569885	161.6960274	11:34	796.9066772
0.438624771	349.6553955	162.3803277	11:37	797.1629028
0.458906413	365.7906494	163.0728724	11:39	797.092041
0.478853183	381.7218018	163.75	11:42	797.1583252
0.499011593	397.753418	164.4261835	11:45	797.0825195
0.51879733	413.5565491	165.1179815	11:48	797.1447144
0.538796053	429.5690308	165.8182104	11:52	797.2757568
0.558833127	445.5037537	166.4878784	11:54	797.2035522
0.578876261	461.5341492	167.2050928	11:57	797.2932739
0.598736703	477.4625549	167.8967331	12:00	797.4499512
0.618880163	493.5568542	168.613425	12:03	797.4998779
0.638983136	509.5294189	169.3049253	12:05	797.4066772
0.658667419	525.3555298	170.033164	12:08	797.6036377
0.679023008	541.6630859	170.7634573	12:11	797.7094727
0.698682933	557.3676147	171.519338	12:13	797.7404175
0.71896536	573.4932251	172.32346	12:17	797.6646118
0.738708234	589.2668457	173.1673453	12:20	797.6990356

0.759482221	605.8851929	174.1055113	12:24	797.7608643
0.778756636	621.1987305	174.9948404	12:27	797.6801758
0.798900422	637.3914185	175.9529837	12:31	797.8358765
0.818869609	653.3969727	176.9329132	12:34	797.9255371
0.838813208	669.2662964	177.9443992	12:37	797.8728638
0.858769816	685.2113037	179.00101	12:40	797.8986816
0.878713254	701.2086182	180.0947337	12:43	797.994812
0.898844965	717.3197021	181.2208761	12:46	798.0460815
0.918538973	733.1712036	182.3971968	12:49	798.1928101
0.938516447	749.1387329	183.6382907	12:52	798.2158813
0.958548148	765.2059326	184.9592657	12:55	798.296814
0.978154697	780.9284058	186.7598186	12:59	798.3690186
0.98826245	789.0352783	188.2918394	13:02	798.4066162
0.993948131	793.5440063	189.5282777	13:05	798.3756714
0.98355913	785.4752197	189.2338118	13:08	798.6049805
0.973311349	777.5150146	188.6262239	13:10	798.8348389
0.950351328	759.2458496	187.5214382	13:13	798.9107056
0.924859143	738.8571777	186.1309423	13:16	798.8861694
0.899067941	718.3427734	184.8686541	13:19	798.986084
0.874281311	698.6266479	183.7834409	13:22	799.086792
0.849431827	678.7827148	182.812402	13:25	799.1020508
0.824391836	658.7706909	181.9363971	13:27	799.098999
0.799333385	638.8775024	181.1106302	13:30	799.2628784
0.774413184	618.9816895	180.3277295	13:33	799.2912598
0.749479192	599.1151123	179.5759652	13:36	799.3752441
0.724227571	578.9607544	178.8497605	13:39	799.4182739
0.699136629	559.0487061	178.1769252	13:42	799.6272583
0.67414305	539.0111084	177.4926038	13:44	799.55
0.649099271	519.0665894	176.811391	13:47	799.6721191
0.62436922	499.2680969	176.1552441	13:50	799.6359863
0.599532074	479.359375	175.5137534	13:53	799.5558472
0.550714897	440.4921875	174.2732189	13:56	799.8552246
0.49946336	399.4938049	172.8894917	13:59	799.8460693
0.45214112	361.7498474	166.5340381	14:07	800.0817261
0.398411898	318.8372192	163.5176878	14:12	800.2703247
0.345010062	276.143219	161.4386763	14:16	800.3917847
0.30097138	240.9318695	159.7962326	14:20	800.5142212
0.250921501	200.8818817	157.8313139	14:24	800.5765991
0.200966158	160.7662048	155.6346126	14:29	799.9665527

0.140804489	112.6675339	152.545004	14:33	800.17

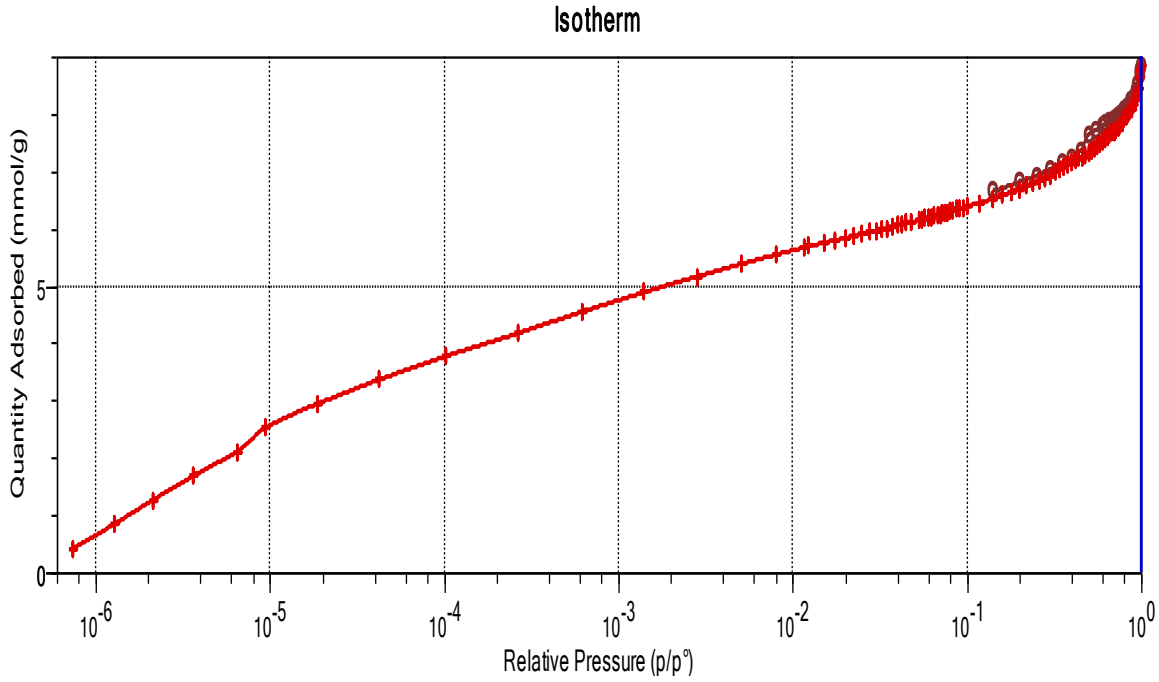

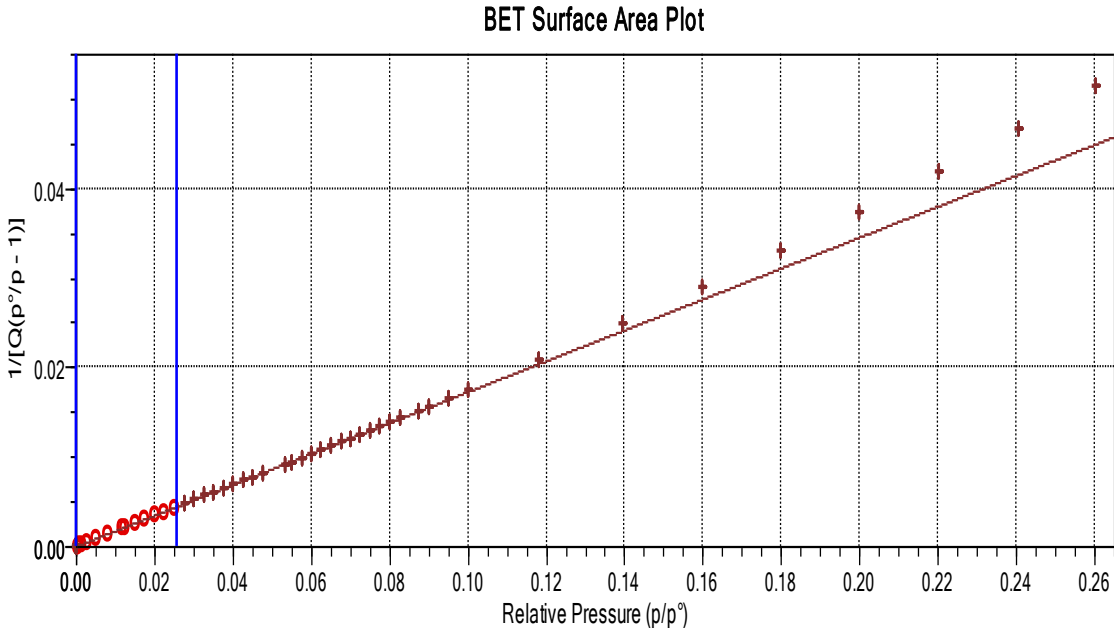
BET Surface Area Plot
1/[Q(P°/P - 1)]
0.04
0.02
0.00
0.00
0.02
0.04
0.06
0.08
0.10
0.12
0.14
0.16
0.18
0.20
0.22
0.24
0.26
Relative Pressure (p/p°)

Appendix B

BET surface area and porosity analysis report of the GAC

micromeritics®

3Flex Share 4.04 | 3Flex Version 4.04 Serial # 652 Unit 1 Port 3 | Page 1

Sample: GAC
Operator: Victoria
Submitter: Victoria
File: C:\Users\afsoon's\Desktop\000-357.SMP

Started:	11/8/2018 2:09:07 PM	Analysis adsorptive:	N2
Completed:	11/9/2018 9:00:59 AM	Analysis bath temp.:	77.754 K
Report time:	12/11/2018 8:17:17 PM	Thermal correction:	No
Sample mass:	0.0916 g	Ambient free space:	10.0589 cm³ Measured
Analysis free space:	30.1610 cm³	Equilibration interval:	10 to 30 s
Low pressure dose:	0.44615 mmol/g	Sample density:	1.000 g/cm³
Automatic degas:	No		

Summary Report

Surface Area

Single point surface area at p/p° = 0.047381813: 585.8724 m²/g

BET Surface Area: 588.4034 m²/g

Pore Volume

Single point adsorption total pore volume of pores less than 3,178.983 Å width at p/p° = 0.993948131: 0.294523 cm³/g

Single point desorption total pore volume of pores less than 1,934.646 Å width at p/p° = 0.990000000: 0.294349 cm³/g

Pore Size

Adsorption average pore diameter (4V/A by BET): 20.022 Å

Desorption average pore diameter (4V/A by BET): 20.010 Å

Isotherm Tabular Report				
Relative Pressure (p/p°)	Absolute Pressure (mmHg)	Quantity Adsorbed (cm^3/g STP)	Elapsed Time (h:min)	Saturation Pressure (mmHg)
			01:16	784.656311
7.36398E-07	0.0005788	9.410792299	01:37	785.9877319
1.28225E-06	0.00100852	18.83921077	01:44	786.5249634
2.13001E-06	0.001676868	28.2711519	01:50	787.2576294
3.65507E-06	0.002879074	37.69379837	01:57	787.692688
6.47431E-06	0.005103404	47.11566448	02:03	788.2531128
9.52094E-06	0.007512042	56.51437891	02:13	789.0013428
1.8911E-05	0.014929525	65.89547925	02:25	789.4608765
4.23882E-05	0.033475388	75.26957247	02:37	789.7321777
0.000103075	0.081416108	84.52020873	02:52	789.8741455
0.000266731	0.210749969	93.46959968	03:13	790.1213379
0.000625778	0.494994909	101.9146375	04:02	791.0067139
0.001411799	1.118664026	109.4276447	05:23	792.368042
0.002825659	2.243042231	115.6788182	07:27	793.8121338
0.005083101	4.041742325	120.5218929	09:17	795.1332397
0.008033754	6.400860786	124.2424175	10:55	796.7459717
0.011636848	9.27569294	127.0210651	11:44	797.0966797
0.012387896	9.874526978	127.4972814	11:48	797.1109009
0.01511463	12.05045319	128.7910072	11:53	797.270813
0.017403006	13.87532711	129.7410293	11:59	797.2948608
0.020016327	15.96111488	130.6683371	12:03	797.4018555
0.022492961	17.94023514	131.4792464	12:08	797.5933228
0.025020038	19.9597187	132.2038679	12:13	797.7493286
0.027543207	21.96850014	132.8448877	12:16	797.6013794
0.030042648	23.96654892	133.4589898	12:20	797.7491455
0.032567643	25.98	134.029595	12:23	797.7265625
0.03505705	27.96926308	134.5730096	12:27	797.8213501
0.037614955	30.00850105	135.0993774	12:30	797.7811279
0.040085602	31.98594475	135.572472	12:33	797.9403687
0.042614408	34.00179291	136.0158193	12:36	797.8942871
0.045020658	35.92082977	136.4437598	12:39	797.8743896
0.047644432	38.0185585	136.8555966	12:42	797.9643555
0.053237212	42.4781189	137.671776	12:45	797.902771
0.054906421	43.822258	137.9467821	12:48	798.1262817
0.057640257	46.00759888	138.3391473	12:51	798.1851807

0.060122895	47.99834824	138.6985334	12:54	798.3372803
0.062527155	49.91834641	139.0208314	12:57	798.3466797
0.065127388	52.00100327	139.36259	13:00	798.4506226
0.067663086	54.02595901	139.6777483	13:03	798.4554443
0.070123992	55.98698425	139.97	13:06	798.3998413
0.072541176	57.93995285	140.2667199	13:09	798.7181396
0.07499605	59.9107666	140.5664741	13:12	798.8522949
0.07758253	61.98049545	140.8609937	13:15	798.897583
0.07997422	63.90153503	141.1122491	13:18	799.0266724
0.082678924	66.0671463	141.3933846	13:20	799.0808716
0.087489962	69.91604614	141.8552081	13:23	799.1322021
0.09020368	72.08657074	142.1165556	13:26	799.1533203
0.095068647	75.98139954	142.5734798	13:29	799.2266846
0.100200874	80.09091187	143.0166023	13:32	799.3035278
0.11822559	94.50812531	144.4766709	13:35	799.3880615
0.139647068	111.6584854	146.0458149	13:38	799.5762939
0.15973883	127.7086792	147.4130159	13:41	799.4842529
0.179911357	143.8143463	148.7040919	13:43	799.3622437
0.199912277	159.8527069	149.8955784	13:46	799.6142578
0.220381251	176.2302399	151.0755176	13:49	799.6607666
0.240640592	192.4141846	152.2147667	13:52	799.5915527
0.260376949	208.2598419	153.2757703	13:55	799.8397827
0.28112548	224.8464203	154.3303361	13:58	799.8080444
0.300947849	240.7165833	155.3035901	14:00	799.8614502
0.321543492	257.2539673	156.3051756	14:03	800.0596313
0.341770885	273.440155	157.2738226	14:06	800.0686035
0.35898189	287.1999512	158.0734724	14:09	800.0402222
0.378806698	303.1385803	158.9699777	14:11	800.2460938
0.398909968	319.249176	159.8903371	14:14	800.303833
0.418906568	335.2927246	160.7876752	14:17	800.3997803
0.439024944	351.4538574	161.6565332	14:20	800.5327759
0.458974625	367.4454651	162.5297883	14:24	800.5790405
0.479556736	383.6905518	163.3356974	14:26	800.0941772
0.498943805	399.1618347	164.0758193	14:29	800.0136108
0.519150368	415.3687744	164.9521363	14:33	800.0933838
0.539431136	431.53	165.8514318	14:35	799.9724731
0.559019626	447.387085	166.7377394	14:38	800.3065796
0.579316415	463.6360779	167.5774657	14:41	800.3157959
0.599142416	479.5258484	168.3508638	14:43	800.3536987

0.619105151	495.602478	169.1251819	14:46	800.5142212
0.639212629	511.7217407	169.9245953	14:49	800.5501099
0.65926316	527.7624512	170.7253221	14:51	800.5338135
0.678814402	543.510376	171.5827504	14:54	800.6759644
0.699134299	559.78	172.4419429	14:57	800.6759644
0.719101389	575.8031006	173.2947126	14:59	800.7258911
0.739195678	591.9394531	174.2045038	15:02	800.7885742
0.758809989	607.7614136	175.0626826	15:05	800.9401855
0.779297474	624.0754395	176.0004472	15:07	800.8179932
0.79917985	640.112915	177.0056815	15:10	800.9622803
0.818913541	655.8930664	177.9828677	15:13	800.9307861
0.83866854	671.9315186	179.0416922	15:15	801.1884155
0.85922992	688.3966675	180.2153819	15:18	801.1786499
0.879418507	704.5627441	181.4321728	15:21	801.1688843
0.898957695	720.3555298	182.7310345	15:23	801.3230591
0.918730428	736.3032227	184.2617423	15:26	801.4355469
0.938834248	752.5703125	186.213164	15:29	801.6008301
0.958947568	768.4106445	189.04656	15:31	801.3062134
0.978290969	784.1796265	193.191946	15:34	801.5811768
0.988724198	792.5089722	196.2174417	15:37	801.5470581
0.993860258	796.7299805	198.4413805	15:40	801.6519165
0.985619447	790.1990356	196.7248895	15:42	801.7283325
0.976034574	782.4990234	194.8235798	15:45	801.7124023
0.949689969	761.3066406	190.6242081	15:49	801.6370239
0.925717912	742.2026978	187.8970681	15:51	801.7590332
0.900734198	722.2290649	185.8774619	15:54	801.8226318
0.875853711	702.2786865	184.4023842	15:57	801.8218994
0.849752062	681.6588745	183.1140482	16:00	802.1856079
0.824882791	661.8051147	182.0463109	16:02	802.302002
0.799991039	641.8956909	181.0675758	16:05	802.3786011
0.775141867	621.8452148	180.185741	16:08	802.2340698
0.75038817	602.0123291	179.3047215	16:11	802.2678833
0.725205179	581.9012451	178.4534575	16:14	802.3953247
0.700587917	562.1978149	177.6379713	16:16	802.4657593
0.675604408	542.1332397	176.8456163	16:19	802.4418335
0.650384112	522.0601196	176.0630735	16:22	802.6950684
0.625325799	502.069519	175.2817742	16:25	802.8927002
0.600556651	482.089447	174.5198702	16:27	802.7376709
0.55185539	443.063385	173.0011929	16:30	802.8613892

0.500794519	402.0236816	171.2707792	16:33	802.7717285
0.44982403	361.2044678	165.2143656	16:37	802.9906006
0.398849256	320.3332825	162.0750663	16:40	803.1437378
0.351282618	282.1455078	159.9024243	16:43	803.1866455
0.300408832	241.3164673	157.6339503	16:46	803.2935181
0.250538194	201.2484283	155.2718259	16:48	803.2644653
0.200387159	160.973877	152.6671195	16:51	803.3143311
0.140223732	112.6825638	149.0476576	16:54	803.5912476

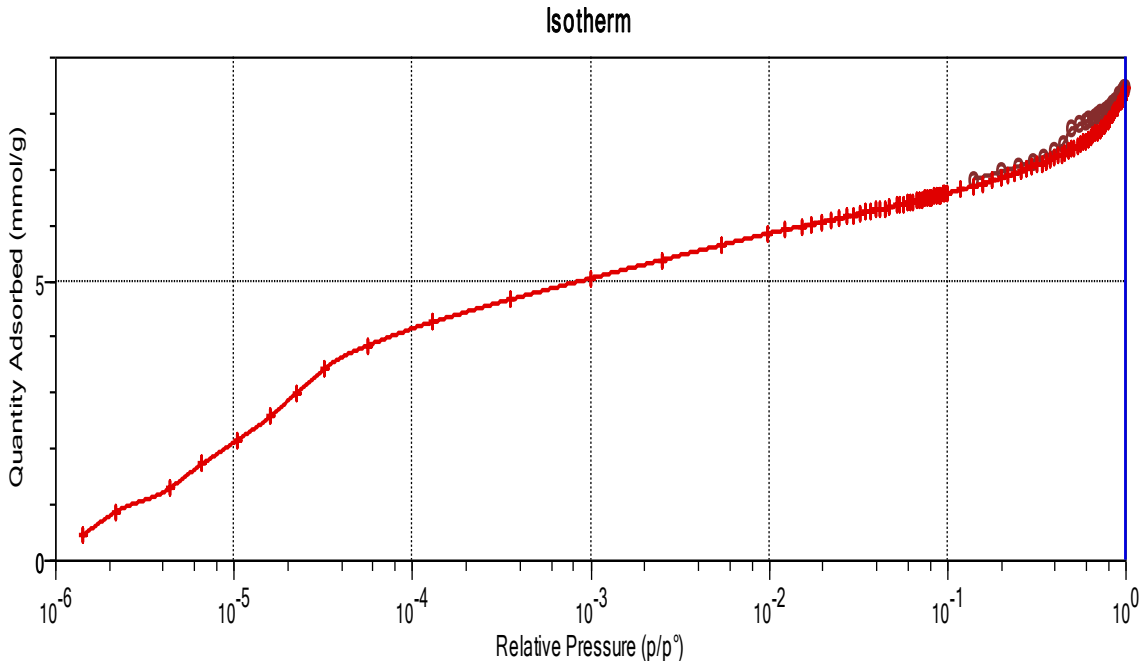

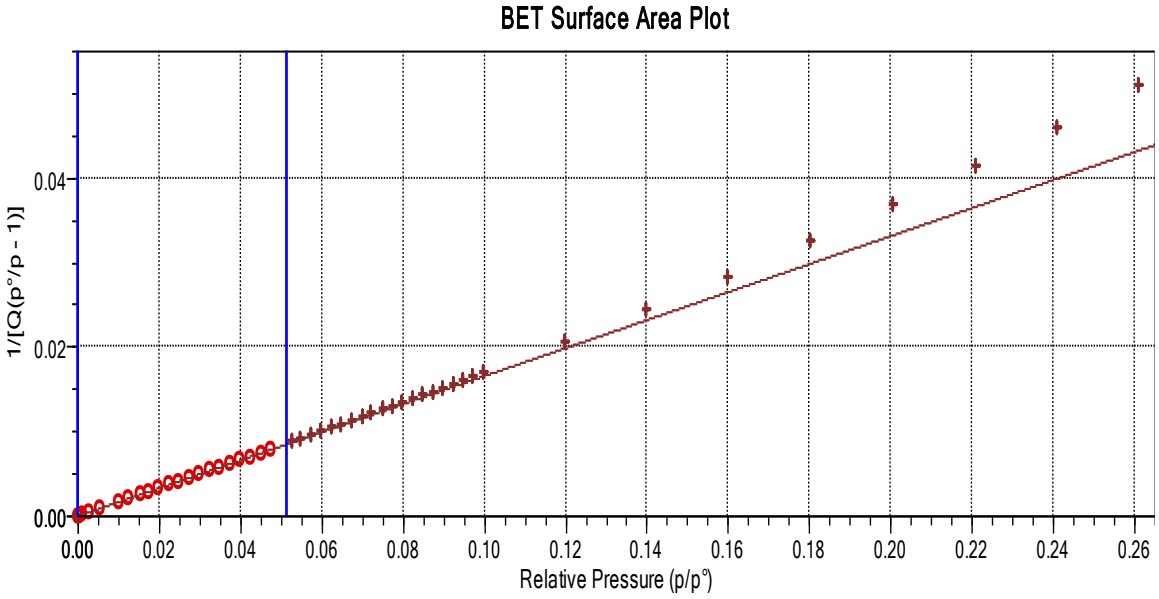
BET Surface Area Plot
1/[Q(p°/p - 1)]
0.04
0.02
0.00
0.00
0.02
0.04
0.06
0.08
0.10
0.12
0.14
0.16
0.18
0.20
0.22
0.24
0.26
Relative Pressure (p/p°)